NTNU – Trondheim
Norwegian University of
Science and Technology

Experimental validation of dynamic stationkeeping capability analysis

The next level DP capability analysis

Brede Børhaug

Master of Science in Engineering Cybernetics
Submission date: June 2012
Supervisor: Thor Inge Fossen, ITK
Co-supervisor: Luca Pivano, Marine Cybernetics AS

Norwegian University of Science and Technology
Department of Engineering Cybernetics

NTNU
Norwegian University of
Science and Technology

Faculty of Information Technology,
Mathematics and Electrical Engineering
Department of Engineering Cybernetics

MSC THESIS DESCRIPTION SHEET

Name:	Brede Børhaug
Department:	Engineering Cybernetics
Thesis title (Norwegian):	Eksperimentell validering av dynamisk kapabilitetsanalyse
Thesis title (English):	Experimental Validation of Dynamic Stationkeeping Capability Analysis

Background: Vessel stationkeeping performance is typically provided by the traditional DP Capability analysis, which is inherently quasi-static, meaning that several important assumptions and simplifications must be done to facilitate the analysis. Dynamic Station-keeping Capability analysis (DynCap) is a new tool that is being developed to provide a detailed study of a vessel's stationkeeping capability in realistic dynamic conditions.

DynCap is carried out with systematic time-domain simulations with a sophisticated 6-DOF vessel model, including dynamic environmental loads, a complete propulsion system including thrust losses, power system, sensors, and a control system with observer, DP controller and thrust allocation.

Thesis description

- Give a brief description of dynamic station keeping capability analysis.
- Give a brief description of the theoretical foundation of capability analysis.
- Give a brief description of the CyberSea Vessel Simulator. Discuss the complexity and realism of the simulator.
- Configure and tune the Marine CyberSea Vessel Simulator based on available data for CyberShip III.
- Define the configuration parameters that affect the results of the dynamic capability analysis. Chose the configuration parameter for running the analysis and discuss the impact that they may have on the results.
- Run dynamic capability analysis with the selected configuration parameters using the Marine Cybernetics DynCap tool employing the Marine CyberSea Vessel Simulator for CyberShip III.
- Run experiments to validate the CyberSea Vessel Simulator with the CyberShip III configuration.
- Run experiments to compare the DynCap results obtained during simulations with the experimental DynCap results.
- Comment and discuss the results obtained.

Tentative: Conduct a static capability analysis according to industry standard methods. Compare and discuss the results to that of the DynCap analysis and experimental data.

Guidelines
The report shall be written in English and contain the following elements: Abstract, acknowledgements, table of contents, main body, conclusion with recommendations for further work, list of symbols and acronyms, references and (optional) appendices. All figures, tables and equations shall be enumerated.

Start date:	2012-01-09
Due date:	2012-06-11

Thesis performed at:	Department of Engineering Cybernetics, NTNU
Supervisor:	Professor Thor I. Fossen, Dept. of Eng. Cybernetics, NTNU
Co-Supervisor:	Luca Pivano, PhD, R&D Manager at Marine Cybernetics AS

Abstract

This thesis considers two main issues: the theoretical aspects of stationkeeping capability analysis in general, and dynamic capability (DynCap) analysis in particular; further there has been conducted capability analyses of the model vessel, CyberShip III, including an experimental validation of the results.

This thesis presents the most comprehensive investigation into the differences between the DynCap analysis and the industry standard DP capability analysis (DPCap), published to date, as far as both Marine Cybernetics AS and the author are aware of. The mathematical foundation of DynCap has been investigated in detail, and it has been shown that by applying the simplifications and assumptions proposed in the industry used IMCA M140 specifications for DP capability plots to the equations of DynCap, it is possible to arrive at the DPCap equations. The review of the mathematical foundation of capability analysis, highlights the benefits of employing the DynCap analysis in favor of the DPCap analysis, and provides the necessary mathematical motivation for choosing the DynCap analysis in favor of the DPCap analysis.

This thesis also presents multiple stationkeeping capability analyses of CyberShip III. The stationkeeping capability of CyberShip III was obtained through both DPCap analysis and DynCap analysis. In addition, an experiment using the model vessel CyberShip III was conducted, in order to obtain the true stationkeeping capability of CyberShip III. The results obtained revealed that the traditional DPCap analysis, seems repeatedly to be too optimistic, and that the DynCap results seems to be more realistic. The experimental results show that the relative reduction in depicted capability between the result obtained through DynCap anal-

ysis and experimental data obtained, is approximately 10%. In contrast, the relative reduction from DPCap results, compared to the experimental data, where found to be approximately 60%.

By combining the theoretical foundation of DynCap, the simulations conducted and the experimental data obtained, the thesis is able to validate the DynCap stationkeeping capability analysis. The superior performance of the DynCap analysis, relative the DPCap analysis, provides additional arguments for employing the DynCap method in favor of the industry standard DPCap. Further the thesis highlights possible shortcomings of the DynCap analysis, including remarks in regard to the complexity and accuracy of the models used during the DynCap simulations.

The implications of the results presented in this thesis may be regarded as considerable. The results show that without a well defined standard for DPCap analysis, the validity of the results are uncertain. The uncertainty in turn limits the use of the obtained results. This thesis proposes that by employing the DynCap analysis, the operators, ship owners and oil companies, will be able to make decisions based on more accurate data, which will enhance security, and reduce non-productive time. With well defined limits of operation for a vessel, it will be possible to utilize the resources in a more productive manner. By basing decisions on accurate data, the selected vessel may be able to operate closer to the limit, without compromising security. This will in turn reduce costs and possibly increase profits.

Keywords: Dynamic Positioning, DP, DP Capability, DPCap, Dynamic Stationkeeping Capability, DynCap

Norwegian Translation of the Abstract

Denne avhandlingen vurderer to hovedområder: de teoretiske sidene ved DP kapabilitetsanalyse generelt, og dynamisk kapabilitetsanalyse (DynCap) spesielt; videre har det vært gjennomført kapabilitetsanalyser av modellbåten CyberShip III, inkludert en eksperimentell validering.

Denne avhandlingen presenterer den mest omfattende gjennomgangen av forskjellene mellom DynCap analyse, og den tradisjonelle DP kapa-

bilitetsanalysen (DPCap), utgitt i skrivende stund, så langt både Marine Cybernetics AS og forfatteren er kjent med. Det matematiske grunnlaget for DynCap er undersøkt i detalj, og det blir vist hvordan man ved å anvende de forenklingene og forutsetninger som er foreslått i bransjen normen IMCA M140, på ligninger for DynCap, kan komme frem til DPCap ligningene. Den grundige gjennomgangen av det matematiske grunnlaget for kapabilitetsanalyse, gir en økt forståelse og fremhever fordelene ved å benytte DynCap analyse, i tillegg til den nødvendige matematiske motivasjonen for å bruke DynCap analyse i favør av DPCap analysen.

Avhandlingen presenterer også flere kapabilitetsanalyser av båten CyberShip III. Kapabilitetsanalysen av CyberShip III ble gjennomført både ved DPCap analyse og DynCap analyse. I tillegg ble kapabiliteten til CyberShip III bestemt eksperimentelt, ved hjelp av modellfartøyet CyberShip III. Resultatene funnet, avslører at de tradisjonelle DPCap analyseresultatene, gjentatte ganger, ser ut til å være for optimistisk. Vider indikerer resultatene at DynCap synes å gi et mer realistisk bilde. De eksperimentelle resultatene viser at den relative reduksjonen i kapabilitet mellom resultatet funnet gjennom DynCap analyse, og de funnet eksperimentelt, er ca 10 %. I motsetning viser det seg at den relative reduksjon mellom DPCap og eksperimentelle data, ble funnet å være i gjennomsnitt ca 60 %.

Ved å kombinere det teoretiske grunnlaget for DynCap, simuleringer og eksperimentelle data, var det mulig å validere DynCap kapabilitetsanalysen. Den overlegne ytelsen til DynCap analysen, relativ DPCap analysen, styrker motivasjonen for å benytte DynCap metoden i favør av industristandarden DPCap. Videre blir mulige svakheter ved DynCap analysen generelt, samt den gjennomførte analysen belyst, hvor blant annet i hvilken grad kompleksiteten og nøyaktigheten av modellene som brukes i DynCap simuleringene, kan sies å være tilfredsstillende.

Implikasjonene av resultatene presentert i denne oppgaven kan betraktes som betydelig. Resultatene viser at uten en veldefinert standard for DPCap, kan det være vanskelig å avgjøre i hvor stor grad man kan stole på resultatene. Usikkerheten legger videre begrensninger på bruken. Avhandlingen foreslår at ved å benytte DynCap analysen, vil operatørene, redere og oljeselskaper, kunne ta beslutninger basert på mer nøyaktige data, noe som vil forbedre sikkerheten. Med godt definerte operasjonsvinduer for

det enkelte fartøy, vil det være mulig å utnytte ressursene på en mer produktiv måte. Ved å basere avgjørelser på nøyaktige data, kan det enkelte fartøyet operere nærmere grensen av hva det kan håndtere, uten at det går på bekostning av sikkerheten. Det vil i sin tur medføre redusere kostnader, og muligheter for økt fortjeneste.

Acknowledgments

Most of all I would like to thank my supervisor, Professor Thor I. Fossen at the Department of Engineering Cybernetics: first for taking me in as a MS'c student, and for being my supervisor during this master thesis. I would like to thank Professor Fossen, for being a great advisor, with a spectacular dedication and for being a great inspiration for me academically as well as personally.

In addition I would like to thank my co-supervisor Dr. Luca Pivano, R&D Manager at Marine Cybernetics AS; first of all for always taking the time to help me out and supporting my efforts, and for giving me the opportunity to work so closely with the exciting technology of Marine Cybernetics AS.

In addition I would like to thank all the employees at Marine Cybernetics AS. This thesis would not been possible without the dedication and patience of all the employees. In particular the author is thankful for the dedication of the R&D team at Marine Cybernetics AS, and in particular Kristoffer Eide and dr. Dong Trong Nguyen.

Finally I would like to thank my dearest Guri Eriksrød Skauen, for her endless love, support and encouragement in our daily life, and particularly during my thesis.

Brede Børhaug, June 2012

Contents

List of Figures

List of Tables

Nomenclature

ABS American Bureau of Shipping

CB Center of Buoyancy

CF Center of Flotation

CFD Computational fluid dynamic

CO Center of Gravity

DOF Degrees-of-Freedom

DPCap Stationkeeping Capability Analysis

DP Dynamic Positioning

DynCap Dynamic Stationkeeping Capability Analysis

ECEF Earth-center Earth-fixed

ECI Earth-center inertial

GA General Arrangement

Hs Significant wave hight

IMCA International Marine Contractors Association

LRS Lloyd's Register

NED North, East, Down

UGAS uniformly globally asymptotically stable

Chapter 1

Introduction

The subject of this thesis is experimental validation of dynamic stationkeeping capability (DynCap) analysis. DynCap is a new tool that aim to improve on todays methods for vessel capability analysis. Vessel stationkeeping performance is today typically provided by the traditional Dynamic Positioning (DP) capability analysis, which is inherently quasi-static, meaning that several important assumptions and simplifications must be done to facilitate the analysis, according to Pivano et al. (2012). DynCap analysis is being developed to provide a more detailed study of a vessels stationkeeping capability in realistic dynamic conditions.

DynCap is carried out with systematic time-domain simulations with a sophisticated 6-degrees-of-freedom (DOF) vessel model, including dynamic environmental loads, a complete propulsion system including thrust losses, power system, sensors, and control system with observer and thrust allocation. DynCap is a tool designed to give a more accurate capability plot for a DP vessel, than the current industry standard static DP capability analysis.

1.1 Background and Motivation for Dynamic Stationkeeping Analysis

In the last 10 years the number of DP units has increased dramatically driven by an increased offshore activity. At the same time the operational safety has also drawn more attention. One of the challenges in the offshore

industry is to make sure that a vessel or floating structure is able to perform its tasks in a safe and efficient manner, Pivano et al. (2012). To be able to plan safe and efficient operation it is important to know the window of operation, the maximum environmental load the particular vessel can withstand, while still maintaining position and heading. During critical operations such as drilling, diving, and offloading, the stationkeeping precision requirements are high, regardless of the environmental conditions. It is thus important to know the positioning capability of the vessel in order plan and execute operations in a safe manner, according to Pivano et al. (2012). To provide the necessary capability information, a stationkeeping capability analysis must be performed. The determination of this capability can be done by static DP capability (DPCap), which conducts this analysis by basically balancing the forces acting on the vessel, or through time-domain simulations. Today the static calculations, DPCap, of a floating offshore structure is recommended performed by ISO 19901-7 and IMCA M140, where the latter is considered as the current industrial standard, Pivano et al. (2012). The background for the use of somewhat standardized methods for conducting stationmaster capability analysis, like the IMCA M140 specification, is to enable a direct comparison of individual vessel's performance, which provide an indication of stationkeeping capability in a common and understandable format, Pivano et al. (2012). Since by the use of DPCap, several important assumptions has to be made in order to compute the capability analysis, in accordance to the IMCA M140, like effects of dynamics and thruster losses, concerns of how accurate the DPCap is, have been raised.

To meet the concerns of the operators, oil companies and the ship yards, the use of time-domain simulations have been proposed as a possible solution. The time-domain approach to stationkeeping capability analysis, a dynamic capability analysis (DynCap), aims to bridge the gap between the DPCap and the true capability of the individual vessel. The principles of a time-domain simulation, by nature indicate a more accurate result of a capability analysis than the DPCap, since dynamics, control systems etc. can be considered in the analysis. With time-domain simulations, one may include dynamics, transition time, and time constants, but at the same time possibly introduce errors as well, which can obscure, or mask the results. In order to establish the DynCap analysis as a next-generation

stationkeeping analysis, and possibly show that time-domain simulation is not only better than DPCap, but a requirement for obtaining satisfyingly accurate stationkeeping capability results, some sort of validation of the approach is needed.

1.2 Previous Work

Since the first developed DP system, the capability of a vessel to maintain position in increasing weather, has been subject to discussion, research and numerous publications. All DP vessels have a DPCap analysis conducted as part of the DP classification, and the theory is well documented. The impact of dynamics of a vessel, on the DPCap analysis has also been subject to research and discussion for years. The DynCap analysis on the other hand is relatively new in the marked, and the only known publication on DynCap, is the in proc. paper Pivano et al. (2012). The paper briefly describes the method on a conceptual level, and highlights the differences conceptually.

1.3 Contribution and Scope of the Thesis

We discuss the contribution of the two parts of this thesis separately.

1.3.1 Dynamic stationkeeping capability

The main focus of Part 1 of this thesis is the concepts and the mathematical foundation of capability analysis, and dynamic capability analysis in particular. The part attempts to summarize the theory of DynCap analysis, and by investigating the mathematical foundation of both analysis, show the mathematical relationship between DynCap and DPCap. Both the DPCap and DynCap analysis are based upon first-principle equations, and from that it is shown that one may apply the assumptions of the IMCA M140 specifications, to the DynCap equations and eventually end up with the fundamental equations of DPCap. By providing a through review of the DynCap analysis theoretically, the part provides the most detailed examination of the DynCap analysis published to date.

1.3.2 Capability Analysis and Experimental Validation

The main focus of Part 2 of this thesis, as well as the main motivation for writing this thesis, is experimental validation of DynCap analysis. First both DPCap analysis and DynCap analysis is conducted. The results are discussed, and compared to earlier DPCap and DynCap results. According to Marine Cybernetics AS, and the knowledge of the author, the worlds first experimental validation of DynCap analysis is then conducted. An extensive, three week experiment undertaken, which obtained the true stationkeeping capability of the vessel. The results enabled both a validation of the DynCap analysis, as well as a validation of the Vessel Simulator used. Further, the results of this thesis, give insight into not only the accuracy of the DynCap results, but the DPCap results as well.

As an added benefit of the extensive system identification process conducted during the DynCap analysis, quality vessel data was obtained, and have already shown to be of great benefit to other master students working on the CyberShip III the spring of 2012.

1.4 Organization of this Thesis

This thesis is organized into 12 chapters and 8 appendices. The chapters are labeled 1 to 12 respectively, and the appendices are labeled A to H.

Following is a short preview of the chapters and appendices:

Chapter 2 gives a brief presentation of some of the notation used in this thesis. Multiple aspects, including coordinate systems and coordinate transformations are addressed. The vessel, CyberShip III, considered in this thesis will be presented.

Part I: Stationkeeping capability analysis theory

Chapter 3 presents the concept of capability analysis, and the dynamic capability analysis in particular.

Chapter 4 investigates the differences between DynCap and DPCap, exemplified by investigating the DPCap and DynCap analysis conducted on an offloading shuttle tanker.

Chapter 5 presents the mathematical foundation of DPCap, as specified by the IMCA M140 specifications.

Chapter 6 presents the fundamental mathematical equations behind the DynCap analysis. By applying the assumptions stated in the IMCA M140 specifications, it is shown how the DynCap equations become the equations of DPCap.

Part II: Capability Analysis and Experimental Validation

Chapter 7 presents the DPCap analysis of CyberShip III. The analysis is conducted in compliance with the IMCA M140 specifications. An analysis where no thrust is reserved for dynamics is presented, as well as one where 20% thrust is reserved to account for the dynamics.

Chapter 8 will present a short overview of the CyberSea Vessel Simulator, in addition to the parameters needed to conduct the DynCap analysis.

Chapter 9 presents an extensive test-program applied to the simulator, and simulator configurations, which seek to validate the configurations of the CyberSea simulator. The tests conducted are based upon a combination of the Marine Cybernetics AS internal routines for configuration testing and tests developed by the author. The main purpose of conducting the tests, was to verify that no human errors had occurred during the input of configuration files to the simulator, ensure that the described parameters, as well as the hydrodynamic calculations correspond with the behavior of the vessel in the simulator, and the predicted and observed behavior of CyberShip III.

Chapter 10 presents the DynCap analysis conducted for CyberShip III. The acceptance criteria selected for the analysis is presented and justified. The results of the DynCap analysis are presented, followed by a brief discussion.

Chapter 11 presents an extensive experiment conducted to obtain the true stationkeeping capability of CyberShip III. The chapter presents the control system and thrust allocation algorithm used

during the experiment. The results are then presented, followed by a discussion, where the results are compared to that of the DP-Cap analysis and DynCap analysis. In addition the results are compared to the results presented in Chapter 4, for the offloading shuttle tanker.

Chapter 12 contains the conclusion of the thesis, and the recommendations for future work.

Appendices

Appendix A contains the complete vessel configuration, and key vessel parameters. The appendix is intended as a reference for all simulations presented in this thesis, and as a source of reliable and verified data for others working on CyberShip III.

Appendix B contains the plots generated on the basis of the results from WAMIT.

Appendix C contains the raw transcript from WAMIT. The units used in the transcript are intended for large vessels, tankers, AHTS, rigs, etc. so the interested reader may consult Chapter A.2 for values in SI units.

Appendix D contains the plots generated on the basis of the hull configurations and the hydrodynamic data acquired from WAMIT.

Appendix E contains the thruster combinator curves used during simulation and in the experiments.

Appendix F states some definitions on stability, that are of relevance to the control system designed in Chapter 11.

Appendix G contains the laboratory log, from the CyberShip III capability experiment at MCLab.

Appendix H contains the technical drawings of the wind generator rig, as well as a picture of the assembled wind generator.

Chapter 2

Preliminaries

2.1 Introduction

This chapter will give a brief introduction to notation used through out this thesis, in addition to some key mathematical concepts. For more thorough explanations, and additional reading on the mathematics presented, the interested reader may consult Fossen (2011a), Sørensen (2011), Vik (2011), Khalil (2002), Børhaug (2011), IMCA M140 (2012) or DNV (2011) (2011). The simulations and experiments conducted during this thesis are conduted on the scale model vessel CyberShip III. A brief overview of the vessel will therefor also be presented in this chapter.

2.2 Vessel Motion Variables

A marine vessel is moving in 6 *degrees-of-freedom* (DOF), and six independent coordinates are then required to determine the position and orientation, Fossen (2011a). In the case of a vessel, the six different motion components are defined as *surge, sway, heave, roll, pitch* and *yaw*, Fossen (2011a). The six different motion components are depicted in Figure 2.1.

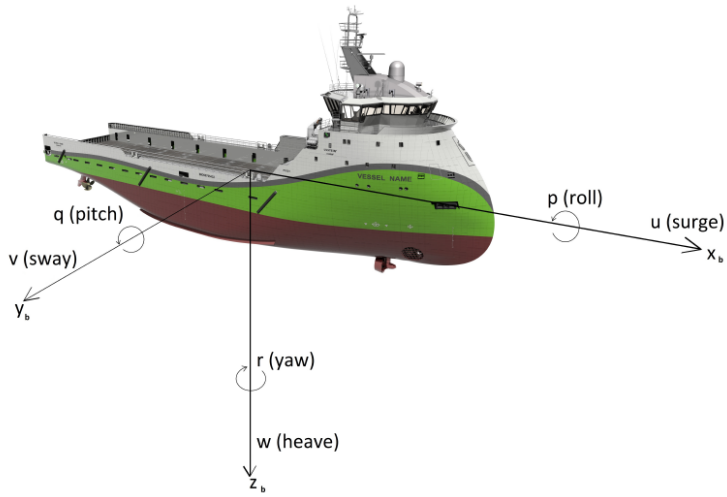

Figure 2.1: 6-DOF velocities u, v, w, p, q and r in the body-fixed coordinate system

This thesis will use the SNAME (1950) notation for marine vessels to give the position, orientation, and the corresponding velocities and accelerations of the vessel, as presented by Fossen (2011a). The notation is given in Table 2.1.

DOF		Forces and moments	Linear and angular velocities	Position and Euler Angles
1	motion in the x direction (surge)	X	u	x
2	motion in the y direction (sway)	Y	v	y
3	motion in the z direction (heave)	Z	w	z
4	rotation about the x axis (roll)	K	p	ϕ
5	rotation about the y axis (pitch)	M	q	θ
6	rotation about the z axis (yaw)	N	r	ψ

Table 2.1: SNAME (1950) notation

2.2.1 Vessel variables and dynamic positioning

In the case of DP control systems, all six motion variables are seldom used. Most DP systems operate in 3DOF; surge, sway and yaw. Some vessels also do roll stabilization, but such cases are outside the scope of this thesis. For simplicity, the DynCap and DPCap equations in this thesis will be presented in 3DOF, while the vessel simulator used for dynamic capability analysis in Part 2, will be in full 6DOF. The interested reader may consult Fossen (2011a), or Sørensen (2011) for additional reading.

2.2.2 Reference frames

Representation of marine vessels can be given in several different coordinate systems. These include Earth-center inertial (ECI) frame, Earth-center Earth-fixed (ECEF) , North, East, Down (NED) frame, and the body-fixed frame. The body fixed coordinate systems can be oriented in a variety of ways, i.e fixed in center of gravity (CO) , center of buoyancy (CB) or center of flotation (CF). In conjunction with DP control systems, the main coordinate systems to consider are the NED and body-fixed coordinate system.

North, East, Down frame The NED coordinate system is a coordinate system that is valid in a relative small area. It assumes flat earth, and is fixed to a point on the surface of the Earth. The x-axis points towards the true north and the y axis points to the east. According to the right hand rule, this result in the z axis pointing straight down, giving us {n} $o_n = (x_n, y_n, z_n)$. This is in many ways the coordinate system we relate to in our daily life, and is well suited for navigation in a relatively contained area, or stationkeeping.

Body-fixed frames

The body-fixed frame is a frame that move with some body, e.g the vessel. The location of the origin of the coordinate system may vary. The body-axis coordinate system, denoted body {b}, have the origin in the center of gravity, and the x-axis pointing straight forward, and the y-axis towards starboard. Following the right-hand-rule we get the z-axis down.

Additional Body frames Some additional body frames do exist, including several platform frames and instrument frames. The interested reader may consult Vik (2011) for additional reading.

2.2.3 Coordinate transformation

There are three basic method to represent one three dimensional coordinate system with respect to another, Euler angles, direct cosine and quaternions. In this thesis only Euler angles will be used, but the interested reader may consult Fossen (2011a), Sørensen (2011), Vik (2011) or Børhaug (2011), for additional reading on quaternions, and direct cosine.

The Euler angles are three angles introduced by Leonhard Euler to describe the orientation of a rigid body. In order to describe the orientation three parameters are required. Wikipedia (2011). The three parameters are the rotation about x (roll), y (pitch) and z (yaw), and we then have the following vector:

$$\Theta = [\phi, \theta, \psi]^T \tag{2.1}$$

The principal rotations for roll, pitch and yaw respectively, are then given by:

$$\begin{aligned} R_{x,\phi} &= \begin{bmatrix} 1 & 0 & 0 \\ 0 & \cos\phi & -\sin\phi \\ 0 & -\sin\phi & \cos\phi \end{bmatrix}, \quad R_{y,\theta} = \begin{bmatrix} \cos\theta & 0 & \sin\theta \\ 0 & 1 & 0 \\ -\sin\theta & 0 & \cos\theta \end{bmatrix} \\ R_{z,\psi} &= \begin{bmatrix} \cos\psi & -\sin\psi & 0 \\ \sin\psi & \cos\psi & 0 \\ 0 & 0 & 1 \end{bmatrix} \end{aligned} \tag{2.2}$$

The resulting rotation from the three angles can be expressed by multiplying the three matrices together. The order of which the matrices are multiplied does not change the result of the transformation as long as one stay true to one convention throughout the equations. Flowing the Euler angle representation the following multiplication is used:

$$R(\Theta) = R_{z,\psi} \cdot R_{y,\theta} \cdot R_{x,\phi} \tag{2.3}$$

resulting in the general form:

$$\boldsymbol{R}(\boldsymbol{\Theta}) = \begin{bmatrix} \cos\psi\cos\theta & -\sin\psi\cos\phi + \cos\psi\sin\theta\sin\phi & \sin\psi\sin\phi + \cos\psi\cos\phi\sin\theta \\ \sin\psi\cos\theta & \cos\psi\cos\phi + \sin\phi\sin\theta\sin\psi & -\cos\psi\sin\phi + \sin\theta\sin\psi\cos\phi \\ -\sin\theta & \cos\theta\sin\phi & \cos\theta\cos\phi \end{bmatrix} \tag{2.4}$$

The transformation matrix $\boldsymbol{T}_{\boldsymbol{\Theta}_{nb}}$ is given by Fossen (2011a):

$$\boldsymbol{T}_{\boldsymbol{\Theta}_{nb}} = \begin{bmatrix} 1 & \sin(\phi)\tan(\theta) & \cos\phi\tan\theta \\ 0 & \cos\phi & -\sin\phi \\ 0 & \frac{\sin\phi}{\cos(\theta)} & \frac{\cos\phi}{\cos\theta} \end{bmatrix} \tag{2.5}$$

By investigating the elements of the transformation matrix, we can clearly see that the transformation matrix, when using Euler angles, is singular. The singularity occur in pitch $\pm\frac{\pi}{2}$. The angles where the singularities are located is possible to move, but this method will always have singularities. In the case of marine vessels the singularity will not be problematic, as long as the singularities are placed in a non-plausible orientation of the vessel. It is usually safe to assume that the vessel will never have a pitch angle equal to $\pm\frac{\pi}{2}$, and this assumption will also be used throughout this thesis.

Remark 1. *When using Euler angles, $\boldsymbol{R}_{zyx}$, the resulting transformation matrix (2.5), will have singularity in $\pm\frac{\pi}{2}$ in pitch.*

2.3 CyberShip Overview

CyberShip III is a scale model of a 60 meter vessel. The vessel is equipped with three azimuth thrusters, one in the bow, and two in the stern. Figure 2.2 shows the general arrangement drawings of the CyberSea III vessel, where Table 2.2 shows the general arrangements table:

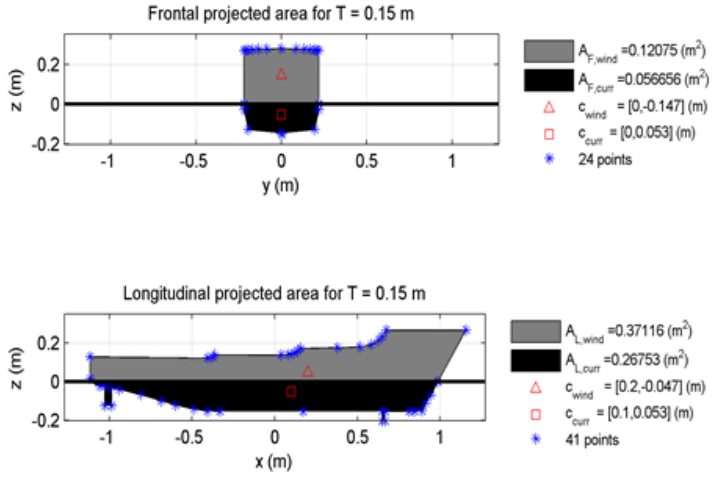

Figure 2.2: CyberShip III General Arrangement

Vessel name	CyberShip III
Vessel type	AHTS
Classification	DP 0
Dynamic positioning system	MC/BB
Power system	No main prime movers
	No auxiliary prime movers
	1 main generators
	No auxiliary generators
	1 switchboard
Propulsion and steering system	Bow Azimuth
	Port Pod
	Starboard Pod
Position reference systems	1 GPS
Other sensors	1 Gyro
	1 VRU

Table 2.2: CyberShip III General Arrangement

We note that the sensors listed are the sensors used during simulation, while the actual vessel get the equivalent data from an external measurement system, which will be described in detail in Chapter 11.

The main particulars of CyberShip III are summarized in Table 2.3. For detailed information on how this data was obtained, one may consult Appendix A.

Parameter	Description	WL1	Unit
Loa	Length over all	2.275	m
Lpp	Length between perpendiculars	1.971	m
B	Breadth	0.437	m
T	Draft	0.153	m
m	Mass	74.2	kg
V	Volume displacement	0.075	m3
C_B	Block coefficient	0.57	-
A_w	Water plane area	0.8	m2
GM_T	Transverse metacenter height	0.04	m
GM_L	Longitudinal metacenter height	2.75	m
Rii	Radii of gyration R44,R55,R66	[0.157,0.512,0.512]	m
LCG	Horizontal location of CG from AP	1.02	m
VCG	Vertical location of CG from baseline (KG)	0.20	m
r_CG	CG w.r.t to CO = [LPP/2 0 WL] in DWL (x-forward, z-down)	[0.04,0.0,-0.04]	m

Table 2.3: Main particulars of CyberShip III

Part I

Dynamic Stationkeeping Capability Analysis

Chapter 3

Concept of Capability Analysis

3.1 Introduction

In the 1960's the first Dynamic Positioning (DP) systems were developed. These systems were simple single-input single-output (SISO) PID controller, which built upon the existing heading autopilots. This combined system, capable of controlling a vessel in three horizontal planes (surge, sway and yaw), are today known as Dynamic Positioning systems. According to Sørensen (2011) we can define such a system as:

Definition 1. *Dynamic Positioning (DP) vessel is by the class societies e.g Det Norske Veritas (DNV), American Bureau of Shipping (ABS) and Lloyd's Register (LRS or Lloyd's), defined as a vessel that maintains its position and heading (fixed location or predetermined track) exclusively by means of active thrusters. This is obtained either by installing tunnel thrusters in addition to the main screw(s), or by using azimuthing thrusters, which can produce thrust in different directions. Sørensen (2011)*

A DP vessel is designed to keep the position of a vessel within certain excursion limits within a specified weather window, or so-called design environment, according to Sørensen (2011). In order to ensure that the vessel is capable of holding position within the defined excursion limits,

a capability analysis is necessary. The capability analysis can be done either statically, or dynamically by time-domain simulation. The latter is the subject of this thesis, and the upcoming chapters will present some key aspects related to a dynamic capability analysis. In this chapter the fundamental concepts of capability analysis will be explained, including current rules and guidelines associated with capability analysis. Chapter 4 will highlight some differences which can be expected when capability analysis is conducted by time-domain simulation, in favor of static capability analysis. This will then be followed by a short discussion of some challenges associated with todays most used capability analysis method, static capability analysis. Some concerns raised by several oil companies, ship owners and yards, in relation to todays capability methods, will also be presented.

3.2 DP Capability

The goal of a DP capability analysis is to calculate and predict the environmental limits, in which a DP vessel is capable of maintaining position and heading. The angle of which the sum of environmental forces act on the vessel are calculated for all 360 degrees, and according to the IMCA M149 specification for static capability analysis (DPCap), are to be presented in a polar coordinate plot. Figure 3.1 shows an example of such a plot.

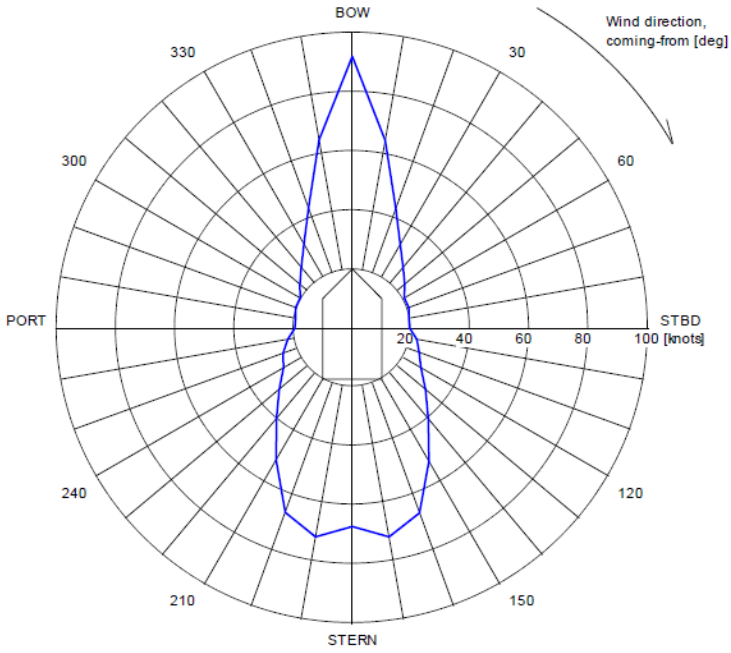

Figure 3.1: Example DPCap according to the IMCA M140 specifications

The above plot shows a typical *wind speed envelope* for a DP Vessel, computed by regular DPCap analysis. The limiting weather is computed by balancing the forces and moments acting on the vessel, which according to the IMCA M140 specifications are:

$$\boldsymbol{\tau_{Environment} + \tau_{Thrust} = 0} \tag{3.1}$$

The resulting limiting weather condition is obtained as a combination of a mean wind speed, significant wave height and a sea current speed. In compliance with the IMCA M140 spesifications for DPCap, the weather is taken as coming from the same direction. The polar plot we have in Figure 3.1 is often referred to as a DP capability envelope, or wind-envelope. This thesis will use the term *wind envelope*.

3.3 Todays DP Capability Standard

The standard used in the industry today is the International Marine Contractors Association (IMCA) M140 specifications for stationkeeping capability analysis. The IMCA M140 allows for the analysis to be computed with environmental forces from non-vessel-specific coefficients, thruster forces from rules-of-thumb coefficients, and without giving specifications on how to account for the DP control system, observer design nor differences and shortcomings of the thrust allocation, Pivano et al. (2012). It is possible to add additional components to the capability analysis, by adding more realistic assumptions and coefficients. The latter is though not a requirement in the IMCA M140 specifications, nor standardized how to be done. One may use actual vessel data recorded for wind, current, and wave-drift coefficients, realistic thruster models, and realistic static thrust allocation including e.g. forbidden zones and thrust loss effects based on actual allocated thrust, Pivano et al. (2012), but this is not the industry norm.

A considerable drawback of the relaxed requirements stated for how to calculate the DPCap, makes it difficult to compare DPCap results of different vessels. This also indicates that a considerable divination from the true vessel capability might exist, since one analysis method may use simple force balancing equations, while others may include thruster dynamics and time constants. E.g one may assume in the analysis that the azimuth thrusters may provide almost instantaneous bollard force in any direction, while as we will see in Part 2, this is not the case. This leads us to summarize that there might not be trivial to assess how realistic the results from the analysis are compared to the actual performance, nor to which extent two vessel DPCap plots can be compared.

A key simplification that the DPCap analysis does, in accordance with the IMCA M140, is that it typically reserves 15%-20% of the thrust to account for dynamic loads. This is often referred to as dynamic allowance. In Part 2 we will see how this may not be a realistic, nor a sufficient assumption in all cases.

We note that even if the regular DPCap may have some critical drawbacks, when the results are used during operation, and in weather conditions close to the limit, it might still be a very powerfull tool in the early stages of a design process. As a design verification and concept develop-

ment tool, one may argue that such an analysis may be adequate, since it is fast and relatively simple, and requires limited model knowledge. A looming question is still which effects the non-modeled dynamics have on the true environmental limits of the vessel. The latter question will be a returning question throughout this thesis.

3.4 Introduction to the Dynamic Capability Analysis

DynCap is an extension, and an improvement, of the regular DPCap, based on systematic time-domain simulations with a complete 6-DOF vessel model. For now we assume that this holds, without further elaboration. In Chapter 6 we will substantiate this claim, by investigating the mathematical relationship. DynCap do not aim to change the way in which the capability results are presented, or the need for the information, but rather present the environmental limits based on more substantiate and accurate data. In order to do so, an accurate and sophisticated vessel model is needed. In this thesis the Marine Cybernetics AS DP-HiL vessel simulator, CyberSea, has bin utilized to simulate the vessel dynamics. The author is not at liberty to disclose all the details associated with inner workings of the CyberSea simulator, but the basic structure is given in Figure 3.2, Pivano et al. (2012):

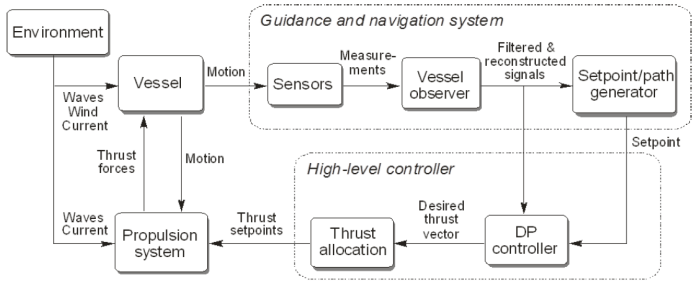

Figure 3.2: Basic structure of the vessel simulator

In contrast to the regular DPCap, the vessel is in DynCap allowed to move. One may argue that one of the strongest assumptions of the regular

DPCap, the vessel does not move, has been removed. In addition we note that we do not need to assume a certain amount of thrust reserved for dynamic loads as for the traditional DPCap, according to Pivano et al. (2012), since the dynamics now are included in the analysis. We also note how the environmental forces acting on the vessel now also are a function of varying heading. It is to be expected that even a DP vessel which experiences environmental forces, will not be able to have a heading error equal to zero for all time. The impact of small heading divinations during a DPCap analysis, may severely effect the results. Consider a large offshore vessels or freighter, a small change in heading, e.g 1-3 degrees, may result in a significant increase in projected wind and current area, dependent upon the shape of the vessel. In addition the introduction of the simulator depicted in Figure 3.2, we also see that it allows the employment of dynamic wind and current loads, 1st and 2nd order wave loads including slowly-varying wave drift, dynamics of the propulsion system and power system, according to Pivano et al. (2012).

Finally we note that complete DP control system model is also included, with observers, DP controller and thrust allocation, sensors, and position reference systems. The performance of the DP controller, thrust allocation, sensor system and observers then become a part of the analysis. This might introduce time constants and transient time, which we in Part 2, will see have a significant impact on the final result, compared to regular DPCap. In addition the introduction of a power system, and a detailed propulsion system, enables the possibility of investigating actuator rate limits and computation of dynamic thrust loss effects such as the interaction between thrusters, interaction between thrusters and hull, ventilation, out-of-water effects, and transversal losses, Pivano et al. (2012).

3.5 Acceptance Criteria

DPCap define the limit based upon balancing the forces acting on the hull. A benefit of the dynamic approach, is that one may specify some set of acceptance criteria. According to Pivano et al. (2012), one may define the position and heading excursion limits, to allow a wide or narrow footprint, or the acceptance criteria can be based on other vessel performance e.g.

sea keeping, motion of a crane tip or other critical point, or dynamic power load. By defining different acceptance criteria, one may be able to tailor the analysis to investigate the performance of the vessel under the operation in which the vessel is supposed to undertake. In this way one may argue that the DynCap can increase the safety for personnel and equipment during operation, compared to regular DPCap analysis.

In Figure 3.3 one may see an example of position and heading acceptance criteria. In the analysis in Figure 3.3 the wind envelope plot is found by increasing the wind speed, while investigating if the vessel footprint and heading fulfills the predefined position and heading limits.

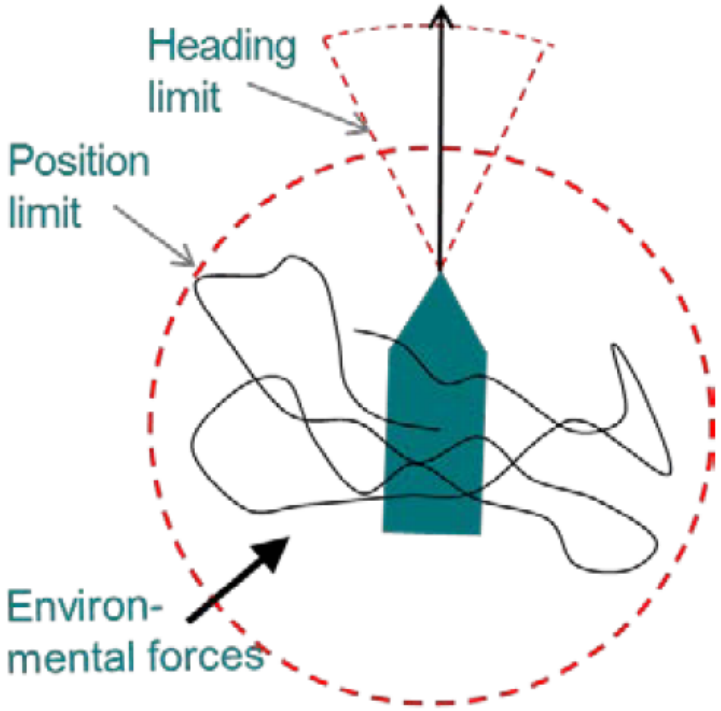

Figure 3.3: Example of wind envelope, with acceptance criteria

Chapter 4

Comparison Between DPCap and DynCap

4.1 Introduction

In the previous chapter an introduction to the concept of DynCap was given. In this chapter we want to additionally motivate, and highlight the possible benefits of the results from a time-domain simulation in comparison to a static capability analysis. The results from a DPCap and DynCap analysis performed by the R&D department at Marine Cybernetics AS, will be presented to investigate the differences. According to Pivano et al. (2012) the goal of the project was to aid development, and verify the design of a Direct Shuttle Loading (DSL), from a storage platform, using a innovative offshore loading shuttle. The offload shuttle vessel utilized a stern loading concept, in contrast to the more conventional bow loading method. Figure 4.1 shows a model of the shuttle tanker.

Figure 4.1: Model of the Offloading Shuttle tanker

4.2 Offloading Shuttle Tanker DynCap and DP-Cap

Consider the key vessel parameter given in Table 4.1, for the Offloading Shuttle tanker.

Description	Unit	Value
Loading condition name	-	Loaded SG=0.94, Departure
Length overall	m	215.7
Length between perpendiculars	m	200
Breadth	m	38
Draught	m	11.6
Mass displacement	tons	73140

Table 4.1: Offloading Shuttle tanker parameters

Figure 4.2 shows the resulting DPCap plot, Pivano et al. (2012).

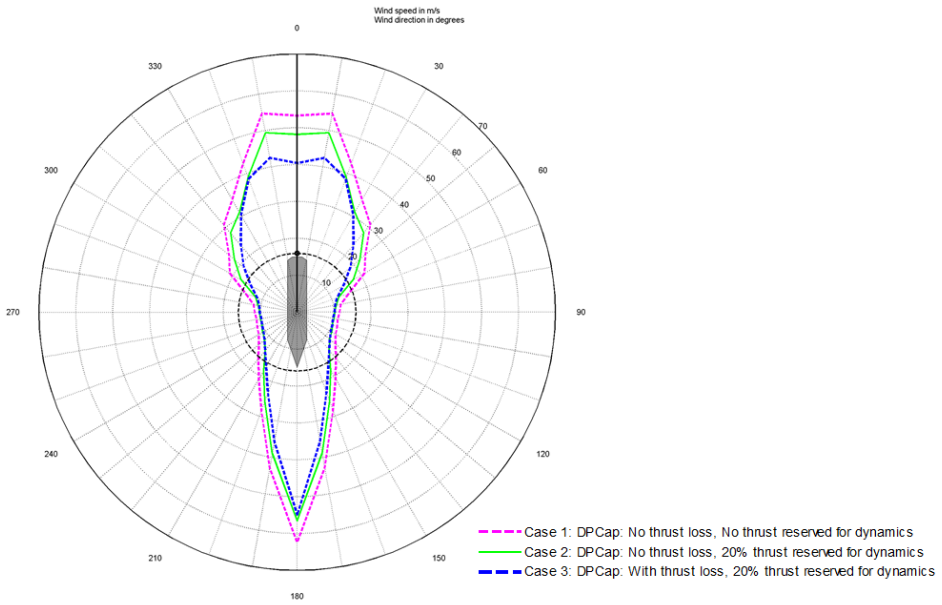

Figure 4.2: Offloading Shuttle Tanker DPCap

The outermost curves in Figure 4.2 was obtained without the inclusion of thrust loss, and with no thrust reserved for dynamic loads. Considering a typical offloading operation where the vessel would try to minimize the environmental forces by placing the stern against the environmental loads, the plot shows that the vessel would be able to maintain position with wind of about 54 m/s (0 deg of angle of attack), according to Pivano et al. (2012). This limiting wind speed corresponds to a significant wave height (Hs) of 28 m. The results where shown to an experienced Captain, which stated that from his experience this limiting weather appears too large, compared to a real vessel's capability. Further we observe how the limiting weather, when coming from 90 deg, indicate a limit of 13 m/s. This is to be expected, since the projected area on the vessel is much larger, which then results in a significant larger environmental force acting on the vessel.

The green line in the plot, shows the wind envelope, obtained by including 20% reservation of thrust, to account for dynamics. We then can see that the limiting wind speeds are smaller, which are to be expected. Further we have that by including in DPCap both the thrust losses and

the reserved thrust for dynamic loads the capability is further reduced as shown with the dashed blue line, according to Pivano et al. (2012).

By defining two acceptance criteria, 15m/10deg limit and 5m/3deg limit, and introducing DynCap simulation, we according to Pivano et al. (2012) get the results shown in Figure 4.3.

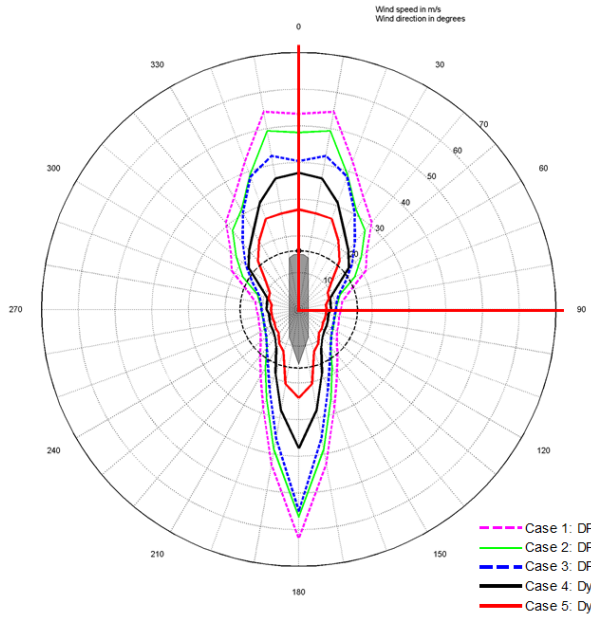

Limit wind speed [m/s]

Case	0 deg	90 deg
1	54	13
2	48	11
3	40	10
4	37	8
5	27	7

Figure 4.3: Offloading Shuttle Tanker DPCap and DynCap results

Figure 4.3 shows wind envelope plot, obtained from both the DPCap and the DynCap with different settings. The black line represents the wind envelope obtained through simulation with acceptancs criteria 15m/3deg, where the red line represents the 5m/3deg limitation.

From the results presented in Figure 4.3, we can conclude that two approaches, static and dynamic, in this case, depicts a substantial difference in the vessel stationkeeping capability. The results obtained with the traditional analysis appear to be too optimistic while the results computed with DynCap look more restrictive. At the same time one may question to what extent the DynCap depicts the true performance, which will be addressed in Part 2 of this thesis.

Investigating the logs from the experiment conducted at Marine Cybernetics, the large difference for wind directions coming from 0 can be explained by the fact that DynCap finds the limiting environmental conditions through simulations. By investigating the thrust allocation, when closing in on the limiting condition, the environmental forces towards the stern give significant heading motion due to the difference in frontal and side vessel areas. The bow thrusters struggle to control the heading, switching between maximum positive to maximum negative force, according to Pivano et al. (2012). This indicates that the dynamics of the thruster might not have been accounted for in a satisfying way in the DPCap.

Due to the relaxed requirements of the IMCA M140 specifications, in particular in conjunction with the effect of the dynamics to be included in the analysis, it may be of particular interest to investigate case 1 vs case 5. We note that the capability of the vessel in case 5, is exactly half of the capability in case 1, at the 0 degree heading environmental direction. Based upon the difference between case 1 and 5, one may state that the security risk during operation, is considerable, or even alarming, if the DynCap can be verified to even be close to the true capability of the vessel.

One may argue that, case 3 is a more common DPCap analysis, or the availability of all three, but the difference between the results are still noticeable, and could constitute a considerable risk to the environment, personnel and equipment on board the vessel. From the presented results, one may argue not only for the need for the time-domain simulation in conjunction with DP capability analysis, but also a review of the specifications of the IMCA M140 specifications used today.

4.3 Summerizing the DynCap and DPCap Differences

Based on the results presented in the previous section and according to Pivano et al. (2012), we can summerize the DPCap and the DynCap according to Table 4.2.

Property	DPCap	DynCap
Balance between environmental and thruster forces	Static	Dynamic
Dynamic environmental loads	Statistical considerations may be included	Included
Vessel position	Fixed: No dynamic vessel response	Free floating
Thruster capacity	Uses 80-85% of the thruster capacity - dynamic allowance of 15-20%	All available thruster capacity utilized
Thruster and rudder dynamics	Not included	Included
Thruster losses	Static losses may be included	Dynamic losses included
DP system	Dynamics of the DP system is not accounted for	DP controller, DP observer and thrust allocation included
External loads	Static may be included	Dynamic loads may be included
Transient effects	Not included	Included
Computational requirements	Low	High
Model complexity	Low to Medium	High
Flexibility	Low	High

Table 4.2: Summery of the DPCap and DynCap

We note that the computational requirements of the DynCap is stated to be high. This is a combination of the complexity needed, but also the duration of the simulation. The duration of the simulation need to be long, in order to ensure the accuracy of the result, an to account for peak fluctuations in the environmental forces.

4.4 Reflections on Industry Challenges and Concerns

In the light of material presented in the past chapters, it might be reasonable to question whether or not the IMCA M140 specification is to basic. In particular it might be reasonable to question whether or not the environmental forces from estimation methods are an accurate enough method

to calculate the capability of a vessel. Further the IMCA M140 state that thruster forces are to be calculated based on generic rules-of-thumb. In addition the effect of the thrust allocation algorithms are not accounted for in the IMCA M140 spesifications for DP capability analysis.

One might want to argue that it is possible to extend DPCap with more realistic assumptions and parameters. One problem related to this statement is that the extensions are not standardized, which apply for both DPCap and DynCap. In a competitive marked, where the vessels capability can determine whether or not a vessel owner will get a contract, such non-required extensions might not be a desirable option for a vessel owner, if the results indicate a decrease in capability, even if the improved method might be closer to the true capability. We then see that a possible conflict of interest is emerging, which not only effect the DPCap, but the DynCap as well. By including the actual vessel model data, like wind, current and wavedrift coefficients, realistic thruster models, and realistic thruster allocation, including e.g. forbidden zones etc., one may arrive at a point where the capability plots, static and dynamic, are closer to the true capability. In order for the latter to be the industry norm, it is likely that the class society must tighten the regulations concerning DP capability analysis, static as well as dynamic.

Summarizing the stated claims and questions above, we arrive at the motivation for the further investigation into capability analysis, and the accuracy of the analysis methods. According to Pivano et al. (2012), the open issues often addressed by operators, vessel owners, oil companies and ship yards are: How much can we trust the results from the traditional capability analysis? Do they convey a realistic picture of a vessel's station-keeping capability in dynamic operating conditions? Are they conservative or optimistic? By further examining the capability analysis methods, this thesis aims to shed some light on these issues, and to some extent answer the questions.

Chapter 5

Static Capability Analysis in Compliance with IMCA M140

According to IMCA, the main reason for the development of the IMCA M140 specifications, is to ensure a standardization in the production of capability plots for DP vessels. According to IMCA M140 (2012), by the use of the IMCA M140 standardization, one will be able to make direct comparisons of individual vessel's performances and provide an indication of stationkeeping ability in a common format. This chapter will present how such an analysis should be conducted, and the mathematical equations needed to compute the capability plots for any DP vessel.

5.1 Environmental Forces

The IMCA M140 spesifications, state the forces which must be considered in order to calculate the environmental limits of the vessel in question. According to IMCA M140 (2012), the end objective is to be able to solve the following equation:

$$\boldsymbol{\tau_{Env}} + \boldsymbol{\tau_{Alloc_{optimal}}} = 0 \tag{5.1}$$

where $\boldsymbol{\tau_{Alloc_{optimal}}}$ is available optimal allocated force from the thrusters. $\boldsymbol{\tau_{env}}$ is the environmental forces, and according to IMCA M140 (2012), the following environmental forces are to be considered:

- wind forces
- wave forces
- current forces

5.1.1 Wind forces

According to IMCA M140, the wind forces can be calculated as follows:

$$F_{wx}(hull) = \frac{1}{2}\rho v_w^2 C_{wx}(\alpha_w) A_T(hull) \tag{5.2}$$

$$F_{wy}(hull) = \frac{1}{2}\rho v_w^2 C_{wy}(\alpha_w) A_L(hull) \tag{5.3}$$

$$F_{wn}(hull) = \frac{1}{2}\rho v_w^2 C_{wn}(\alpha_w) A_L(hull) L_{pp} \tag{5.4}$$

where we have that

$$\begin{aligned}
F_{wx}(hull) &= \text{wind force in surge [kN]} \\
F_{wy}(hull) &= \text{wind force in sway [kN]} \\
F_{wn}(hull) &= \text{wind force in yaw [kNm]} \\
\alpha_w &= \text{wind direction [deg]} \\
C_{wx}, C_{wy}, C_{wn} &= \text{hull wind coefficients for given wind directions} \\
\rho &= \text{density of air (1.23 x 10-3) [t/}m^3\text{]} \\
v_w &= \text{wind speed} \\
A_T &= \text{transverse wind area of hull } [m^2] \\
A_L &= \text{longitudinal wind area of hull } [m^2] \\
L_{pp} &= \text{Length between perpendiculars [m]}
\end{aligned} \tag{5.5}$$

The IMCA M140 specifications do not specify any requirements for the method used to obtain the wind force coefficients, but it does propose that

they might be calculated as follows:

$$C_{wx}(\alpha_w) = 0.423\cos(\alpha_w) \tag{5.6}$$
$$C_{wy}(\alpha_w) = 0.8\sin(\alpha_w) \tag{5.7}$$
$$C_{wn}(\alpha_w) = -0.143\sin(2\alpha_w) \tag{5.8}$$

We note that if the wind force coefficients are calculated as proposed in equation (5.6), (5.7) and (5.8), the vessel is considered completely symmetrical in terms of the projected area. This is seldom the case, except for box shaped vessels.

The IMCA M140 specifications state that the wind forces on the superstructure are to be calculated by the use of the API method, which results in each force component of the superstructure is given by a projected longitudinal and transverse area, a shape coefficient and a height coefficient, according to IMCA M140 (2012). The wind force on each component is then found to be given on the form:

$$F_{wx}(ss) = C_w(C_sC_hA_T(ss))v_w^2 \tag{5.9}$$
$$F_{wy}(ss) = C_w(C_sC_hA_L(ss))v_w^2 \tag{5.10}$$

where

C_w = API wind coefficient (0.615 x 10-3 to give force in kN)
C_s = shape coefficient
C_h = height coefficient
$C_T(ss)$ = superstructure transverse projected area $[m^2]$
$C_L(ss)$ = superstructure longitudinal projected area $[m^2]$

According to IMCA M140 (2012), the wind moment component on the superstructure, is calculated by multiplying the total transverse superstructure force by the distance of the centroid of the total transverse superstructure area from midships. This yields the following expression

$$F_{wn}(ss) = F_{wy}(ss)X_{wc} \tag{5.11}$$

where

X_{wc} = distance between centroid of total transverse superstructure area from midships [m]

Further we then find that for intermediate headings, between 0-90, can be obtained by the API interpolation procedure, which according to IMCA M140 (2012), which suggests that:

$$F_w(\alpha_w) = F_{wy}(90)\left[\frac{2\sin^2(\alpha_w)}{1+\sin^2(\alpha_w)}\right] + F_{wx}(0)\left[\frac{2\cos^2(\alpha_w)}{1+\cos^2(\alpha_w)}\right] \quad (5.12)$$

where we have that

$$\begin{aligned} \alpha_w &= \text{wind heading angle [deg]} \\ F_w(\alpha_w) &= \text{resultant wind force at heading angle } \alpha_w \text{ [kN]} \\ F_wy(90) &= \text{wind force in sway [kN]} \\ F_wx(0) &= \text{wind force in surge [kN]} \end{aligned}$$

According to the IMCA M140 specifications, we then have that the longitudinal and transverse components at the heading angle α_w are obtained by resolving the resultant

$$F_{wx}(\alpha_w) = F_w(\alpha)\cos(\alpha_w) \quad (5.13)$$
$$F_{wy}(\alpha_w) = F_w(\alpha)\sin(\alpha_w) \quad (5.14)$$

which finally yields that the wind yaw moment on the superstructure, at intermediate heading angles α_w, is given by:

$$F_{wn}(\alpha_w) = F_{wy}(\alpha_w)X_{wc} \quad (5.15)$$

where X_{wc} becomes the leaver arm. It is also to be noted that the wind speed should be the one minute mean, at a height of 10m. The reason for the use of the one minute mean, is to account for some of the wind gusts. According to IMCA M140 (2012) the one minute mean can be approximated to about 1.12-1.17 times the hourly mean. It is to be noted that this approximation might be subject to discussions, since different locations, might have very different wind characteristics, which might have a profound effect on the results.

5.1.2 Wave drift forces

According to IMCA M140 (2012), the mean wind drift force used in DP-Cap, can be calculated as follows

$$\omega' = \omega\sqrt{\frac{V^{\frac{1}{3}}}{g}} \tag{5.16}$$

where we have that

$$\begin{aligned} \omega &= \text{dimensional frequency } \left[\frac{rads}{sec}\right] \\ V &= \text{volume of displacement } [m^3] \\ g &= \text{acceleration of gravity } \left[\frac{m}{s^2}\right] \end{aligned}$$

According to IMCA M140 (2012), we have that the surge and sway forces, as a consequence of wave drift, are given by

$$F_{wvx} = \frac{1}{2}C_{wvx}g\rho a^2 V^{\frac{1}{3}} \tag{5.17}$$

$$F_{wvy} = \frac{1}{2}C_{wvy}g\rho a^2 V^{\frac{1}{3}} \tag{5.18}$$

where

$$\begin{aligned} a &= \text{wave amplitude [m]} \\ \rho &= \text{density of water } \left[\frac{t}{m^3}\right] \\ C_{wvx} &= \text{non-dimensional regular wave drift force coefficient } \left[\frac{kN}{m^2}\right] \\ C_{wvy} &= \text{non-dimensional regular wave drift force coefficient } \left[\frac{kN}{m^2}\right] \end{aligned}$$

We further have that the yaw moment, due to wave drift is given by

$$F_{wvn} = \frac{1}{2}C_{wvn}g\rho a^2 V^{\frac{2}{3}} \tag{5.19}$$

where C_{wvxn} is the non-dimensional regular wave drift force coefficient. We note that the coefficients are not explicitly defined, nor does the IMCA M140 state how they are to be calculated. This gives room for interpretation, and may contribute to limit the possibility of comparing plots calculated on the basis of the IMCA M140.

5.1.3 Current Forces

According to IMCA M140 (2012) the current forces are given by

$$F_{cx} = \frac{1}{2}\rho v_c^2 C_{cx}(\alpha_c) BT \tag{5.20}$$

$$F_{cy} = \frac{1}{2}\rho v_c^2 C_{cy}(\alpha_c) L_p pT \tag{5.21}$$

$$F_{cn} = \frac{1}{2}\rho v_c^2 C_{cn}(\alpha_c) L_p p^2 T \tag{5.22}$$

where we have that

$$\begin{aligned} \alpha_c &= \text{current direction [deg]} \\ C_{cx}, C_{cy}, C_{cn} &= \text{hull current coefficients given for current directions} \\ \rho &= \text{density of sea water } \frac{t}{m^3} \\ v_c &= \text{current speed } \left[\frac{m}{s}\right] \\ T &= \text{vessel draft [m]} \\ B &= \text{vessel beam [m]} \end{aligned}$$

Again we find that the method of obtaining the coefficients are not stated, and it is advised to use coefficients from similar vessels.

5.2 DPCap Equation

We now arrive at the point where we are able to state the complete equation to solve, in order to obtain the DPCap results

$$\mathbf{0} = \boldsymbol{\tau}_{\boldsymbol{Alloc}_{\boldsymbol{optimal}}} + \boldsymbol{\tau}_{\boldsymbol{Env}} \tag{5.23}$$

$$\mathbf{0} = \boldsymbol{\tau}_{\boldsymbol{Alloc}_{\boldsymbol{optimal}}} + \boldsymbol{\tau}_{\boldsymbol{wind}} + \boldsymbol{\tau}_{\boldsymbol{wave}} + \boldsymbol{\tau}_{\boldsymbol{current}} \tag{5.24}$$

where

$$\boldsymbol{\tau_{wind}} = \begin{bmatrix} F_{wx} + F_{wx}(hull) \\ F_{wy} + F_{wy}(hull) \\ F_{wn} + F_{wn}(hull) \end{bmatrix} \tag{5.25}$$

$$\boldsymbol{\tau_{wave}} = \begin{bmatrix} F_{wvx} \\ F_{wvy} \\ F_{wvn} \end{bmatrix} \tag{5.26}$$

$$\boldsymbol{\tau_{current}} = \begin{bmatrix} F_{cx} \\ F_{cy} \\ F_{cn} \end{bmatrix} \tag{5.27}$$

By defining

$$\alpha_w = \alpha_{wv} = \alpha_c \tag{5.28}$$

and by conducting a line search, where the wind speed, and corresponding wave height are changed, one can be able to find the limit where the $\boldsymbol{\tau_{Alloc_{optimal}}}$ satisfies (5.23). It is also recommended that the available thrust should be limited to 80-85% of the available thrust, to account for the dynamics. In the next chapter, we will investigate the mathematical equations of DynCap, and compare which effects the differences will have on the calculated limits.

Chapter 6

Dynamic Capability Analysis

In Chapter 5 the mathematical foundation of DPCap was presented. In this chapter we will see that it is possible to extend the DPCap equations to the point where they become the DynCap equations. We will see that by applying the key simplifications of the IMCA M140 to the DynCap equations, they become the DPCap equations. In addition the fundamental difference between the equations of DPCap and DynCap will be introduced, the addition of the dynamics. For simplicity, the equations will be presented in 3 DOF, but it is worth noticing that in the simulations done in Part 2, a full 6-DOF-vessel model was used. It is also to be noted that the CyberSea vessel simulator, used to create the dynamics, differ to some extent from the explanations in this chapter. This chapter only aims to highlight core mathematics behind the DynCap analysis.

6.1 Deriving the DynCap equations

Consider the following equation of motion of a vessel i water, which according to Fossen (2011a) is the governing model for vessels in water:

$$\dot{\boldsymbol{\eta}} = \boldsymbol{J}(\boldsymbol{\eta})\boldsymbol{\nu} \tag{6.1}$$

$$\boldsymbol{M}(\boldsymbol{\nu},\boldsymbol{\omega})\dot{\boldsymbol{\nu}} + \boldsymbol{C}(\boldsymbol{\nu},\boldsymbol{\omega})\boldsymbol{\nu} + \boldsymbol{D}(\boldsymbol{\nu}) + \boldsymbol{g}(\boldsymbol{\eta}) = \boldsymbol{\tau}_{Thrust} + \boldsymbol{\tau}_{Env} \tag{6.2}$$

where $\boldsymbol{\eta} \in \mathbb{R}^3$, and is given by $\boldsymbol{\eta} = [x\ y\ \psi]^T$. Further we have that $\boldsymbol{\tau_{Thrust}} \in \mathbb{R}^3$ and $\boldsymbol{\tau_{Env}} \in \mathbb{R}^3$. According to Fossen (2011a), we have that $\boldsymbol{J(\eta)}$ is the kinematic transformation matrix. Further we have $\boldsymbol{M(\nu, \omega)} = \boldsymbol{M_{RB}(\nu)} + \boldsymbol{M_A}(\omega)$, where $\boldsymbol{M_{RB}}$ is the rigid body and inertia matrix, and $\boldsymbol{M_A}$ is the frequency dependent added mass matrix. We have that $\boldsymbol{C(\eta, \omega)} = \boldsymbol{C_{RB}(\eta)} + \boldsymbol{C_A}(\omega)$, where $\boldsymbol{C_{RB}(\eta)}$ is rigid body Coriolis and centripetal matrix, and $\boldsymbol{C_A}(\omega)$ is the frequency dependent added Coriolis and centripetal matrix. We have that $\boldsymbol{D(\nu)} = \boldsymbol{D_L\nu} + \boldsymbol{d_{NL}(\nu, \gamma)}$, which are the linear and non-linear damping respectively. γ is the relative drag angle. The term $\boldsymbol{g(\eta)}$ accounts for gravity and buoyancy. The interested reader may consult Fossen (2011a) for additional details on how to compute the individual matrices.

According to Fossen (2011a), in the case of stationkeeping, both the added mass and the added Coriolis and centripetal matrix, get evaluated at the infinity frequency, which also give that the fluid memory effect, $\boldsymbol{\mu}$, must be added as a separate component. $\boldsymbol{\mu}$ according to Fossen (2011a) take the form

$$\boldsymbol{\mu}(\eta) = \int_0^\infty \boldsymbol{K}(t-\tau)[\boldsymbol{\eta(\tau)} - U\boldsymbol{e}_1]\ d\tau \tag{6.3}$$

which gives us

$$\boldsymbol{M(\nu)\dot{\nu} + C(\nu)\nu + D(\nu) + g(\eta) + \mu(\eta)} \quad = \quad \boldsymbol{\tau_{Thrust} + \tau_{Env}} \tag{6.4}$$

We have that $\boldsymbol{\tau_{Thrust}}$ represents the actual thrust force, and can be considered as a function $\boldsymbol{\tau_{Thrust}}(\nu.\dot{\nu}, \mu, ..)$, where the forces involved can be approximated as,

$$\boldsymbol{\tau_{Thrust}(\nu, \dot{\nu}, \mu) = \tau_{Alloc}\beta(\nu, \dot{\nu}, \mu)} \tag{6.5}$$

where $\boldsymbol{\beta} \in \mathbb{R}^3$, is the loss factor, accounting for i.a the coanda effect, thruster-thruster and thruster-rudder interaction, propeller spin etc. For now we assume that the $\boldsymbol{\tau_{Alloc}}$ can be take the following form

$$\boldsymbol{\tau_{Alloc} = B(\alpha)T} \tag{6.6}$$

where B is the orientation matrix, and the solution is found by solving a optimization problem, which take the general form as

$$\boldsymbol{g} = min(\boldsymbol{J, \alpha, T, l_{bX}, u_{bX}}) \tag{6.7}$$

where $\boldsymbol{J}$ is the cost function, $\boldsymbol{\alpha}$ and $\boldsymbol{T}$ are the optimizing parameters, and $\boldsymbol{l_{bX}}$ and $\boldsymbol{u_{bX}}$ are nonlinear constraints. The interested reader may consult Fossen (2011a) or Sørensen (2011) for additional reading on thrust allocation.

Further we note that the desired $\boldsymbol{\tau_{DP}}$ provided by the DP system to the thrust allocation algorithm, is not calculated on the basis of solving this (6.4), but a result of the DP controller, where the environmental forces, have to be estimated, and where the environmental forces are estimated. In addition the control system does not have the exact vessel parameters, but the best available estimation. The combination of simplifications in the control system, unknown environmental forces, and biases, give that one may assume that no controller will be able to provide a thrust $\tau_{desired}$, which would result in exactly $\boldsymbol{\nu} = \boldsymbol{\eta} = \mathbf{0}\ \forall t$ in reality. Small deviations will occur, and in harsh weather, this deviations may be considerable.

By allowing allowing $\boldsymbol{\eta} \neq \mathbf{0}$, but within a defined acceptance criteria, and investigating (6.4) by time domain simulation, with increasing $\boldsymbol{\tau_{env}}$, we have arrived at the DynCap method. We then may then consider (6.4) to be seen as the fundamental equation of dynamic capability analysis.

6.2 Extending DPCap to Become DynCap

To show mathematical relationship between (6.4) of the DPCap equation, and DynCap, we start by defining the same assumptions as in DPCap, and state that $\boldsymbol{\nu} = \mathbf{0}$, and $\boldsymbol{\eta} = \mathbf{0}$, as well as no thruster losses. We assume $\boldsymbol{\beta} = \boldsymbol{I}$. We then see that we have

$$\boldsymbol{M(0)0} + \boldsymbol{C(0)0} + \boldsymbol{C_A}(zero)\mathbf{0} + (\boldsymbol{D} + \boldsymbol{D(0)})\mathbf{0} + \boldsymbol{g(0)} + \boldsymbol{\mu} \quad = \quad \boldsymbol{\tau_{Thrust}} + \boldsymbol{\tau_{Env}} \tag{6.8}$$

where

$$\boldsymbol{\mu} = \int_0^\infty \boldsymbol{K}(t-\tau)[\boldsymbol{eta(\tau)} - U\boldsymbol{e}_1]\ d\tau = \mathbf{0} \tag{6.9}$$

By assuming no thruster dynamics, and optimal allocated forces, $\boldsymbol{\tau_{Thrust}} = \boldsymbol{\tau_{Alloc_{Optima}}}$, we arrive at

$$\mathbf{0} \quad = \quad \boldsymbol{\tau_{Alloc_{Optimal}}} + \boldsymbol{\tau_{Env}} \tag{6.10}$$

We now see that the dynamic capability equation, have become the (5.1), which is the fundamental DPCap equation. This show that DynCap may

be considered as an extension, or a development of the DPCap. There is also to be noted that we now assume the environmental forces are a constant, which is not the case in DynCap.

Reflecting on the relationship between the DPCap equation, (5.1), and the DynCap equation, (6.4), one may consider the DynCap as the natural development in capability analysis. One may consider DynCap to have followed the development of theory on dynamic systems, as well as the development in computer science, while the DPCap has remained where it started. In that light, one may say that DynCap is the next generation of DPCap analysis.

Part 1 of this thesis have stated several claims, without the necessary validation, nor the necessary mathematical proof in the strictest form. It has been assumed that (6.4), represent a close approximation of the true dynamics of a vessel. One may argue that (6.4) is widely used within modeling of marine vessel, according to Fossen (2011a), but any conclusions can not be drawn on that statement alone. In order to further support the claims of DynCap being a superior method for computing the capability of a vessel further investigation is needed. In order to contribute to this investigation, Part 2 will now conduct a DPCap analysis, in compliance with IMCA M140, a DynCap analysis according to Marine Cybernetics AS internal guidelines, and finally an experiment, which aims to acquire the true capability of the vessel used in the two analysis methods. The author then aim to substantiate the claims of DynCap being a more accurate method for determining the capability of a vessel, as well as being able validate the DynCap analysis as a method for determining a vessels stationkeeping capability.

Part II

Capability Analysis and Experimental Validation

Chapter 7

DP Capability Analysis

The first part of this thesis gave a strong motivation for investigating alternative ways of computing a vessels stationkeeping capability. In addition the mathematical foundation for the industry standard, DPCap, and the DynCap method were presented. We now want to further investigate both the differences between DPCap and DynCap, and in particular investigate the accuracy of the DynCap analysis, opposed to the DPCap analysis. To do so, we will now conduct a DPCap analysis, a DynCap analysis, and finally an experiment which seeks to obtain the true capability of the vessel subject to the analysis.

Chapter 7 will present the DPCap analysis of CyberShip III. The analysis was conducted in compliance with the IMCA M140 specifications. An analysis where no thrust is reserved for dynamics will be presented, as well as one where 20% thrust is reserved to account for the dynamics. Chapter 8 will then present the simulator used to conduct the DynCap analysis, in addition to the key configurations used. Chapter 9 will present a series of tests, conducted to strengthen the credibility of both the simulator and the configurations used during simulations. Chapter 10 will present the DynCap analysis and result. Finally Chapter 11 will present the experiment conducted, and the result obtained. A detailed discussion of the result will then follow.

7.1 Prerequisites and Assumptions

The DPCap analysis conducted of CyberShip III was performed in compliance with the IMCA M140 specifications. During the analysis the environmental loads were set to be collinear, i.e wind and waves from the same direction. The current is not considered in the analysis, since current was not available at the laboratory used to obtain the true stationkeeping capability of CyberShp III, as described in Chapter 11. The wind to wave relationship was taken from the IMCA M140 specification, valid for the North Sea.

The analysis was conducted on the CyberShip III vessel with scaled wind and waves, according to BIS scale, where the scaling factor is $\lambda = 30$, consult Fossen (2011a) for details. The results will be presented in full scale, to make the results more comparable to other wind envelop plots.

7.2 DPCap Analysis of CyberSip III

We start by recalling (5.1):

$$\boldsymbol{\tau_{Env}} + \boldsymbol{\tau_{Alloc_{optimal}}} = 0 \tag{7.1}$$

where $\boldsymbol{\tau_{Alloc_{optimal}}}$ is the actual thrust outputted by the thrusters, where the thrust is optimally allocated to counteract the environmental forces. Further $\boldsymbol{\tau_{Env}}$ represents the environmental forces, which now is given by

$$\boldsymbol{\tau_{Env}} = \boldsymbol{F_{wind}} + \boldsymbol{F_{wave}} \tag{7.2}$$

The wind and wave drift force is calculated according to:

$$F_{wind} = \begin{bmatrix} \frac{1}{2}\rho_a v_w^2 C_{wx}(\alpha_w) A_T(hull) \\ \frac{1}{2}\rho_a v_w^2 C_{wy}(\alpha_w) A_L(hull) \\ \frac{1}{2}\rho_a v_w^2 C_{wn}(\alpha_w) A_L(hull) L_{pp} \end{bmatrix} \tag{7.3}$$

$$F_{wave} = \begin{bmatrix} \frac{1}{2} C_{wvx} g \rho_w a^2 V^{\frac{1}{3}} \\ \frac{1}{2} C_{wvy} g \rho_w a^2 V^{\frac{1}{3}} \\ \frac{1}{2} C_{wvn} g \rho_w a^2 V^{\frac{2}{3}} \end{bmatrix} \tag{7.4}$$

where the parameters are defined as described in Chapter 5. In order to increase the accuracy of the DPCap analysis the current and wave coefficients are taken from the computational fluid dynamic (CFD) analysis

conducted on the 3D model of CyberShip III, as described in Appendix A.2. The IMCA M140 state that if such data is available, it is advices to use, but not necessary.

The $\boldsymbol{\tau_{Alloc_{optimal}}}$ was calculated according to Fossen (2011a),

$$\boldsymbol{\tau_{Alloc_{optimal}}} = \boldsymbol{T(\alpha)f} \tag{7.5}$$

where $\boldsymbol{f}$ is the thrust force vector, and $\boldsymbol{T(\alpha)}$ is the actuator configuration matrix. By limiting the available thrust from each thruster, one can reserve thrust to account for dynamics, as recommended by the IMCA M140 specifications. Both 0% and 20% reserved for dynamics were calculated.

To obtain the allocated force, one may solve (7.5), by means of the pseudo-inverse, for a given τ. In order to simplify the calculations, and reduce analysis time, the optimal allocated thrust was obtained by the use of a Marine Cybernetics AS script for optimal thrust allocation. The environmental forces was calculated by solving (7.2). The script solving this equation, can be found in the digital Appendix. By conducting a line search with 7 iteration for each heading, the wind envelop shown in Figure 7.1 was computed for CyberShip III.

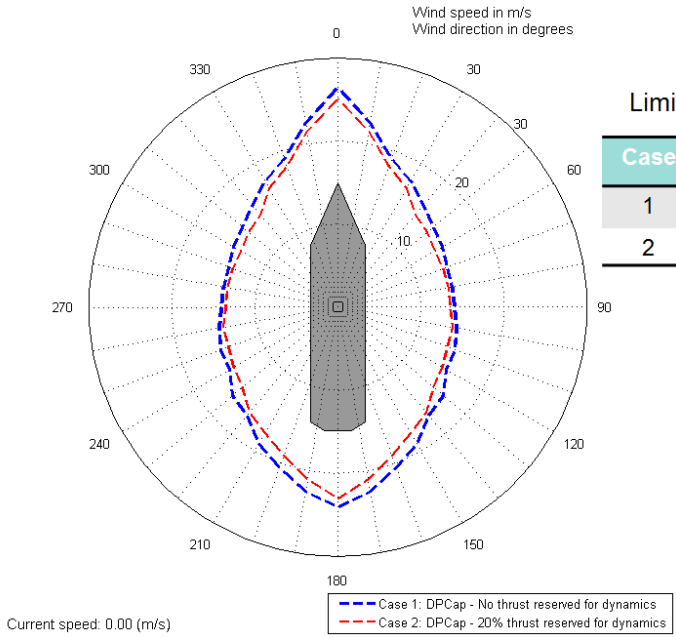

Figure 7.1: CyberShip III DPCap

Figure 7.1 shows the calculated wind envelop plot, obtained from the DPCap analysis. Case 1 shows the DPCap of CyberShip III, where no thrust is reserved to account for the dynamics. The limiting windspeed is calculated to be 26.5 m/s at the 0 degree environmental heading, and 14 m/s wind at the 90 degree environment angle. We note that the plot, compared to that of the offloading shuttle tanker presented in Chapter 4, is rounder in shape. This is expected, since CyberShip III got three azimuth thrusters, which enables the thrust to be more efficiently distributed, which increases the thruster utilization.

In Case 2, the DPCap was conducted with 20% of the thrust available, reserved to account for dynamics. We see that in Case 2, the plot has a similar shape, but with a smaller amplitude than in Case 1. This is an expected result, since less thrust is available. We also note that the difference between Case 1 and Case 2, is less at the 90 degree angle than at the 0 degree angle. This is similar to the results for the offloading shuttle tanker presented in Chapter 4.

We have that the significant wave height, corresponding to the 26.5 m/s wind, according toFossen (2011a) is given by:

$$\text{Hs} = 0.21\frac{U_{19.5}^2}{g} = 0.21\frac{26.5^2}{g} = 15.03m \tag{7.6}$$

and investigating the in scale value:

$$\text{Hs}_{Scale} = \frac{11.826}{30} = 0.501m \tag{7.7}$$

Considering the size of the CyberShip III model, Lpp = 1.975m, we might argue that the DPCap analysis seems to be a bit optimistic. At the same time, the size of the vessel, and consequently low weight, does result in low damping, which may indicate that the IMCA M140 recommendation of 20% thrust reserved for dynamics may be too low in this case. The discussion on how to calculate the optimal reserve for dynamics is outside the scope of this thesis, and will not be further investigated. One may consult Fossen (2011a) or Sørensen (2011) for additional details on effects of dynamics on vessels.

Remark 2. *The results of the analysis was briefly reviewed by dr. Nguyen and dr. Pivano at Marine Cybernetics AS, who agreed that both the calculations and results seemed to be reasonable.*

Remark 3. *The wind wave ratio was calculated in full scale, and then both scaled to model scale, by the use of BIS-scaling. The same method will be used throughout this thesis. In addition symmetry was assumed, and the calculations where therefor limited to 0-180 degrees. The resolution was 10 degrees. The same resolution and assumption will be used throughout this thesis.*

Chapter 8

CyberSea Vessel Simulator Overview

8.1 Introduction

In the previous chapter a DPCap analysis was conducted, and the results presented. We will now investigate the capability of CyberShip III, by means of the DynCap analysis. This chapter will give a short overview of the CyberSea Vessel Simulator, and the parameters needed to conduct the DynCap analysis. The detailed explanation of the configurations, and how they were computed can be found in Appendix A.

8.2 Simulator Overview

The CyberSea Vessel Simulator consist of a library of advanced mathematical modules, which aims to simulate all aspects of a marine vessel. The general structure of the vessel simulator, as configured for DynCap ,is given by Figure 8.1:

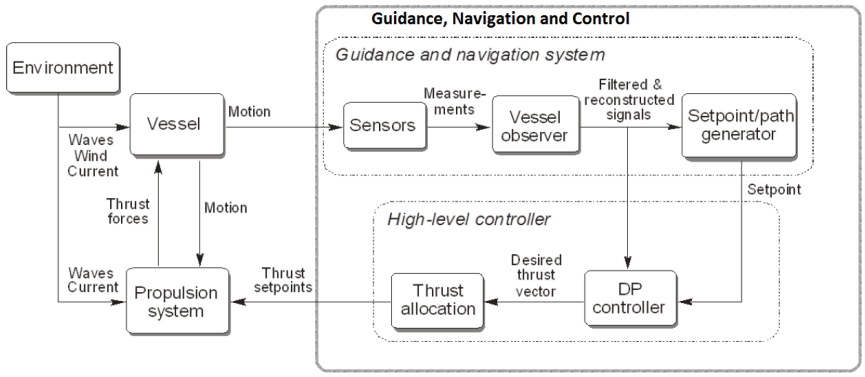

Figure 8.1: Vessel Simulator general overview

The modules which must be included to conduct the DynCap analysis, are:

- *Environmental module*, containing environmental models, and calculations of the environmental forces acting on the vessel.

- *Vessel module*, containing the equations of motion, where the correct vessel parameters, hull configurations, loads and hydrodynamic coefficients are important.

- *Propulsion System module*, containing thruster data, as well as account for effects like thruster losses, coanda effects and thruster-thruster interaction. In addition the module considers the thruster dynamics.

- *Guidance, Navigation and Control System modules*, which contains the sensor simulator, vessel observer, guidance system, and control system.

- *Thrust Allocation module*, which allocates the desired forces of the control system, to the individual thrusters. In the case of vessels operating close to the limit, the thrust allocation algorithm is critical, and will be subject to discussion in the chapters to come.

- *Power module*, which can be of particular interest when investigating the different failiour conditions, and the impact that may have on the vessels capability.

We note that in the case of the DynCap analysis of CyberShip III, some of the modules, including environmental module and thruster allocation algorithm, had to be modified in order for the simulations to be possible. The modules had to be changed, so that the scaling was according to that of the DPCap and the experiment to be presented in Chapter 11.

8.3 Simulator Configuration

In order to configure the CyberSea simulator, an extensive system identification had to be conducted, including 3D modeling, CFD analysis, hydrodynamic computations etc. The process of obtaining the parameters, and the parameters used, will not be discussed in this section, while a detailed description of both the process of obtaining the data and the parameters used, can be found in Appendix A.

8.4 Simulator Accuracy and Shortcomings

All simulations are simplifications of real world phenomenas. For that reason it is of particular importance to acknowledge the shortcomings of the simulator used, and highlight the possible uncertainties in the model and simulations. In the case of the CyberSea simulator, the models are well tested, and probably the weakest link is the configurations. In the case of the configurations of CyberShip III, there are two areas of particular interest, based on the results presented in Appendix A, the environmental model and the thruster data obtained.

The Environmental model has been verified by the Marine Cybernetics R&D team, and successfully been used for years. At the same time, one may question how the model compare to that of the real world. The wave model used, is based upon the Pierson-Moskowitz spectrum, which is given by:

$$S(\omega) = A\omega^{-5}e^{-B\omega^{-4}} \tag{8.1}$$

where

$$A = 8.1 \times 10^{-3} g^2 \tag{8.2}$$

$$B = 0.74 \left(\frac{g}{V_{19.4}} \right)^4 \tag{8.3}$$

where we have that $V_{19.4}$ is the wind speed at a height of 19.4 meters above the sea surface. This model has shown to be a good approximation to the waves in the North Atlantic Ocean. At the same time one may question; how do one measure the environment. The best measurements become estimations. Further we have that the spectrum may not be applicable for the location the vessel operates in. In particular we note that the CyberShip III, has a relative small above water area, which make the mean wave drift more important. If the operational area of a vessel is in territories with waves significantly different from that of the North Atlantic Ocean, one may use an other spectrum, but the accuracy of the spectrum still remain unknown. Further we have that the random seeds needed to calculate the the waves, may influence the results.

An other concern when reflecting on the accuracy of the configured simulator, is the thruster data. The thruster data provided by MarinTek, was incomplete at best. It was stated that the maximum bollard pull of the thrusters where 10 N for the bow azimuth, and 21.9 N for each of the stern azimuths. The accuracy of this data was difficult to confirm. Further the provided data, did not include accurate data on propeller rise time, thruster characteristics, azimuth turning rpm or mapping from thrust to propeller rpm. Several assumptions, as described in Appendix A, had to be made. The raise time and azimuth turning rpm where measured using a stop watch in dry dock, and do probably not reflect the true parameters exactly. If the azimuth rpm is incorrect, the simulator will provide thrust in a given direction faster or slower than CyberShip III would be able to do. This will have a direct impact on the result, and contribute to show that the vessel have a larger window of operation in the case of to high rpm, or smaller window of operation in the case of a too low configured rpm.

Chapter 9

Configurations Testing

9.1 Introduction

This chapter will seek to validate the configurations given in the previous chapter and presented in detail in Appendix A. The tests done, are based upon a combination of the Marine Cybernetics AS internal routines for configuration testing and tests developed by the author. The main purpose of the tests are to verify that no human errors have occurred during the input of configuration files to the simulator, ensure that the described parameters, as well as the hydrodynamic calculations correspond with the behavior of the vessel in the simulator, and the predicted and observed behavior of CyberShip III.

9.2 Forces

The first test aims to examine the response of the vessel, to external forces on the hull. By applying force to the hull, we would expect the vessel to move. Further we would expect that there should not be any significant motion in other DOF than the one where force or moments are applied. Small couplings in sway and yaw may be expected. The response should be sensible considering the type of vessel and the size of its thrusters.

Table 9.1 shows the forces applied to the hull of the vessel in the simulator, while the DP system was deactivated and the thrusters turned of.

No	Description and method	Observed response	Remark
1	Force forward: 20 N	u = 1.4 m/s v = 0.0 m/s r = 0.0 deg/s	OK
2	Force backward: -20 N	u = 1.3 m/s v = 0.0 m/s r = 0.0 deg/s	OK
3	Force starboard: 40 N	u = 0.0 m/s v = 0.6 m/s r = 0.2 deg/s	OK
4	Force port: -40 N	u = 0.0 m/s v = -0.6 m/s r = -0.2 deg/s	OK
5	Moment starboard: 20 Nm	u = 0.1 m/s v = -0.0 m/s r = 46.0 deg/s	OK
6	Moment port: -20 Nm	u = 0.1 m/s v = 0.0 m/s r = -46.0 deg/s	OK

Table 9.1: Configuration check of forces applied to the hull

We note that all tests were labeled as OK. In particular we note that the vessel has a high yaw rate when the forces are applied. This corresponds well with the observed behavior of CyberShip III, where it seems that the vessel is significantly over-powered.

9.3 Current

We now want to investigate the effects of current on the hull. This test was performed by setting current speed and direction, and by disabling all current fluctuations. The expected response of the vessel would be that the vessel drifts with close to current speed and direction. Further one would expect that the heading will stabilize. The gyros and position reference systems should show values according to the vessel state. The results of the tests can be found in Table 9.2

No	Description and method	Observed response	Remark
1	Current dir.: 90 deg Current speed: 1.0 m/s	Drift speed: 1.0 m/s Drift course: 90 deg Drift heading: -22 deg	OK
2	Current dir.: 0 deg Current speed: 0.5 m/s	Drift speed: 0.5 m/s Drift course: 0 deg Drift heading: -115 deg	OK
3	Current dir.: 270 deg Current speed: 1.5 m/s	Drift speed: 1.5 m/s Drift course: -90 deg Drift heading: 20 deg	OK

Table 9.2: Configuration check of current applied to the vessel

All tests concluded with that the configurations seemed to be correct, and that the heading stabilized after some time. The latter indicated that the vessel then floats along with the current, in a way which was expected. We note that current will not be used during the simulations, since such forces are not available at the Marine Cybernetics Laboratory at NTNU, Tyholt. At the other hand, the test is useful to ensure that the hull behaves in an expected way, which will strengthen the results.

9.4 Wind

The wind tests aimed to examine the effect of wind on the above water projected area. The tests were conducted by setting wind speed and direction manually in the simulator. During the tests, wind gusts and fluctuations were disabled. The results needed to be interpreted based on the GA drawings and the parameters of the above water area. The results from the tests can be found in Table 9.3

No	Description and method	Observed response	Remark
1	Wind dir = 180.0 deg Wind speed = 2.0 m/s Random effects disabled	Drift speed: 0.1 m/s Drift course: 156.8 deg Drift heading: 108.0 deg	OK
2	Wind dir = 90.0 deg Wind speed = 2.5 m/s Random effects disabled	Drift speed: 0.1 m/s Drift course: 24.0 deg Drift heading: 16.9 deg	OK

Table 9.3: Configuration check of forces applied to the vessel

We note that the vessel drifted along with the wind, at a low speed. By consulting with Marine Cybernetics AS employees, it was concluded that the drift speed, heading and course, corresponded well with the anticipated behavior. In particular we note that the vessel does have a side-slip angle, which is to be expected based on the location of CG and the distribution of the above water area.

9.5 Propulsion system

This section presents the results of the tests carried out for the propulsion system. We note that due to thrust losses, forces can vary with varying vessel speed. The tests were performed with thrust in surge provided by the aft azimuths, in both forward and backward direction. In addition tests were conducted to investigate thrust in sway without causing significant yaw motion, and finally yaw moment using all thrusters.

The expected results would be that the vessel should stabilize at realistic speed and rotational rate in sway and yaw. In surge, the speed may be too low because of the surge damping model, which is mainly tuned for low-speed testing. The test results can be found in Table 9.4

No	Description and method	Observed response	Remark
1	Thr1: 0 % Thr2: 25 % Thr3: 25 %	Max surge force: 10.72 N Max surge velocity: 1.45 m/s Small motions in sway-yaw: Yes	OK
2	Thr1: 60 % (90 deg) Thr2: 10 % (75 deg) Thr3: 10 % (105 deg)	Max sway force: 9.98 N Max sway velocity: 0.29 m/s Small motions in surge-yaw: Yes	OK
3	Thr1: 50 % (90 deg) Thr2: 10 % (270 deg) Thr3: 10 % (270 deg)	Max yaw moment: 6.39 Nm Max yaw rate: 25.5 deg/s Small motions in surge-sway: Yes	OK
4	Thr1: 0 % Thr2: 25 % (180 deg) Thr3: 25 % (180 deg)	Max surge force: -8.79 N Max surge velocity: -1.12 m/s Small motions in sway-yaw: Yes	OK

Table 9.4: Configuration check for propulsion system check

By calculating the theoretical thrust to be expected, and comparing to the simulator output, it was possible to conclude that the forces and moments closely matched the expected values. Consulting with Marine Cybernetics AS test employee, dr. Dong, we concluded that the behavior of the vessel was as expected, and indicated that the configurations were correct.

9.6 Individual thruster tests

This section presents the tests of the individual thrusters. The goal of these tests were to investigate if the thrusters behaved according to the configurations and the expected behavior for the individual thrusters. The tests were conducted by activating full manual control of all thrusters. During tests of one thruster, the other thrusters were locked in position with $\alpha = 0$ and thrust equal to 0.

The expected behavior would be that the thrust should saturate at 100%, and the response time from zero to full should be approx. 2.5-3 seconds, based on observation of CyberShip III at MarinTek. The max forces should be close to the bollard pull thrust, and the maximum power close to the rated power for the thruster. The rotational speed of the bow azimuth should be about 3 rpm (10 seconds from 0 to 180 deg), while the

aft azimuth thrusters should be 2 rpm, which was the configured speed of CyberShip III thrusters in the low level thruster controller. The test results for Thruster 1, can be found in Table 9.5

No	RPM [%]	Pitch/ Thrust [%]	Azimuth/ Rudder	X, Y, N [N, Nm]	Pow [W]	Resp time [s]	SAT [%]	CMD ACT FB
1	0 to 100	0	0 deg	0, 0, 0	0	0	0	NA
2	100	0 to 100	0 deg	10, 0, 0	33.8	2.8	100	OK
3	0 to -100	0 to -100	90 deg	0, -10, -5.5	33.8	2.8	100	OK
4	100	100	90 to -90 deg	0, -10, -5.5	33.8	11	100	OK
5	100	100	0 to 100%	-10, 0, 0	33.8	11	100	OK
6	100	100	0 to -100%	-10, 0, 0	33.8	11	100	OK

Table 9.5: Configuration check for Thruster 1

We note that the tests closely match the predicted behavior. The power consumption at full power is 33.8 W, which is the maximum shaft power stated in the thruster spec. In addition the rotation and rise time of the thrusters closely match that of the observed behavior of CyberShip III. Saturation of the thrusters are at 100%, which is in compliance with the predicted behavior.

The results for Thruster 2 and Thruster 3 can be found in Table 9.6 and Table 9.7.

No	RPM [%]	Pitch/ Thrust [%]	Azimuth/ Rudder	X, Y, N [N, Nm]	Pow [W]	Resp time [s]	SAT [%]	CMD ACT FB
1	0 to 100	0	0 deg	0, 0, 0	0	0	0	NA
2	100	0 to 100	0 deg	21.9, 0, 0	33.8	2.8	100	OK
3	0 to -100	0 to -100	90 deg	0, -14.13, 12.36	33.788	3.5	70	OK
4	100	100	90 to -90 deg	0, -0.02142, 18.75	33.8	15	100	OK
5	100	100	0 to 100%	-17.77, 0, -2.19	33.8	15	81.12	OK
6	100	100	0 to -100%	-17.77, 0, -2.19	33.8	15	81.12	OK

Table 9.6: Configuration check for Thruster 2

No	RPM [%]	Pitch/ Thrust [%]	Azimuth/ Rudder	X, Y, N [N, Nm]	Pow [W]	Resp time [s]	SAT [%]	CMD ACT FB
1	0 to 100	0	0 deg	0, 0, 0	0	0	0	NA
2	100	0 to 100	0 deg	21.9, 0, 0	33.8	2.8	100	OK
3	0 to -100	0 to -100	90 deg	0, -14.13, 12.36	33.788	3.5	70	OK
4	100	100	90 to -90 deg	0, -21.42, 18.75	33.8	15	100	OK
5	100	100	0 to 100%	-17.77, 0, 2.19	33.8	15	81.12	OK
6	100	100	0 to -100%	-17.77, 0, 2.19	33.8	15	81.12	OK

Table 9.7: Configuration check for Thruster 3

We note that the saturation of Thruster 2 and Thruster 3 are not at 100% for all azimuth angles. This is to be expected, since the Thrusters experiences thruster-thruster interaction, and the thrust will not reach 100%. The power consumption and the response time were as expected.

9.7 Power

This section describes the tests conducted in order to ensure that the power configuration was correct. The tests were conducted without any environmental loads, and by increasing the thruster load using manual control. The power system and distribution was then monitored, and it was checked whether or not the behavior was reasonable.

The test results can be found in Table 9.8.

No	Description and method	Observed response	Remark
1	All circuit-breakers closed, all bus-ties open, all thruster setpoints at 50 %	Gen1: 4.03 % Thr1: 50 % Thr2: 50 % Thr3: 50 %	OK
2	All Circuit-breakers closed, bus A1 and A2 closed, thruster 1 and 3 at 100 %	Gen1: 7.06 % Thr1: 100 % Thr2: % Thr3: 100 %	OK
3	All circuit-breakers closed, all bus-ties closed, thruster 1 and 3 at 100 %	Gen1: 7.06 % Thr1: 100 % Thr2: 0 % Thr3: 100 %	OK
4	CB of Generator 1 open, all bus-ties closed, thruster 1 and 3 at 100 %	Gen1: 0 % Thr1: 0 % Thr2: 0 % Thr3: 0 %	OK

Table 9.8: Configuration check of the power system

By reading the power consumption of each of the individual thrusters, adding them together, and calculating the percentage of the total available power, we get

$$P_{used} = P_{Thr1} + P_{Thr2} + P_{Thr3} \tag{9.1}$$

$$Gen1_{Percent} = \frac{P_{used} \cdot 100}{P_{Gen1Spec}} \tag{9.2}$$

where $P_{Gen1Spec}$ is the power limit of generator 1, as explained in the power configurations of Section A.4, we were able to conclude that the power configurations seemed to be correct.

9.8 Sensors

This section tests the sensors configured. The tests were conducted by comparing the output from each sensor, with the true state of the vessel in the simulator. The expected behavior, and acceptance criteria, would be that the sensors did not deviate significantly from the true vessel state. Table 9.9 shows the test results.

Sensor	Test	Remark
GPS1	Current	OK
VRU1	Waves	OK
GYRO1	Waves	OK

Table 9.9: Configuration check of the sensor systems

The output of each sensor was compared with the true state vector outputted by the simulator, which lead us to conclude that all sensors worked according to specifications.

9.9 Configuration Test-Program Conclusion

In this chapter extensive tests of the configurations of the CyberSea Vessel Simulator have been conducted. Since all tests indicate that the configurations are correct, the conclusion must be that the vessel simulator is configured correctly. The parameters used may deviate from the true parameters of CyberShip III, which may lead to deviations, due to configurations, but the general behavior seems to be correct. In particular incorrect hull parameters may influence the DynCap results significantly, since there are unknown factors in that regard, as well as the assumtions in regard to thruster bollard pull and characteristics.

Chapter 10

DynCap Analysis of CyberShip III

10.1 Introduction

This chapter describes the DynCap analysis conducted for CyberShip III. The acceptance criteria selected for the analysis will be presented and justified. Further, the implications of using the selected criteria will be discussed. Finally the results of the DynCap analysis will be presented, followed by a brief discussion.

10.2 Defining the Acceptance Criteria

Static capability analysis does not include any set of acceptance criteria. In order to conduct a DynCap analysis, an acceptance criteria must be defined. The selection of the acceptance criteria, will have a direct implication on the results, as shown in Chapter 4. By selecting a larger allowed deviation from the desired position and heading, the wind envelope will become larger. Since the recommended acceptance criteria for a DP vessel during operation, according to DNV (2011) (2011), is a 5m position deviation and 3 degrees heading deviation, the acceptance criteria to use during the DynCap analysis, was 5m/3deg. By applying the BIS scaling, where we have that $\lambda = 30$, we get an acceptance criteria for the simulation of $\frac{5}{\lambda} = 0.167$ m position deviation, and 3 degrees heading deviation.

10.3 DynCap Simulation

In order to execute the DynCap analysis simulation, a test sequence has to be designed and executed by the CyberSea simulator. The test sequence is an automated testing procedure, which will conduct a search for the limiting environmental conditions for a given heading. The first version of the test sequence was developed by Marine Cybernetics AS, and further developed by the author during the work on this thesis. The current version of the test sequence is not for distribution, and for that reason will not be presented in detail in this thesis.

The DynCap simulations can be executed on any computer running the CyberSea simulator. The CyberSea simulator can either run locally, or at a remote server. DynCap analysis requires a large amount of computation power, and can take up to several days to compute on a normal laptop. To be able to be productive during the time of simulation, DynCap analysis of the CyberShip III was conducted on a remote server. In order to run the simulations, a dedicated server blade was made available to the author, at the Marine Cybernetics servers. The blade was then configured to run one simulator on each core of the blade, eight in total. In addition the author reprogrammed the remote configuration interface, so that also parts of the processor power of the authors workstation was included in the cluster. This multi-core cluster approach increased the real-time factor dramatically, and made it possible to extend the simulation time significantly. By extending the simulation time one could ensure accuracy of the results, and be able to account for random effects in the weather. The vessel was simulated for in excess of 60 minutes for all tested environmental loads, for all headings of the vessel.

10.4 DynCap Analysis Results and Discussion

The DynCap test sequence, returns the limiting environmental forces, in terms of maximum wind speed. The return struct outputted by the DynCap simulation can be found in the digital Appendix. Figure 10.1 shows the wind envelop of CyberShip III, according to the DynCap analysis.

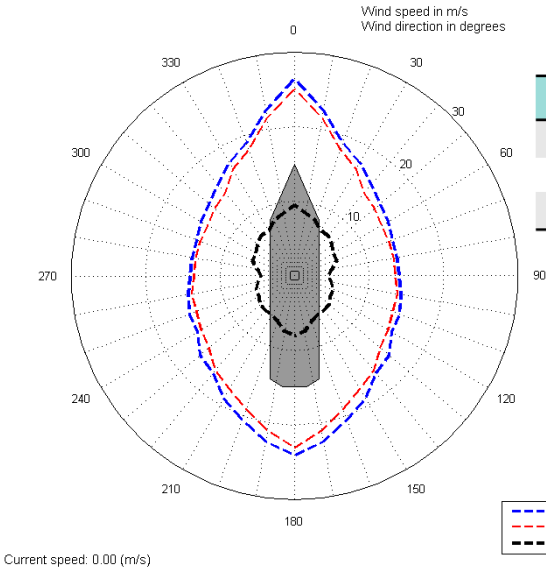

Limit wind speed [m/s]

Case	0 deg	90 deg
1	26.5	14
2	25	13.5
3	9.5	4.5

Figure 10.1: DPCap and DynCap analysis

In Figure 10.1 the black line represents the wind envelop of CyberShip III, according to the DynCap analysis. We see that the DynCap analysis indicates a significantly reduced stationkeeping capability. Comparing Case 2 and Case 3, we see that the DynCap represent only 38% of the capability at the 0 degree heading, and 33% of the capability at the 90 degree heading. We further note that the general shape of all the cases are relatively similar. The round shape is expected, based upon the CyberShip III thruster configuration.

By investigating the logs from the simulation we find that the large difference in the results can be explained by the fact that DynCap finds the limiting environmental conditions through simulations. When closing in on the limiting condition, we find that CyberShip III in 100% of the headings, fails to meet the acceptance criteria due to yaw motion. The thrusters struggle to control the heading, where the controller switching between positive and negative force. Due to the motor dynamics, we find that the thrusters cannot produce the desired forces fast enough, and the vessel fails the heading requirement.

10.5 Discussion

As presented in the previous sections, DPCap analysis and DynCap analysis results indicate a substantial difference in the stationkeeping capability of CyberShip III. If the results where to be validated, the consequences can be profound. If the DynCap analysis shows to be correct, the results obtained with the traditional analysis appear to be significantly optimistic.

When analyzing the results it is also important to emphasize the possible shortcomings of the models and the simulator, and which effects that would have. In particular the lack of thruster data, raise time, and thruster characteristics might have influenced the results. In addition the azimuth turning rate was measured manually with the use of a stop watch, and for practical reasons in dry dock. Further the line drawings, which was the basis for the 3D model, were based upon a pdf file, and then digitized. This method may give rise to imperfections in the model, which in turn will affect the hydrodynamic computations. In addition the CyberSea simulator might have some shortcomings, not know to either the author or the R&D department at Marine Cybernetics AS. Even when taking these possible sources of error into account, it is difficult to asses to what extent errors and imperfections may have affected the result. It is difficult to estimate if the DynCap simulation of CyberShip III is a conservative estimate or not.

We also note that the thrust allocation algorithm would possibly have had a significant impact on the results. At the same time, the thrust allocation algorithm used in the CyberSea Vessel Simulator, have undergone significant testing during development at Marine Cybernetics AS, and have shown to be reliable and accurate over years of Hardware-in-the-Loop (HiL) testing at Marine Cybernetics. To be able to further investigate the performance of the DPCap analysis and the DynCap analysis, the need for more data emerges. In the next chapter an experiment is conducted, designed to obtain the true capability of CyberShip III.

Chapter 11

Experimental Validation of Dynamic Stationkeeping Capability Analysis

11.1 Introduction

The results from Chapter 10, show that there are significant difference between stationkeeping capability obtained through simulation, and that obtained by means of the industry standard DPCap. Based upon the mathematics presented in Part 1, one may argue that some differences would be expected, but the extent may be surprising. The mathematical foundation for the DynCap indicate that the DynCap method should yield a more accurate description of the true capability of the vessel, but in order to show that the result obtained through the use of CyberSea simulator is correct, we now will seek to obtain the true capability of CyberShip III. In this chapter, a series of experiments conducted to establish the actual stationkeeping capability of CyberShip III will be described, and the results presented. Further the accuracy of the results will be discussed, and the results will be compared to that of the DPCap analysis and DynCap analysis.

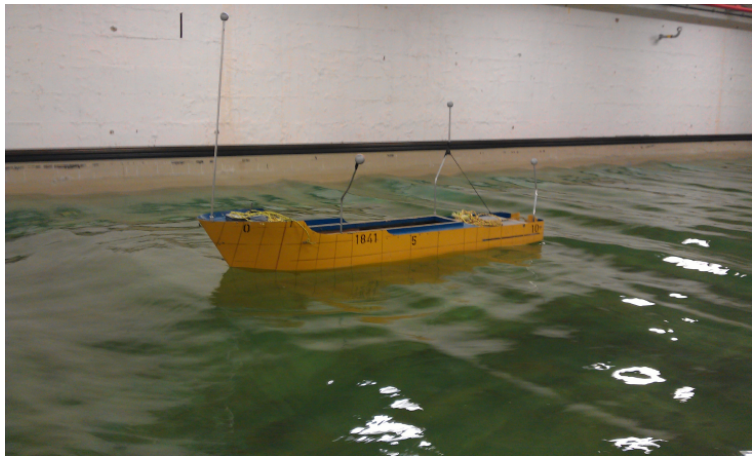

Figure 11.1: CyberShip III

11.2 CyberShip III

The control system designed for CyberShip III was designed to closely resemble that of the control system used during the CyberSea simulations. The control system of CyberSea is a non-linear setpoint controller. Due to practical reasons, porting the code was not possible for the control system. It was therefor decided to use a nonlinear setpoint controller, as described in Fossen (2011a).

Consider the following general PID controller:

$$\boldsymbol{\tau_{PID}} = -\boldsymbol{R^T(\eta)K_p\tilde{\eta}} - \boldsymbol{R^T(\eta)K_dR(\eta)\dot{\tilde{\eta}}} - \boldsymbol{R^T(\eta)}\int_0^t \boldsymbol{\tilde{\eta}(T)dT} \quad (11.1)$$

where we have that

$$\boldsymbol{\tilde{\eta}} \;=\; \boldsymbol{\eta_{ref}} - \boldsymbol{\eta} \quad (11.2)$$

and where the $\boldsymbol{K_p} > \boldsymbol{0}$, $\boldsymbol{K_d} > \boldsymbol{0}$ and $\boldsymbol{K_i} > \boldsymbol{0}$ are the controller gains.

We further have that by introducing a nonlinear passive observer, as

proposed on page 313 in Fossen (2011a), we get

$$\dot{\hat{\boldsymbol{\xi}}} = \boldsymbol{A_w}\hat{\boldsymbol{\xi}} + \boldsymbol{K_1}(\boldsymbol{\omega_0})\tilde{\boldsymbol{y}} \tag{11.3}$$

$$\dot{\boldsymbol{\eta}} = \boldsymbol{R}(y_3)\hat{\boldsymbol{\nu}} + \boldsymbol{K_2}\tilde{\boldsymbol{y}} \tag{11.4}$$

$$\dot{\hat{\boldsymbol{b}}} = -\boldsymbol{T}^{-1}\hat{\boldsymbol{b}} + \boldsymbol{\tau} + \boldsymbol{R}^{\boldsymbol{T}}(y_3)\boldsymbol{K_4}\hat{\boldsymbol{y}} \tag{11.5}$$

$$\boldsymbol{M}\dot{\hat{\boldsymbol{\nu}}} = -\boldsymbol{D}(\hat{\boldsymbol{\eta}}) - \boldsymbol{\tau} + \boldsymbol{R}^{\boldsymbol{T}}(y_3)\boldsymbol{K_4}\hat{\boldsymbol{y}} \tag{11.6}$$

$$\hat{\boldsymbol{y}} = \hat{\boldsymbol{\eta}} + \boldsymbol{C_w}\hat{\boldsymbol{\xi}} \tag{11.7}$$

where we have that $\boldsymbol{K_1} > \boldsymbol{0}$, $\boldsymbol{K_2} > \boldsymbol{0}$, $\boldsymbol{K_3} > \boldsymbol{0}$ and $\boldsymbol{K_4} > \boldsymbol{0}$ are the observer gains. $\boldsymbol{M} \in \mathbb{R}^3$ and $\boldsymbol{D} \in \mathbb{R}^3$ are the mass and damping matrices respectively. We then have that the drift, according to Fossen (2011a), is given by the term $\hat{\boldsymbol{b}}$. By then using the observer bias estimates, $\boldsymbol{R^T}(\psi)\hat{\boldsymbol{b}}$, we according to Loria A., T. I. Fossen and A. Teel (1999), get the following controller law, which was implemented as the CyberShip III DP controller:

$$\boldsymbol{\tau_{PID}} = -\boldsymbol{R^T}(\psi)\boldsymbol{K_p}\tilde{\boldsymbol{\eta}} - \boldsymbol{R^T}(\psi)\boldsymbol{K_d}\boldsymbol{R}(\psi)\dot{\tilde{\boldsymbol{\eta}}} - \boldsymbol{R^T}(\psi)\tilde{\boldsymbol{b}} \tag{11.8}$$

We then note that the integral term has been substituted with the bias term, and we according to Loria A., T. I. Fossen and A. Teel (1999), have that the equilibrium point of the controller can be shown to be uniformly globally asymptotically stable (UGAS) . Consult Appendix F for stability definition. The proof of the stability of the control system will not be explicitly stated, but the proof of the stability is to be found in Loria A., T. I. Fossen and A. Teel (1999).

The control law given by (11.8) was implemented on CyberShip III, together with a *NAN* signal protection system, which was designed to handle loss of signal from the position system. During the experiment, it was observed that the positioning system provided a *NAN* signal to the control system, which resulted in system crashes. The solution was to feedback the last safe signal, until the *NAN* signal was gone. The occurrence of *NAN* was calculated to be less than 0.03 %, and the duration was usually less than 0.1 sec.

The final component of the control system was the thrust allocation. In order to limit the differences in results, due to thrust allocation, it was decided to port the entire thrust allocation code from CyberSea to CyberShip III. The performance and complexity of the Marine Cybernetic thrust

allocation algorithm, is according to Marine Cybernetics AS, comparable to that found on most DP vessels. In order to port the code to run on CyberShip III, all function calls of the Marine Cybernetics thrust allocation had to be review, rewritten, and extensive tested afterwards, to ensure that the behavior of the thrust allocation algorithm had not changed. After the code was ported, an input/output test was conducted. The code running on board CyberShip III, was compared to the code running in CyberSea. Table 11.1, shows the tests, and test results.

Input	CyberSea Output	CyberShip III output	Result
$\boldsymbol{\tau_{DP}} = [\ 0,\ 0,\ 0]'$	$\boldsymbol{T_d} = [\ 0,\ 0,\ 0]'$ $\boldsymbol{\alpha_d} = [\ 0,\ 0,\ 0]'$	$\boldsymbol{T_d} = [\ 0,\ 0,\ 0]'$ $\boldsymbol{\alpha}_d = [\ 0,\ 0,\ 0]'$	OK
$\boldsymbol{\tau_{DP}} = [\ 1,\ 0,\ 0]'$	$\boldsymbol{T_d} = [\ 0.1859,\ 0.4071,\ 0.4071]'$ $\boldsymbol{\alpha_d} = [\ 0,\ 0,\ 0]'$	$\boldsymbol{T_d} = [\ 0.1859,\ 0.4071,\ 0.4071]'$ $\boldsymbol{\alpha}_d = [\ 0,\ 0,\ 0]'$	OK
$\boldsymbol{\tau_{DP}} = [\ -1,\ 0,\ 0]'$	$\boldsymbol{T_d} = [\ 0.1859,\ 0.4071,\ 0.4071]'$ $\boldsymbol{\alpha_d} = [\ 3.142,\ 3.142,\ 3.142]'$	$\boldsymbol{T_d} = [\ 0.1859,\ 0.4071,\ 0.4071]'$ $\boldsymbol{\alpha_d} = [\ 3.142,\ 3.142,\ 3.142]'$	OK
$\boldsymbol{\tau_{DP}} = [\ 0,\ 1,\ 0]'$	$\boldsymbol{T_d} = [\ 0.5976,\ 0.2228,\ 0.2228]'$ $\boldsymbol{\alpha_d} = [\ 1.571,\ 1.127,\ 2.014]'$	$\boldsymbol{T_d} = [\ 0.5976,\ 0.2228,\ 0.2228]'$ $\boldsymbol{\alpha_d} = [\ 1.571,\ 1.127,\ 2.014]'$	OK
$\boldsymbol{\tau_{DP}} = [\ 1,\ 1,\ 0]'$	$\boldsymbol{T_d} = [\ 0.6258,\ 0.5414,\ 0.3708]'$ $\boldsymbol{\alpha_d} = [\ 1.269,\ 0.3808,\ 0.5736]'$	$\boldsymbol{T_d} = [\ 0.6258,\ 0.5414,\ 0.3708]'$ $\boldsymbol{\alpha_d} = [\ 1.269,\ 0.3808,\ 0.5736]'$	OK
$\boldsymbol{\tau_{DP}} = [\ 0,\ 0,\ 1]'$	$\boldsymbol{T_d} = [\ 0.6989,\ 0.3498,\ 0.3498]'$ $\boldsymbol{\alpha_d} = [\ 1.571,\ -1.524,\ -1.617]'$	$\boldsymbol{T_d} = [\ 0.6989,\ 0.3498,\ 0.3498]'$ $\boldsymbol{\alpha_d} = [\ 1.571,\ -1.524,\ -1.617]''$	OK
$\boldsymbol{\tau_{DP}} = [\ 10,\ 15,\ 15]'$	$\boldsymbol{T_d} = [\ 18.87,\ 9.821,\ 2.409]'$ $\boldsymbol{\alpha_d} = [\ 1.47,\ -0.1934,\ -2.241]'$	$\boldsymbol{T_d} = [\ 18.87,\ 9.821,\ 2.409]'$ $\boldsymbol{\alpha_d} = [\ 1.47,\ -0.1934,\ -2.241]'$	OK
$\boldsymbol{\tau_{DP}} = [\ 1000,\ 100,\ 0]'$	$\boldsymbol{T_d} = [\ 10.53,\ 21.98,\ 21.87]'$ $\boldsymbol{\alpha_d} = [\ 0.3182,\ 0.04746,\ 0.0477]'$	$\boldsymbol{T_d} = [\ 10.53,\ 21.98,\ 21.87]'$ $\boldsymbol{\alpha_d} = [\ 0.3182,\ 0.04746,\ 0.0477]'$	OK

Table 11.1: Thrust Allocation Test Results

In table 11.1 we see that for all tested $\boldsymbol{\tau_{DP}}$, sent to the thrust allocation, the same output was returned by the code running on board the CyberShip III, and the thrust allocation module running inside CyberSea. From this we can conclude that the ported code, has retained its functionality.

The simulink diagram has not been included in this thesis, since the system contains a rewritten version of the Marine Cybernetics AS thrust allocation algorithm. For additional details one may contact brede.borhaug@marinecyb.com.

11.3 Experiment Setup: Marine Cybernetics Laboratory

The experiments conducted during the work on this thesis, were conducted at the Marine Cybernetics Laboratory [1] (MCLab) located at NTNU, Tyholt. The experimental laboratory have a pool which is 6.45m wide, 40m long and 1.4m deep. In addition the laboratory is equipped with a movable bridge, and a towing carriage, which is capable of speeds up to 2 m/s. The MCLab is also equipped with a wave maker, which is a 6 meter with single paddle and is operated with an electrical servo actuator. The wave maker is able to produce regular and irregular waves, up to 0.3 meter high. In addition the laboratory has an infrared camera system, which can determine the position and orientation of a floating body equipped with passive infrared markers. The camera system is capable of providing real-time position data, at a rate of 10Hz, which is similar to that of a normal GPS system.

[1] (http://www.ntnu.no/imt/lab/kybernetikk)

(a) MCLab pool

(b) MCLab Wave maker

(c) IR camera system

Figure 11.2: Pictures from the MCLab

11.3.1 Wind generator and measurement

The MCLab is not equipped with a wind maker. To be able to generate wind, a wind generator had to be constructed. Several different sources of wind were investigated, including radiator fans and air condition units. Tests were conducted to investigate the wind output and turbulence of each fan, before finally selecting a centrifugal fan, NICOTRA K48622, designed for ventilation in buildings.

(a) Overview

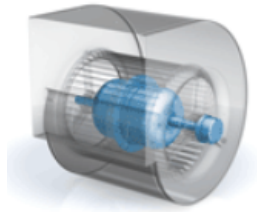

(b) Fan Compontents

Figure 11.3: Wind Generator

The fan was controlled by a 10A variable AC controller. The fan was secured to the movable bridge at the MCLab, by the use of a fan rig. The rig was constructed by welding the two top mounting plates to the two extension rods. The construction describing the top component and

extension rods can be found in Appendix H. The fan was fastened to the rig, by the use of four M6 bolts.

In order to measure the wind speed, a portable wind meter, WindMate WM-350, which was placed in the wind stream, at the location of the center of above water area for the heading to be investigated. For zero degree heading, the fan was located a distance of 10m away from the center of above water area. The wind speed measured were the average wind speed, over a 15 minute time period. In order to be able to conduct only one measurement, which could be used for all headings at a given wind speed, the divination from the measured point, and the center of above water area for the given heading was calculated, and the bridge holding the fan rig was moved accordingly. It is worth noting that the assumption of the wind measured in the center of above water area, might deviate to some extent from the true wind impacting the vessel at all point, since it was observed that the wind was highly dependent on the distance traveled. In addition the WindMate WM-350 has a resolution of 0.1 m/s, which may effect the final result.

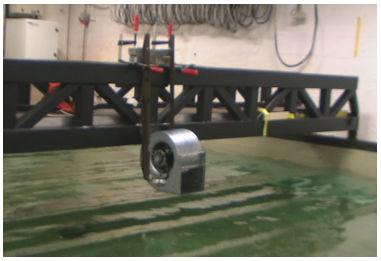

(a) Wind generator

(b) WindMate WM-350

Figure 11.4: Wind Generator

11.4 Capability Experiment Results

In order to obtain the capability of CyberShip III, a line search was conducted, where the environmental loads were varied according to the same method used during the DynCap analysis in Chapter 10. The same acceptance criteria as for the DynCap analysis were used, 5m and 3 degrees. The experiment resulted in 23.5 hours of data retrieved, and over 10 million data points. A detailed laboratory log can be found in Appendix G. Analyzing the data, the stationkeeping capability shown in Figure 11.5 were obtained.

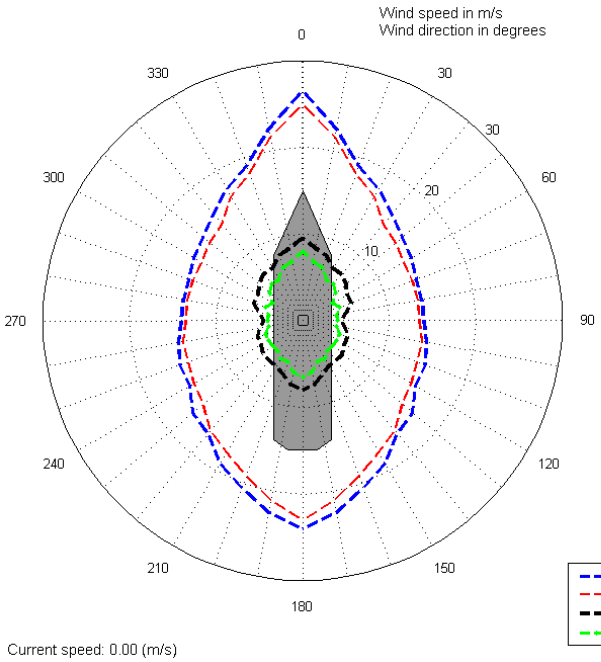

Limit wind speed [m/s]

Case	0 deg	90 deg
1	26.5	14
2	25	13.5
3	9.5	4.5
4	8	4

Figure 11.5: DPCap analysis, DynCap analysis and experimental results

Figure 11.5 shows the wind envelope for CyberShip III, where the results from DPCap, DynCap and experimental data are included. Case 1, Case 2 and Case 3 are the same as presented in Chapter 10, where the green line, Case 4, is the stationkeeping capability obtained from the experimental data. With the environmental loads coming from the 0 degree

angle, the plot shows that the limiting wind speed is 8 m/s. A wind speed of 8 m/s corresponds to a in-scale significant wave height (Hs) of 0.045 m. Further we see that with the environmental loads coming from 90 degrees, the results indicate that the limiting wind speed is 4 m/s. The 4 m/s wind speed, correspond to a Hs of 0.0114 in model scale. We note that this value is significantly smaller that that found by the use of DPCap analysis. Based upon the results presented in Figure 11.5, it seems that the DynCAp analysis is much more realistic, and that the DPCap indeed is too optimistic.

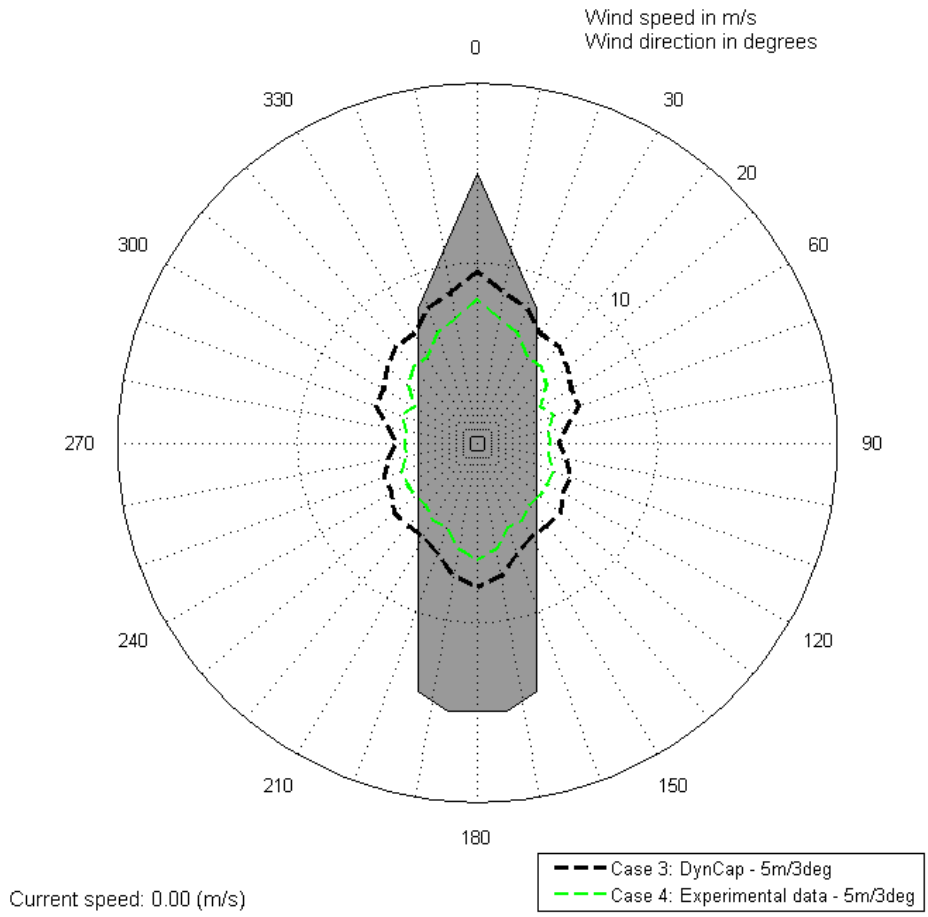

Figure 11.6: DynCap results compared to experimental data

Figure 11.6 shows Case 3 and Case 4 only. We note how the plots are similar in shape. In particular it is interesting to see that both plots have a dip at the 30, 60 and 90 degree angle. The fact that both the simulations, and the experimental results have these unique characteristics, is a strong indication of the accuracy of the DynCap analysis, and the simulator used. It would be interesting to investigate this characteristics in more detail, by increasing the resolution. This would require additional sensors at the MCLab, and for that reason is is not further investigated in this thesis.

Investigating the differences between the DynCap results and the experimental results, we find that the relative reduction between the plots are in average approximately 10%. In Case 2, DPCap with thrust reserved for dynamics, we find that the relative reduction compared to the experimental data is approximately 60%. Comparing this to the results presented in Chapter 4, we note that the results are similar to that of the offloading shuttle tanker, where the average relative difference between the DPCap with 20% thrust reserved, and the DynCap 5m/3deg is approximately 53%. The similarities between the two, give credibility to the the results presented in this chapter.

Investigating the logs of the experiment, it was found that for all headings, the failure to meet the acceptance criteria at the limit, was due to deviation in heading. The bow thrusters struggle to control the heading, where the controller was switching between positive and negative force. Due to the motor dynamics the thrusters could not produce force immediately, thus limiting the vessel heading controllability. This is the same behavior, as observed during the DynCap analysis. This observation may also indicate that the DynCap tool has a future in ship design, or thruster configuration planing.

Finally it is important to emphasize that the position and attitude measurements may have been subject to error. There is also difficult to measure the environment exactly. The wave generator may not be able to produce the correct wave height inputted to the wave maker control station. This may contribute to some uncertainties in the results, and possibly explain the modest differences between Case 3 and Case 4. The assumption of measuring the wind in the center of above water area, may also contributed to uncertainties, and errors in the obtained results.

Remark 4. *All the raw data logs can be found in the digital Appendix.*

11.5 Discussion

The previous section presented results indicating not only that there may be significant differences between the DPCap results and the DynCap results, but that experimental data indicate that the DynCap results are significantly closer to the real stationkeeping capability of the CyberShip III vessel. As in the case of the offloading shuttle tanker presented in

Chapter 4, the results obtained with the traditional DPCap analysis appear to be too optimistic. Further the experimental data indicate that the results obtained by the use of DynCap analysis look more reasonable.

By returning to the questions stated in the final discussion of Chapter 4; How much can we trust the results from the traditional capability analysis? Do they convey a realistic picture of a vessel's stationkeeping capability in dynamic operating conditions? Are they conservative or optimistic? Based upon the results presented in this chapter, we may conclude that if an detailed study of a vessels stationkeeping capability is desired, the traditional DPCap is not adequate. The simplifications and assumptions made when calculating the DPCap, according to the IMCA M140 specifications, seems to result in wind-envelopes which do not reflect the stationkeeping capability of a vessel in a realistic manner. If the capability plot is to be used for determining the vessel operational window or to select a vessel for an operation, it is possible that a more detailed standard should be established. Using results from a DynCap analysis, more accurate results, does not necessarily give reason to select a larger and more expensive vessel for an operation. If the data available is trustworthy, one may select a vessel to operate close to the limit, and in turn optimize the resources available in a more productive way. This should both ensure safe operation, and reduce non-productive.

The final question still remain unanswered; has the DynCap analysis been validated. According to Software Testing Fundamentals (2012), validation can be defined according to:

Definition 2. *Validation (Software Testing Fundamentals (2012))*
To ensure that the product actually meets the user's needs, and that the specifications were correct in the first place. In other words, to demonstrate that the product fulfills its intended use when placed in its intended environment.

Based upon the results presented in this thesis, one may conclude that the DynCap analysis provides a stationkeeping analysis, which is superior that of the DPCap, in terms of accuracy. This conclusion is not solely based upon the experimental results, but the sum of the mathematical foundation, simulations conducted and experimental data. In addition, the correspondence between the obtained results for CyberShip III, and

the results presented for the offloading shuttle tanker in Chapter 4, bring additional credibility to the results. One may argue that the accuracy of the DynCap analysis is not yet sufficiently investigated and several aspects need additional research, which is a reasonable claim. On the other side, the performance of the DynCap analysis have repeatedly shown to be significantly better than that of the DPCap, and in that respect one may argue that the DynCap analysis would be the best available tool at the moment.

Returning to the Definition 2, we may conclude that the product, DynCap, fulfills its intended use when placed in its intended environment. The DynCap has shown to provide the costumer with the most accurate method of analyzing a vessels stationkeeping capability, which in turn implies that the DynCap analysis has been validated.

Chapter 12

Conclusion and Future Work

This thesis has considered two main issues: the theory of capability analysis; conducting a model scale capability analysis, including an experimental validation.

The first part of the thesis, Part 1, considered the theory of capability analysis. It presented the concept of dynamic DP capability analysis (DynCap), and by reviewing a DynCap analysis conducted on a offloading shuttle tanker, the fundamental differences between the results obtained by the use of the DynCap analysis, opposed to the industry standard static DP capability analysis (DPCap), was reviewed. Further the mathematical foundation of DynCap was presented, and it was shown that by applying the simplifications and assumptions proposed in the industry used IMCA M140 specifications to the equations of DynCap, one may obtain the DPCap equations. The mathematical foundation, and the relationship between the DPCap and DynCap method, provide a thorough mathematical understanding of the differences between them, as well as the benefits of employing the DynCap analysis in favor of the DPCap analysis.

The second part of the thesis, i.e . Part 2, consider the stationkeeping capability of CyberShip III. The stationkeeping capability of CyberShip III was obtained through a DPCap analysis, a DynCap analysis, and finally an experiment using the model CyberShip III. The DPCap analysis was conducted in accordance with the industry standard IMCA M140

specifications for DP capability plots. Further the DynCap analysis was conducted by the use of the CyberSea vessel simulator, where an extensive system identification process was undertaken. The results of the DPCap and DynCap analysis showed that there was an considerable difference in the results. The relative reduction in depicted capability from the DPCap to the DynCap results was found to be approximately 50%. These results were also consistent with the DPCap and DynCap analysis conducted by Marine Cybernetics AS, on the offloading shuttle tanker presented in Part 1. The experiment conducted aimed to validate the DynCap analysis results, and provide the validation needed to present DynCap analysis as the next-generation stationkeeping capability analysis. The results showed that the DynCap analysis had an average deviation from the experimental data of approximately 10%, where the relative reduction from DPCap to the experimental data was approximately 60%. The sum of the theoretical foundation, DynCap simulations and experimental data, made it possible to validate the DynCap analysis, which showed to be considerably closer to the experimentally obtained stationkeeping capability of CyberShip III. The superior performance of the DynCap analysis, relative the DPCap analysis, provides additional arguments for employing the DynCap method in favor of the industry standard DPCap. At the same time, the DynCap analysis needs further investigation, to both improve the method, and present more detailed evidence of the performance of the analysis. What is clear, is that by employing the DynCap tool, and considering the complete vessel, environmental forces, and control system dynamics, most of the assumptions needed for the traditional DPCap analysis are removed.

The implications of the results presented in this thesis may be regarded as considerable. The results show that without a well defined standard for DPCap analysis, the validity of the results are uncertain. The uncertainty in turn limits their use. By employing the DynCap analysis the operators, ship owners and oil companies, will be able to make decisions based on more accurate data, which will enhance security, and reduce non-productive time. With well defined limits of operation for a vessel, it will be possible to utilize the resources in a more productive manner. By basing decisions on accurate data, the selected vessel may be able to operate closer to the limit, without compromising security. This will in

turn reduce costs and increase profits.

The DynCap tool is new to the marked. More research and development will lay in its future. Additional investigation of the accuracy of DynCap analysis would be of great interest. In addition a comparison of an DynCap analysis with experimental data from a full scale vessel, would contribute to strengthen the position of DynCap analysis. Further it seems clear that the class society: DNV, Loyds, ABS etc., need to catch up with the technology and development. Time has come to reevaluate the current standards for DP capability analysis. This thesis has shown that if the capability analysis aims to ensure safe operation, the traditional DPCap is not adequate, while the DynCap analysis seems to be the future of capability analysis.

Bibliography

Amerongen, J. V. (1984). Adaptive Steering of Ships—A Model Reference Approach. *Automatica*, 20(1):3–14.

API (1997). Recommended Practice for Design and Analysis of Station-keeping Systems for Floating Structures.

Blendermann, W. (1994). Parameter identification of wind loads on ships. *Journal of Wind Engineering and Industrial Aerodynamics*, 51:339–351.

Board, N. S. (1997). *Twenty-First Symposium on Naval Hydrodynamics*. Compass Series. National Academy Press.

Borhaug, E. and Pettersen, K. (2005). Cross-track control for underactuated autonomous vehicles. In *Decision and Control, 2005 and 2005 European Control Conference. CDC-ECC '05. 44th IEEE Conference on*, pages 602 – 608.

Børhaug, B. (2011). *Guidance And Control of Unmanned Aerial Vehicles in Particular, and Vehicles in General*. Project Thesis, NTNU.

Børhaug, E. (2008). *Nonlinear Control and Synchronization of Mechanical Systems*. PhD thesis, Norwegian University of Science and Technology, Department of Engineering Cybernetics.

Chen, C. (1999). *Linear system theory and design*. The Oxford series in electrical and computer engineering. Oxford University Press.

Chwang, A., Lee, J., and Leung, D. (1996). *Hydrodynamics*. Number v. 1. Balkema.

DNV (2011) (2011). Dynamic Positioning Systems - Operation Guidance, Recommended Practice DNV-RP-E307.

Faltinsen, O. (1993). *Sea Loads on Ships and Offshore Structures*. Cambridge Ocean Technology Series. Cambridge University Press.

Faltinsen, O. (2005). *Hydrodynamics Of High-Speed Marine Vehicles*. Cambridge University Press.

Fossen, T. (2011a). *Handbook of Marine Craft Hydrodynamics and Motion Control*. John Wiley & Sons.

Fossen, T. (2011b). Mathemaatical Models for Control of Aircrafts and Satellites. Department of Engineering Cybernetics, NTNU. Available from: http://www.itk.ntnu.no/fag/gnc.

IMCA M140 (2012). IMCA M140: Specification for DP Capability Plots.

Khalil, H. (2002). *Nonlinear systems*. Prentice Hall.

Lindgaard and Fossen (2003). Fuel Efficient Control Allocation for Surface Vessels with Active Rudder Usage.

Loria A., T. I. Fossen and A. Teel (1999). Non-Autonomous Systems: Applications to Integral Action Control of Ships and Manipulators, Proceedings of the 5th European Control Conference (ECC'99), Karlsruhe, Germany.

Pivano, L., Øyvind Notland Smogeli, and Vik, B. (2012). Dyncap – the next level dynamic dp capability analysis. Marine Cybernetics AS.

Software Testing Fundamentals (2012). Verification vs validation. [Online; accessed 30-may-2012].

Sørensen, A. (2011). *Propulsion and Motion Control of Ships and Ocean structures*. Marine Technology Center, Department of Marine Technology. Lecture notes.

Vik, B. (2011). *Integrated Satellite and Inertial Navigation Systems*. Norwegian University of Science and Technology.

Wikipedia (2011). Euler angles — wikipedia, the free encyclopedia. [Online; accessed 6-October-2011].

Appendix A

Vessel Configuration and Vessel Parameters

A.1 Introduction

This appendix contain the complete vessel configurations and vessel parameters. The appendix is intended to be a reference to the thesis, as well as a source of quality data for others working on CyberShip III. The Appendix consist of the hydrodynamic analysis of CyberShip, and corresponding results. In addition the propulsion, power, sensor and DPSystem configurations are added. Some key parameters and explanations are not included, in order to protect Marine Cybernetics AS property.

A.2 Vessel Hydrodynamics

A.2.1 Introduction to the Vessel Hydrodynamics

In order to describe the flow phenomena associated with the waves and the motion of ships in waves, we need to know the velocity of the fluid and the pressure at different locations on the hull Fossen (2011a). According to Fossen (2011a), the description of the flow and pressure is then given by:

$$div(\boldsymbol{v}) = \nabla \cdot \boldsymbol{v} = \frac{\partial v_1}{\partial x} + \frac{\partial v_2}{\partial y} + \frac{\partial v_3}{\partial z} \tag{A.1}$$

$$\rho \left(\frac{\partial \boldsymbol{v}}{\partial t} + \boldsymbol{v} \cdot \nabla \boldsymbol{v} \right) = \rho \boldsymbol{F} - \nabla p + \mu \nabla^2 \boldsymbol{v} \tag{A.2}$$

were $\boldsymbol{v}(\boldsymbol{x}, t) = [v_1(\boldsymbol{x},\ t),\ v_2(\boldsymbol{x},\ t),\ v_3(\boldsymbol{x},\ t)]^T$. The system of nonlinear partial differential equations given by Equation A.1 and Equation A.2 does not have a analytic solution. One may use the simplifications proposed in Fossen (2011a), which is stated to be satisfactory for control system design, and simple simulation. In the case of more advanced simulations, where among others propeller-rudder-hull interaction is considered, the simplifications stated in Fossen (2011a) is not suited, and a nummerical solution is preferred. The interested reader may consult Fossen (2011a), Chwang et al. (1996), Board (1997) and Faltinsen (2005).

This section will describe the construction of a 3D model of CyberShip III, and the numerical calculations done by the use of the hydrodynamic software WAMIT, resulting in an accurate description of the flow phenomenas related to waves and motion of CyberShip III. In addition the hydrodynamic and hydrostatic configurations of CyberShip III will be presented, and some key parameters resulting from these configurations will be emphasized.

A.2.2 Ship Geometry

The ship geometry files included in the Vessel Simulator are used in the hydrodynamic computations, This includes the computation of added mass, potential damping and hydrostatic terms, 1st and 2nd-order wave loads

as well as viscouse damping due to the anti-roll tanks (if included), bilge keels etc.

In order to generated the geometry files, a 3D model of the vessel needed to be constructed. The model was created with the use of Rhinoceros 4.0, on the basis of line drawings provided by MarinTek. The linedrawings consisted of 20 stations, resulting in a 3D model with 2008 pannels. Figure A.1 show the 3D model of the wetted surface of CyberShip III. The above water surface does not effect the calculations done by WAMIT.

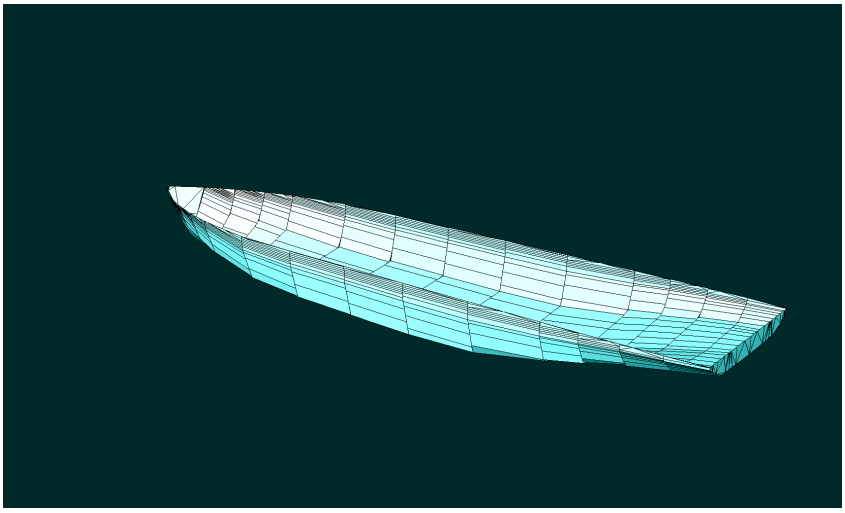

Figure A.1: 3D model of CyberShip III wetted surface

By the use of Rhinoceros 4.0, the geometry files, the .GDF files, were constructed and prepared for hydrodynamic processing by hydrodynamic potential theory program. Table A.1 show the hydrodynamic software program used, and version.

Program	Version	Company
WAMIT	6.4	WAMIT Inc.

Table A.1: Hydrodynamic Software

The processed results from WAMIT can be found in Appendix B, whereas the raw WAMIT output transcript is located in Appendix C.

A.2.3 Wind and Current Configuration

In order to accurately calculate how the wind and current effect the vessel, a General Arrangement (GA) drawing was used. There did not exist any digitized GA drawing of CyberShip III, so the GA drawing was constructed from the 3D-model made in Rhinoceros, and high resolution photographs of CyberShip III. Corresponding centroides are then calculated for the desired water line. Current coefficients was based on experimental data providded by Marine Cybernetics AS, and wind coefficients are based on Helmholtz-Kirchhoffs plate model Blendermann (1994)

Wind and Current Areas

On the basis of the GA drawing the wind and current areas where calculated. Table A.2 show the results of the calculations, and Figure A.2 show the GA drawing.

Parameter	Description	WL1	Unit
A_Fcurr	Frontal current area	0.056	m2
A_Lcurr	Lateral current area	0.267	m2
A_Fwind	Frontal wind area	0.120	m2
A_Lwind	Lateral wind area	0.371	m2

Table A.2: Wind and Current Areas

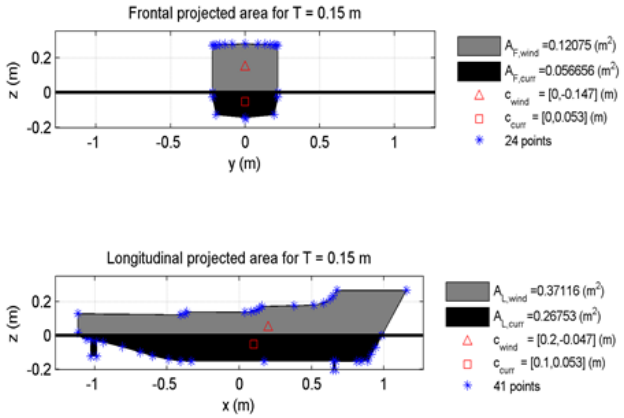

Figure A.2: Wind area, current area and centroids computed for T = 0.153 m

Current and Wind Coefficients

We now arrive at the point were we are able to calculate the wind and drag coefficients. The current was calculated using the cross-flow drag principle, such that the resultant current coefficient matches the given experimental coefficients. The interested reader may consult Faltinsen (1993) for details. The Munk moment was computed using potential coefficients. Figure A.3 and Figure A.4, and Table A.3 and Table A.4 show the current and wind coefficients respectively.

A.2.4 Hull Configuration Tables

A summery of the configurations data needed to be inputted to CyberSea and the hydrodynamic program WAMIT can be found in Table A.5. The data which was not available from MarinTek, had to be found by other means. In particular the displacement was calculated by the use of Rhinoceros and the 3D model developed and the transverse- and longitudinal metacenter height was tuned during the initialization of WAMIT.

The computed surge resistance curves are given in Figure A.5

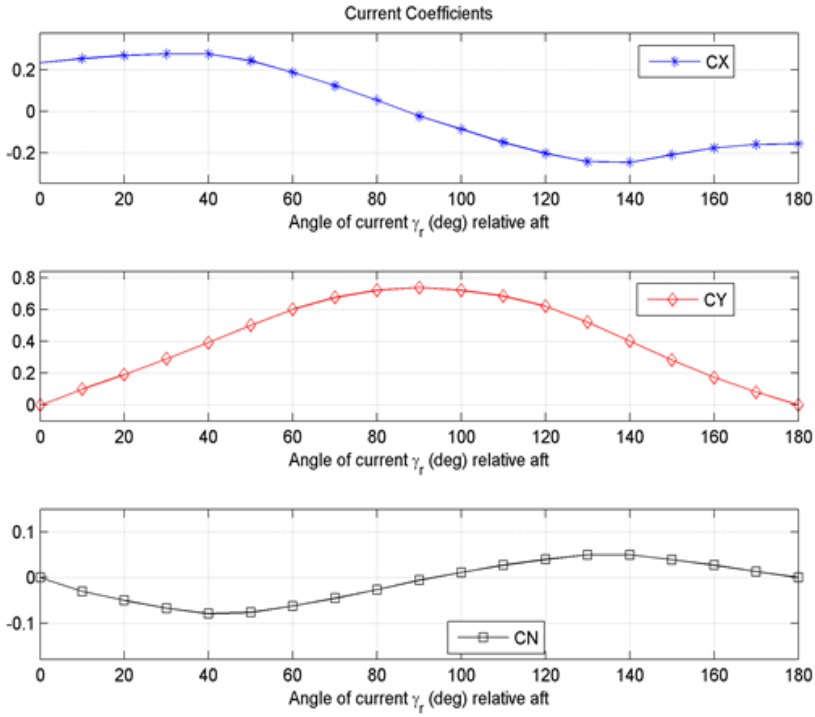

Figure A.3: Current Coefficients

A.2.5 Mass

In CyberSea simulator, the total mass is represented as the rigid-body mass and the hydrodynamic added mass at the infinity frequency, according to Fossen (2011a) giving us:

$$\boldsymbol{M} = \boldsymbol{M_{RB}} + \boldsymbol{M_A} \tag{A.3}$$

$$\boldsymbol{M_{RB}} = \begin{bmatrix} m\boldsymbol{I_{3\times 3}} & -m\boldsymbol{S}(\boldsymbol{r}_g^b) \\ m\boldsymbol{S}(\boldsymbol{r}_g^b) & \boldsymbol{I_b} \end{bmatrix} \tag{A.4}$$

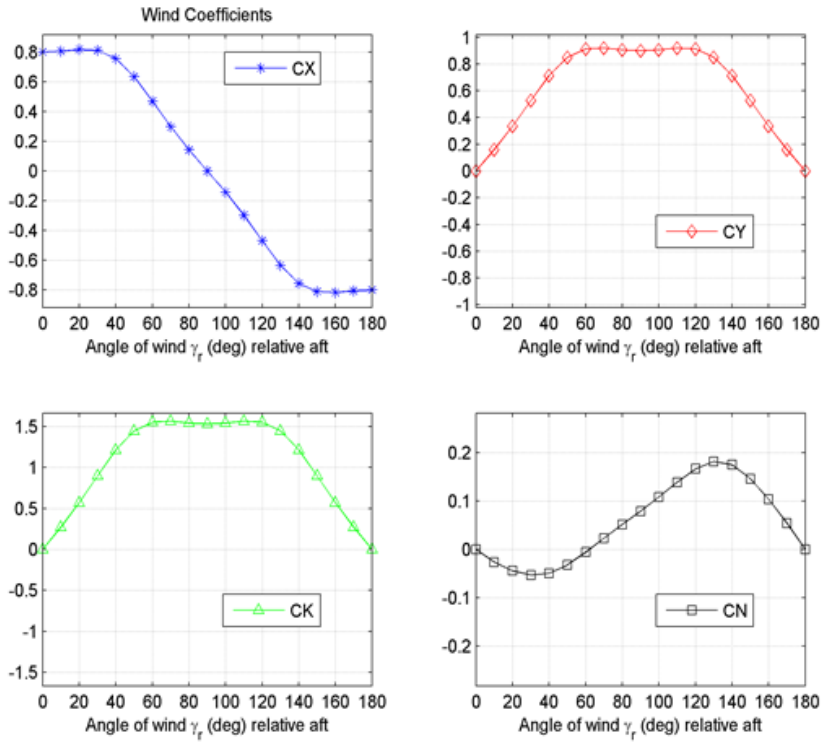

Figure A.4: Wind Coefficients

where $\boldsymbol{S}(\boldsymbol{r}_g^b)$ is the Skew symmetric matrix, and the $\boldsymbol{M_A}$ is the added mass at the infinity infrequence. The rigid-body mass is found to be:

$$\boldsymbol{M_{RB}} = \begin{bmatrix} 74.2000 & 0 & 0 & 0 & -3.1906 & 0 \\ 0 & 74.2000 & 0 & 3.1906 & 0 & 2.6712 \\ 0 & 0 & 74.2000 & 0 & -2.6712 & 0 \\ 0 & 3.1906 & 0 & 1.8730 & 0 & 0.1149 \\ -3.1906 & 0 & -2.6712 & 0 & 18.2493 & 0 \\ 0 & 2.6712 & 0 & 0.1149 & 0 & 18.1121 \end{bmatrix} \quad \text{(A.5)}$$

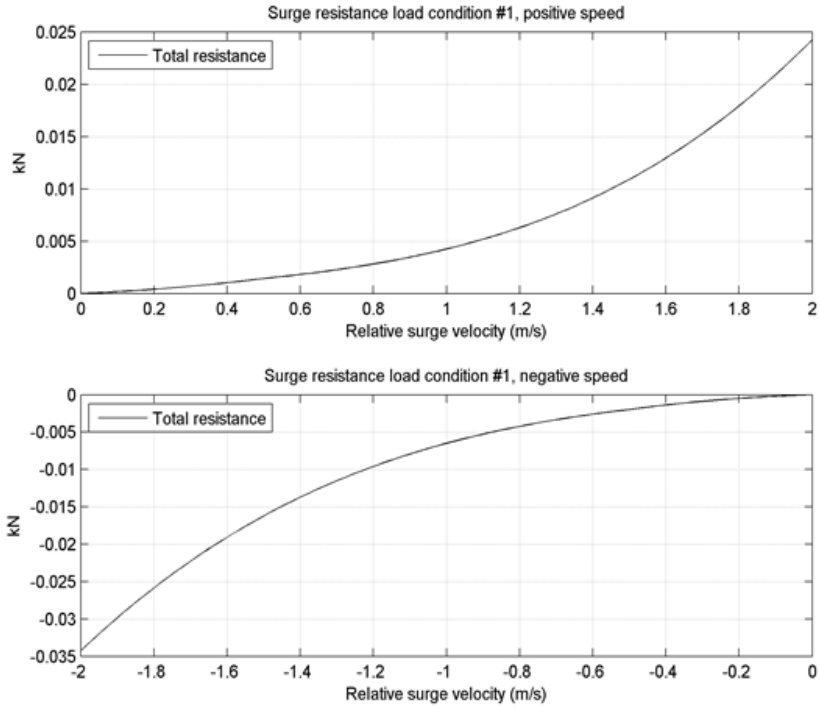

Figure A.5: Surge Resistance Curves relative surge speed

The added mass is is found by the use of WAMIT, and determined to be:

$$\boldsymbol{M_A} = \begin{bmatrix} 2.4480 & 0 & -3.7614 & 0 & -6.3473 & 0 \\ 0 & 22.2892 & 0 & 0.9830 & 0 & 2.0127 \\ -3.7934 & 0 & 120.4109 & 0 & 15.3989 & 0 \\ 0 & 0.9821 & 0 & 0.3711 & 0 & -0.2560 \\ -6.3715 & 0 & 15.4743 & 0 & 22.7731 & 0 \\ 0 & 2.0192 & 0 & -0.2529 & 0 & 4.2847 \end{bmatrix} \quad \text{(A.6)}$$

The total mass is then given by Equation A.3. Table A.6 give the total mass of both the infinity frequency and zero frequency for surge, sway and yaw.

Current direction relative aft (deg)	CX_current (-)	CY_current (-)	CN_current (-)
0.000	0.234	0.000	0.000
10.000	0.254	0.100	-0.030
20.000	0.268	0.192	-0.050
30.000	0.277	0.292	-0.067
40.000	0.277	0.393	-0.079
50.000	0.243	0.502	-0.076
60.000	0.187	0.603	-0.062
70.000	0.123	0.677	-0.045
80.000	0.053	0.722	-0.026
90.000	-0.023	0.740	-0.006
100.000	-0.087	0.721	0.011
110.000	-0.150	0.685	0.027
120.000	-0.203	0.621	0.040
130.000	-0.243	0.521	0.050
140.000	-0.247	0.402	0.050
150.000	-0.210	0.283	0.040
160.000	-0.177	0.174	0.027
170.000	-0.160	0.082	0.013
180.000	-0.157	0.000	0.000

Table A.3: Current Coefficient for 0-180 degrees. Symmetry assumed

Wind direction relative aft (deg)	CX_wind (-)	CY_wind (-)	CK_wind (-)	CN_wind (-)
0.000	0.800	0.000	0.000	-0.000
10.000	0.806	0.160	0.272	-0.026
20.000	0.818	0.335	0.569	-0.044
30.000	0.812	0.527	0.896	-0.053
40.000	0.756	0.714	1.214	-0.049
50.000	0.635	0.851	1.446	-0.032
60.000	0.469	0.913	1.553	-0.006
70.000	0.298	0.920	1.564	0.023
80.000	0.142	0.907	1.542	0.051
90.000	-0.000	0.900	1.530	0.079
100.000	-0.142	0.907	1.542	0.108
110.000	-0.298	0.920	1.564	0.139
120.000	-0.469	0.913	1.553	0.166
130.000	-0.635	0.851	1.446	0.182
140.000	-0.756	0.714	1.214	0.175
150.000	-0.812	0.527	0.896	0.146
160.000	-0.818	0.335	0.569	0.103
170.000	-0.806	0.160	0.272	0.054
180.000	-0.800	0.000	0.000	0.000
190.000	-0.806	-0.160	-0.272	-0.054
200.000	-0.818	-0.335	-0.569	-0.103
210.000	-0.812	-0.527	-0.896	-0.146
220.000	-0.756	-0.714	-1.214	-0.175
230.000	-0.635	-0.851	-1.446	-0.182
240.000	-0.469	-0.913	-1.553	-0.166
250.000	-0.298	-0.920	-1.564	-0.139
260.000	-0.142	-0.907	-1.542	-0.108
270.000	-0.000	-0.900	-1.530	-0.079
280.000	0.142	-0.907	-1.542	-0.051
290.000	0.298	-0.920	-1.564	-0.023
300.000	0.469	-0.913	-1.553	0.006
310.000	0.635	-0.851	-1.446	0.032
320.000	0.756	-0.714	-1.214	0.049
330.000	0.812	-0.527	-0.896	0.053
340.000	0.818	-0.335	-0.569	0.044
350.000	0.806	-0.160	-0.272	0.026
360.000	0.800	-0.000	-0.000	0.000

Table A.4: Wind Coefficient for All Wind Directions.

Para-meter	Description	WL1	Unit
Loa	Length over all	2.275	m
Lpp	Length between perpendiculars	1.971	m
B	Breadth	0.437	m
T	Draft	0.153	m
m	Mass	74.2	kg
V	Volume displacement	0.075	m3
C_B	Block coefficient	0.57	-
A_w	Water plane area	0.8	m2
GM_T	Transverse metacenter height	0.04	m
GM_L	Longitudinal metacenter height	2.75	m
Rii	Radii of gyration R44,R55,R66	[0.157,0.512,0.512]	m
LCG	Horizontal location of CG from AP	1.02	m
VCG	Vertical location of CG from baseline (KG)	0.20	m
r_CG	CG w.r.t to CO = [LPP/2 0 WL] in DWL (x-forward, z-down)	[0.04,0.0,-0.04]	m

Table A.5: Hull Data

DOF	WL1 (ZERO)	WL1 (INF)	Unit
surge	82.0581	79.1642	kg
sway	132.4318	99.1642	kg
yaw	26.9514	22.3968	kg*m2

Table A.6: Total Mass at the zero and infinity frequency

A.3 Propulsion System Configurations

A.3.1 Introduction to the Propulsion System Configurations

The propulsion system on a marine vessel typically consist of prime movers as diesel engines, generators, transmissions and thrusters, Sørensen (2011). In this thesis a *thruster* will be used as a general expression for a propeller unit. In the case of CyberShip III, the vessel is configured with two electric azimuth thrusters in the stern, and one ducted electric azimuth thruster in the bow.

This section will present the configurations done in the CyberSea Vessel simulator, and some key parameters associated with the thrusters. In particular the thruster combinator curves used will be presented, along with the resulting actual power and thrust output from the combinator curves.

A.3.2 Thruster Parameters

We start by labeling the three thrusters on CyberShip III according to Figure A.6

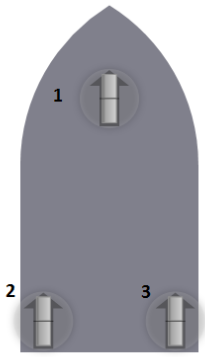

Figure A.6: Thruster Labeling

In order to configure the thrusters to closely match the power load, thrust generated and thrust characteristics of the thruster on CyberShip III, some key parameters needed to be identified. MarinTek provided data on blade dimensions, thruster interface, bollard pull and thrust power. In addition the propeller rise time and location in the z-plane were measured on CyberShip III in MCLab at Tyholt, NTNU. On the basis of the above, the configuration files needed for CyberSea vessel simulator was constructed. Table A.7, Table A.8 and Table A.9 summarizes the key parameters for Thruster1, Thruster2 and Thruster3.

Parameter	Value	Unit
Name/Identification/Tag	Bow Azimuth	-
Thruster type	Azimuth	-
Propeller type	FPP	-
Interface type	thrust with shaft speed/pitch mapping	-
Enabled thrust loss effect (0 = off, 1 = on). [Inline, Transverse, Coanda, Ventilation, Interaction]	[1 1 1 0 0]	-
Diameter	0.04	m
Position w.r.t. CO [x y z]	[0.55 0.00 0.19]	m
Bollard pull thrust ahead (max thrust)	10	N
Propeller shaft speed for bollard pull ahead	4800	RPM
Rated motor power for bollard pull ahead	33.8	W
Bollard pull thrust astern (max thrust)	-10	N
Propeller shaft speed for bollard pull astern	-4800	RPM
Rated motor power for bollard pull astern	33.8	W
Propeller rise time (zero to max)	2.5	s
Azimuth max speed	4800	RPM
Thrust scaling factors (corresponding to +/-100 percent) [min max] for thrust interface)	[-10 10]	N

Table A.7: Thruster 1 Parameters

Parameter	Value	Unit
Name/Identification/Tag	Port Pod	-
Thruster type	Azimuth	-
Propeller type	FPP	-
Interface type	thrust with shaft speed/pitch mapping	-
Enabled thrust loss effect (0 = off, 1 = on). [Inline, Transverse, Coanda, Ventilation, Interaction]	[1 1 1 0 1]	-
Diameter	0.09	m
Position w.r.t. CO [x y z]	[-0.88 -0.12 0.11]	m
Bollard pull thrust ahead (max thrust)	21.9	N
Propeller shaft speed for bollard pull ahead	2400	RPM
Rated motor power for bollard pull ahead	33.8	W
Bollard pull thrust astern (max thrust)	-21.9	N
Propeller shaft speed for bollard pull astern	-2400	RPM
Rated motor power for bollard pull astern	33.8	W
Propeller rise time (zero to max)	2.5	s
Azimuth max speed	2400	RPM
Thrust scaling factors (corresponding to +/-100 percent) [min max] for thrust interface)	[-21.9 21.9]	N

Table A.8: Thruster2 Parameters

Parameter	Value	Unit
Name/Identification/Tag	Starboard Pod	-
Thruster type	Azimuth	-
Propeller type	FPP	-
Interface type	thrust with shaft speed/pitch mapping	-
Enabled thrust loss effect (0 = off, 1 = on). [Inline, Transverse, Coanda, Ventilation, Interaction]	[1 1 1 0 1]	-
Diameter	0.09	m
Position w.r.t. CO [x y z]	[-0.88 0.12 0.11]	m
Bollard pull thrust ahead (max thrust)	21.9	N
Propeller shaft speed for bollard pull ahead	2400	RPM
Rated motor power for bollard pull ahead	33.8	W
Bollard pull thrust astern (max thrust)	-21.9	N
Propeller shaft speed for bollard pull astern	-2400	RPM
Rated motor power for bollard pull astern	33.8	W
Propeller rise time (zero to max)	2.5	s
Azimuth max speed	2400	RPM
Thrust scaling factors (corresponding to +/-100 percent) [min max] for thrust interface)	[-21.9 21.9]	N

Table A.9: Thruster 2 Parameters

A.3.3 Thruster Characteristics

We start by using the above data to find the linear friction component from the power exponent with a least square fit. In addition the bollard pull power used in the propeller characteristics design, such that the total power, including the linear friction component, is correct. This is done by the use of the Marine Cybernetics AS software for thruster configuration. It is important to emphasize that in the case of CyberSSHip III, the thurster data available was severly limited, and calculations were mostly based on the data above, and rough estimates for the unknown parameters to be inputted to the Marine Cybernetics AS software. Figure A.7 and Figure A.8 show the power, as a function of shaft speed, for thruster 1 and thruster 2 and 3 respectively.

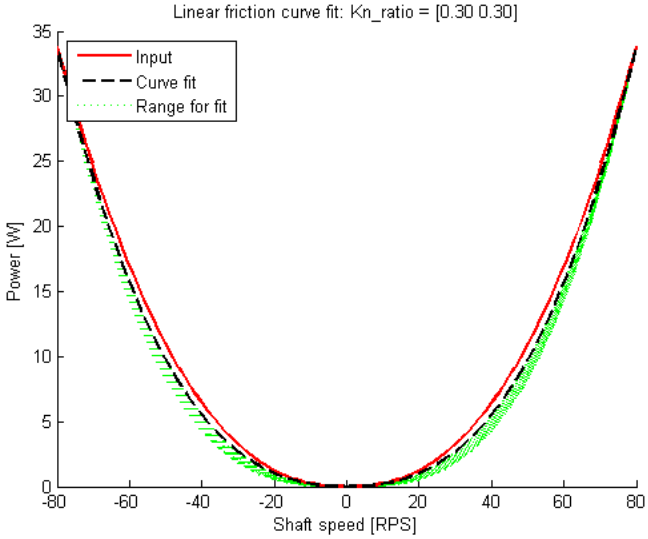

Figure A.7: Thruster 1 power and shaft speed

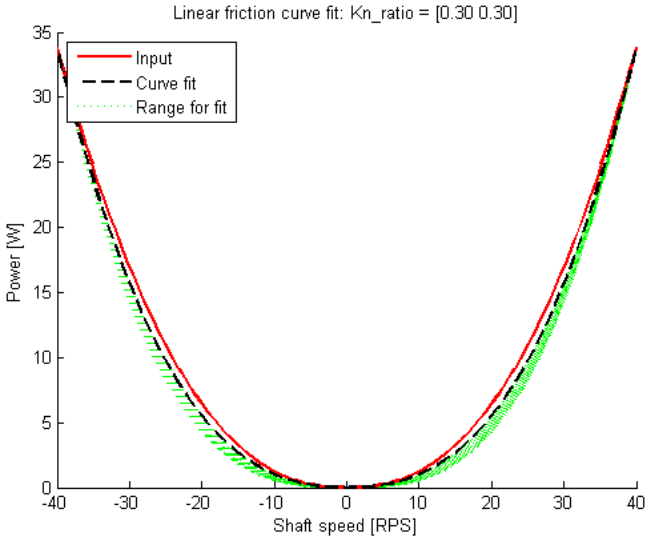

Figure A.8: Thruster 2 and Thruster 3 power and shaft speed

We note that the maximum shaft speed correspond to the maximum power consumption, which indicates that the curves are close to the correct number. We also note that the curves are close to the input, which indicates that the polynomial is a good approximation to the input.

Building upon the configuration we then find advance ratio dependence on thrust and torque coefficients from Wageningen B-series at pitch ratio PD_design. By the use of Marine Cybernetics AS patended software, we then get the n-degree polynomials. In this case we use the 2nd degree polynomials, plotted in Figure A.10 and Figure A.10, for thruster 1, and Thruster 2 and 3 respectively.

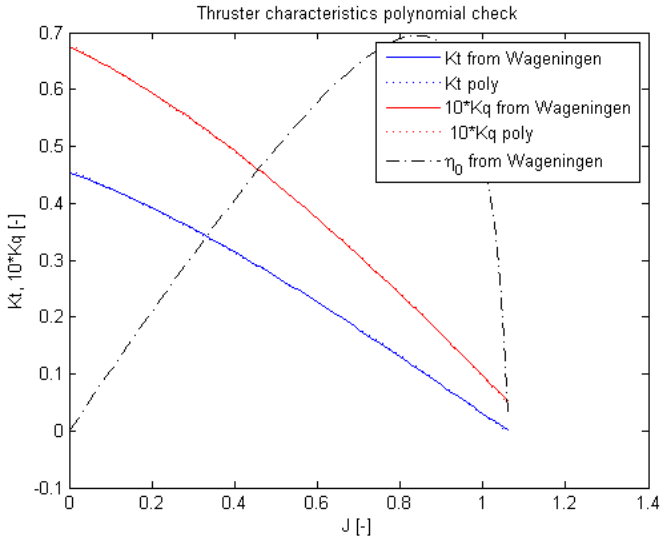

Figure A.9: Thruster 1 2nd degree polynomials

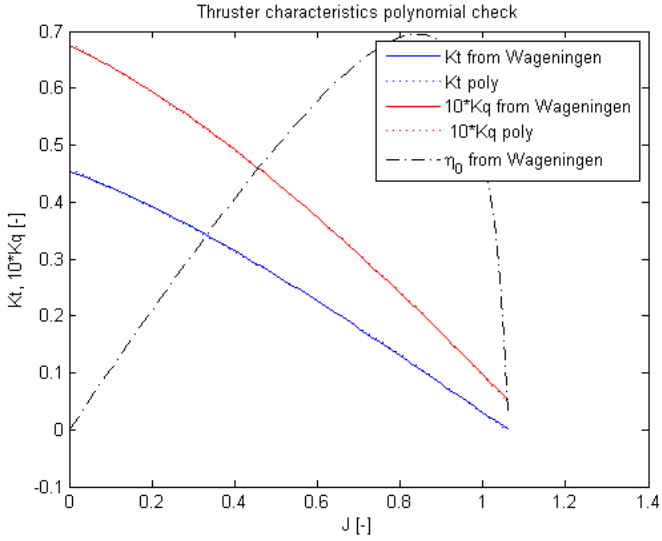

Figure A.10: Thruster 2 and Thruster 3 2nd degree polynomials

The Marine Cybernetics thruster configuration tool have built in checks, and indicated, based upon the configuration, that the results did not have any severe divination from the predicted results. We then map a known open-water propeller characteristics to a full 4-quadrant model. The necessary inputs are the 1-quadrant characteristics and the bollard pull thrust and torque coefficient, in forward and reverse. The model is fitted to match the bollard pull characteristics exactly, and closely match the 1-quadrant characteristics. We note that only the known parts of the model can be expected to be accurate. However, all 4 quadrants of operation are consistently defined using a modification of the Wageningen B4-70 4-quadrant model.In the case of CyberShip III, there are relative large uncertainty related to the characteristics, and the results of the calculations must be seen in this light. Using the Marine Cybernetics software package, we are able to get the following results for the open-water propeller characteristics shown in Figure A.11 for thruster 1, and Figure fig:Thr1OpenWatherChar show the results for Thruster 2 and Thruster3.

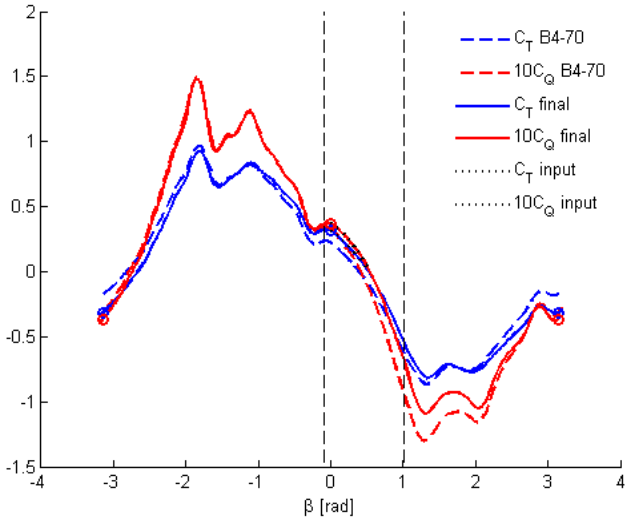

Figure A.11: Thruster 1 propeller characteristics

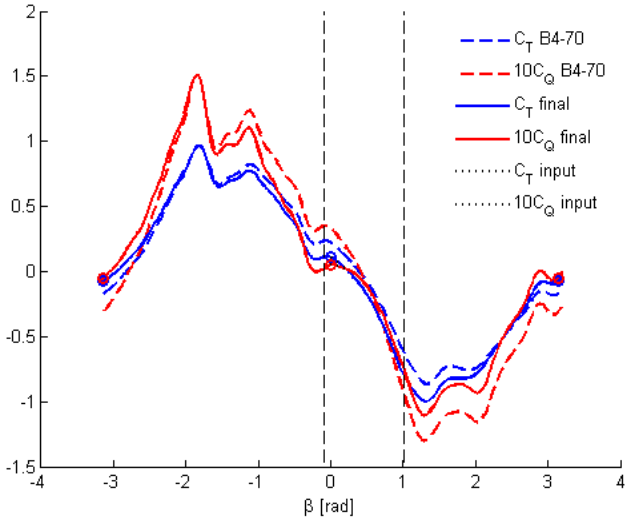

Figure A.12: Thruster 2 and Thruster 3 propeller characteristics

Finally we are able to get the thruster combinator curves. Thruster combinator curves map the RPM-Thrust relationship. This relationship is critical for the lo-level thruster controllers to deliver the desired thrust commanded from the opperator station or the DP system. In the case of CyberShip III, no such combinator could be obtained. It was therefor decided to use the Marine Cybernetics thruster configurator to generate combinator curves based on the data given in Table A.7 Table A.8 and Table A.9. In the case of Thruster 2 and Thruster 3, the combinator curves was assumed to be identical. The generated combinator curves can be sine in Figure A.7 and Figure A.7, where as Figure A.15 and Figure A.16 shows the actual thrust and power based on the combinator curves in Figure A.7 and Figure A.7. We note that the auto-generated combinator curves may deviate to some extent from the true combinator curves exactly, and may be a source to error.

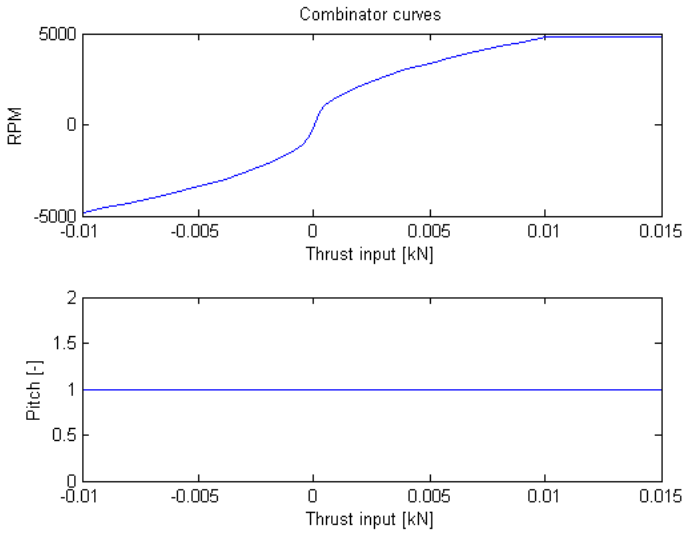

Figure A.13: Thruster 1 Combinator Curve

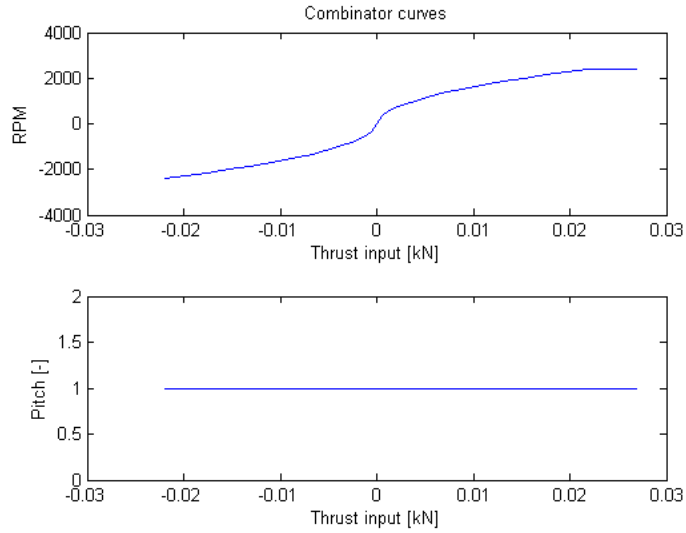

Figure A.14: Thruster 2 and Thruster 3 Combinator Curve

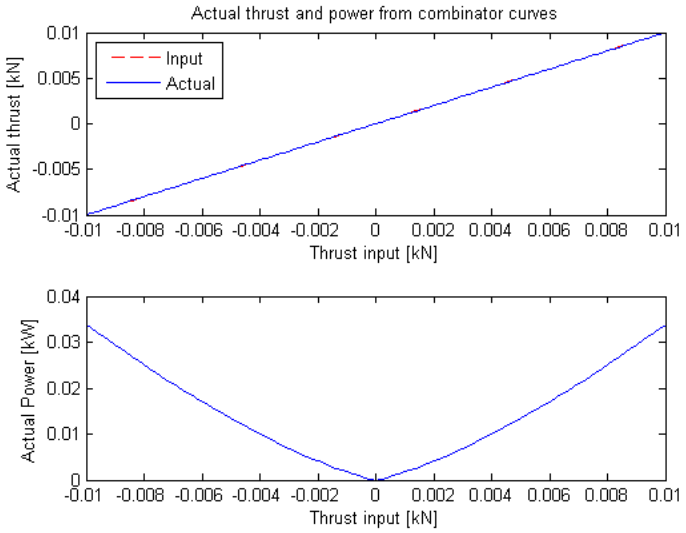

Figure A.15: Thruster 1 Actual Thrust and Power, Based on the Combinator Curves

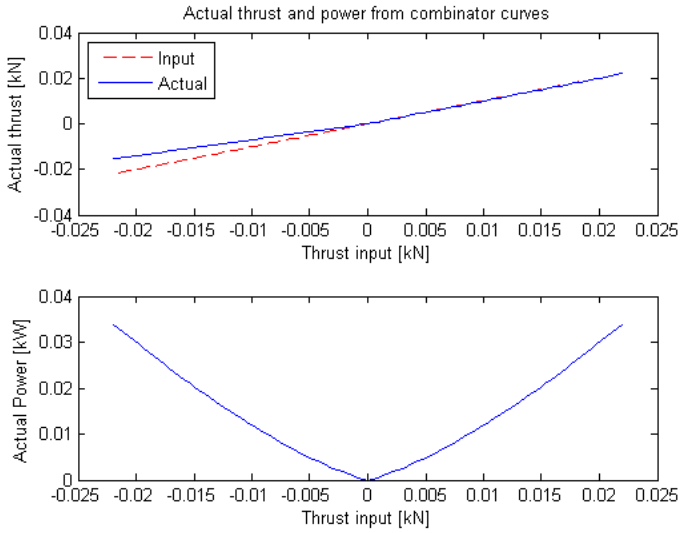

Figure A.16: Thruster 2 and Thruster 3 Actual Thrust and Power, Based on the Combinator Curves

The numerical values for the combinator curves can be found in Appendix E.

A.3.4 Thruster interaction

A thruster may influence other thrusters on a vessel, e.g if a thruster may crate turbulence or influence the speed the water has when passing through an other thruster. In the case of CyberShip III, the bow thruster is assumed to be located a sufficient distance away from the two aft thruster to have any impact on these thrusters. The aft thrusters on the other hand, may cause some interaction. We therefor configure the CyberSea simulator so that:

- Thruster 2 has interaction with thruster 3
- Thruster 3 has interaction with thruster 2

Since CyberShip III does not have any rudders, there will not be any thruster-rudder interaction, and no need for such configurations.

A.4 Power Configurations

This section describes the configuration data of the power system. The power system may have a large impact on a DynCap analysis, in contrast to a static capability analysis. In the case of CyberShip III, the ship is configured with 8 12V batteries in paralleled. At the MCLab, Tyholt, these batteries where tested, and shown to be able to deliver almost instant power, and could be modeled as an ideal voltage source. The following sections will describe the configurations done in order to simulate these batteries as accurately as possible.

A.4.1 Power Configuration Tables

For this reason it was decided to configure the simulator to have a large amount of power relative the maximum thruster power consumption. This was done by configuring one generator connected to a single Bus. In order to circumvent some of the built in checks for wrong configurations, the vessel was also configured with a dummy bus, which only was connected to to main Bus through a bus-tie. Table A.10 show the node setup.

Idx	Tag	Node name	Max. power: (-1 if left out)	Nominal max power	Efficiency: (1.0 if left out)
0	Gen1	Aux. Gen. 1	1 kW		1.0
1	THR1	Bow Azimuth	-1	33.8 W	1.0
2	THR2	Port Pod	-1	33.8 W	1.0
3	THR3	Starboard Pod	-1	33.8 W	1.0
4	Bus1	Main Bus Bar 1 - 690VAC	-1		1.0
5	Bus2	Dummy Bus	-1		-1

Table A.10: Power node setup

A.4.2 Power circuit breakers and bus-ties

In order to simulate the connections onboard CyberShip III, the power distribution was configured according to Table A.11

Index	Tag	From node tag (source)	To node tag (sink)
0	CB1	Gen1	Bus1
1	CB2	Bus1	THR1
2	CB3	Bus1	THR2
3	CB4	Bus1	THR3

Table A.11: Circuit breakers

where CB denotes the circuit breakers and Gen, Bus and THR are the generators, bus, thrusters respectively. In addition the Bus-ties were configured according to Table A.12, and FigurA.17 show a graphical representation of the resulting power configuration.

Index	Tag	Node A Tag	Node B Tag
0	BT1	Bus1	Bus2

Table A.12: Bus-ties

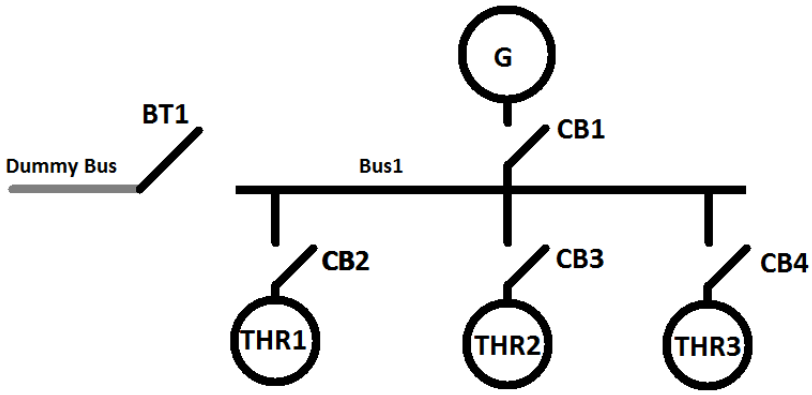

Figure A.17: Power configuration

The resulting power configuration will deliver substantially more power than the system requires, and will then simulate the almost ideal voltage

source the batteries on-board CyberShip III represent.

A.5 Sensors Configurations

A real life DP vessel will have a substantial sensor system on-board, including multiple GPS antennas and VRU's, vindsensors i.l. In the case of the CyberShip experiment, the need for redundancy in the sensor system was not necessary, nor correct. The position and attitude of the vessel during operation at the MCLab, at MarinTek, is provide through a single datalik. In this section the simulator will only be configured to be able to deliver sufficient sensor data to give the current position and attitude of the vessel. The interested reader may consult Fossen (2011a), Sørensen (2011) or Vik (2011) for additional details on sensor systems on board DP vessels and sensor systems in general.

A.5.1 Sensors and Sensor Data

The sensors configured for CyberShip III during simulations was:

- 1 GPS
- 1 VRU
- 1 Gyro compass

The sensors key configuration data is given in Table A.13.

Parameter	Value	Unit
Common reference point w.r.t. CO (r_CRP)	[0.00 0.00 0.00]	m
GPS almanac file	Sem230.txt	-
GPS1 leverarm w.r.t. CRP	[0.2 -0.0 -0.2]	m
GPS1 sample time	0.10	s
VRU1 sample time	0.20	s
Gyro1 sample time	0.20	s

Table A.13: Sensors Configuration Parameters

On the basis of the above parameters, the CyberSea simulator generated the sensorsystem used in the DynCap simulations.

A.6 DP System Configurations

The Marine Cybernetics DP-HiL Simulator CyberSea uses a nonlinear DP controller. The author is not at liberty to disclose all detail surrounding the controller module, but the general structure of the controller is similar to the controller stated in Fossen (2011a). Consider the controller law:

$$\boldsymbol{\tau} = \hat{\boldsymbol{\tau}}_{\boldsymbol{wind}} - \boldsymbol{R^T(\eta)K_p\tilde{\eta}} - \boldsymbol{R^T(\eta)K_dR(\eta)\tilde{\nu}} - \boldsymbol{R^T(\eta)K_i}\int_0^t \tilde{\boldsymbol{\eta}}(\tau)\, d\tau \tag{A.7}$$

where $\boldsymbol{K_p}$, $\boldsymbol{K_d}$ and $\boldsymbol{K_i}$ are the controller gains, and we have that

$$\text{error}_{\boldsymbol{\nu}} = \tilde{\boldsymbol{\nu}} = \boldsymbol{\nu_{ref}} - \boldsymbol{\nu} \tag{A.8}$$

$$\text{error}_{\boldsymbol{\eta}} = \tilde{\boldsymbol{\eta}} = \boldsymbol{\eta_{ref}} - \boldsymbol{\eta} \tag{A.9}$$

further we denote

$$K_d^* = -R^T(\eta)K_dR(\eta) \tag{A.10}$$

According to Fossen (2011a), it is common to select the $\boldsymbol{K_d^*}$ gain as a diagonal matrix, giving us that $K_d^* = K_d$. In the case of full-state feedback, we can according to Fossen (2011a) show that the controller is asymptotically stable by Lyapunov analysis. The Interested reader may consult Fossen (2011a) and Khalil (2002) for details.

We note that in the case of CyberShip III, wind sensor is not available, and the controller law then become:

$$\boldsymbol{\tau} = -\boldsymbol{R^T(\eta)K_p\tilde{\eta}} - \boldsymbol{R^T(\eta)K_dR(\eta)\tilde{\nu}} - \boldsymbol{R^T(\eta)K_i}\int_0^t \tilde{\boldsymbol{\eta}}(\tau)\, d\tau \tag{A.11}$$

The controller gains were then calculated based on the pole-placement algorithm described in Fossen (2011a), giving us:

$$K_p = \frac{\omega_n^2 T}{K} > 0 \tag{A.12}$$

$$K_d = \frac{2\zeta\omega T - 1}{K} > 0 \tag{A.13}$$

$$K_i = \frac{\omega_n^3 T}{10K} > 0 \tag{A.14}$$

where we have that

$$\omega_n = \frac{1}{\sqrt{1-2\zeta^2+\sqrt{4\zeta^4-4\zeta^2+2}}}\omega_b \tag{A.15}$$

$$m = \frac{T}{K} \tag{A.16}$$

$$d = \frac{1}{K} \tag{A.17}$$

where ω_b is the bandwidth of the controller and ζ is the relative damping ratio. Based upon the above equations, the controller was tuned to match the gains used during the experiment described in Part 3. A more detailed examination of the DP system is presented in Part 2. The interested reader may consult Fossen (2011a) and Sørensen (2011).

Appendix B

WAMIT Results

This Appendix contains the plots generated on the basis the results from WAMIT.

B.1 csWamitPlots

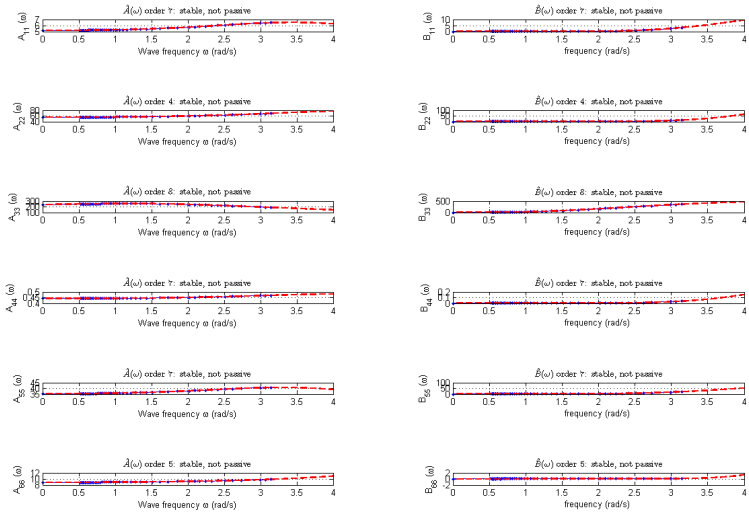

Figure B.1: A(i,i) and B(i, i)

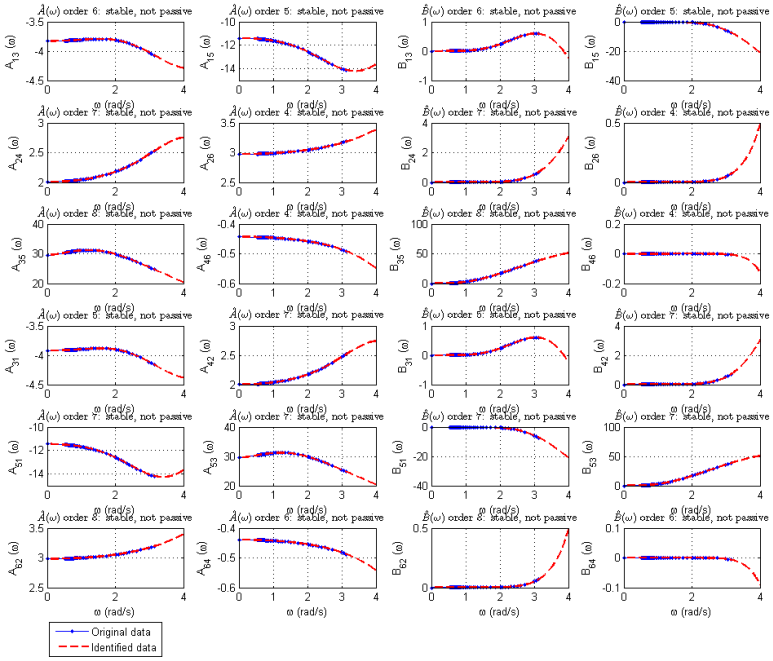
Original data
Identified data
ω (rad/s)

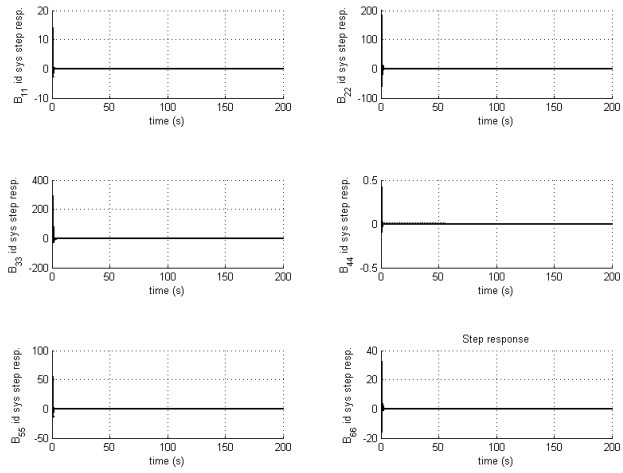

Figure B.2: B(i, i) system identification step response

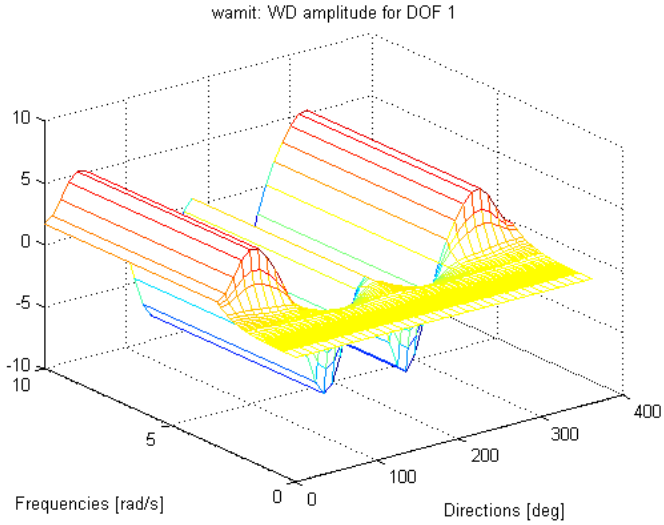

Figure B.3: WD amplitude for DOF 1

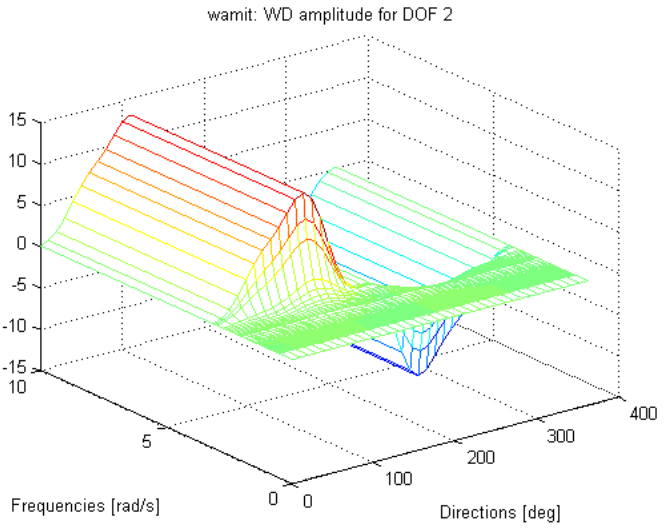

Figure B.4: WD amplitude for DOF 2

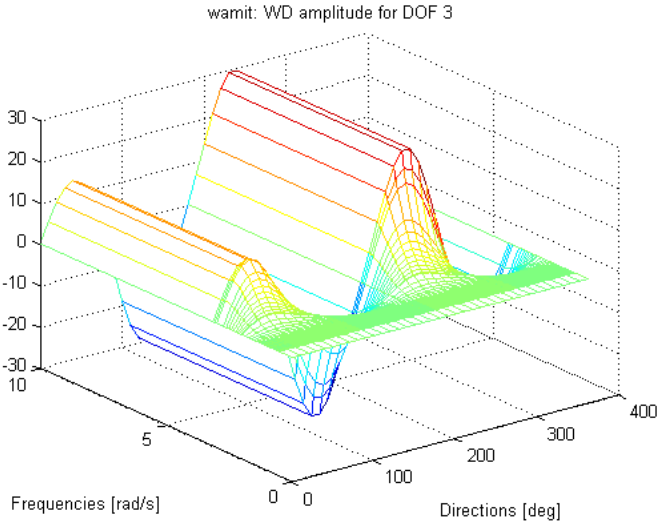

Figure B.5: WD amplitude for DOF 3

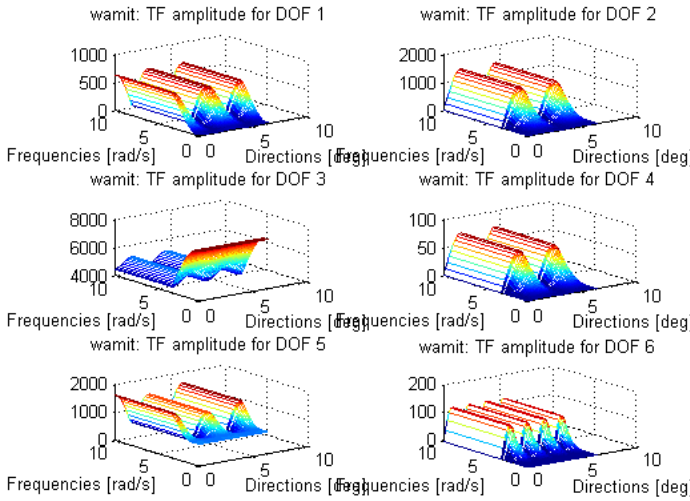

Figure B.6: TF amplitude for DOF 1 and DOF 2

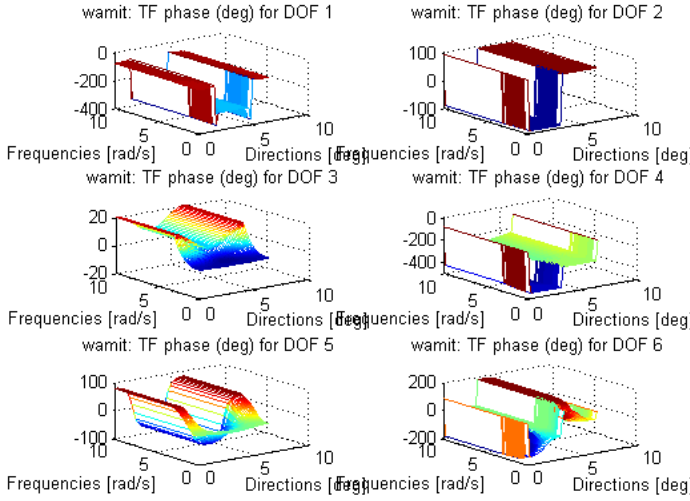

Figure B.7: TF phase for DOF 1 and DOF 2

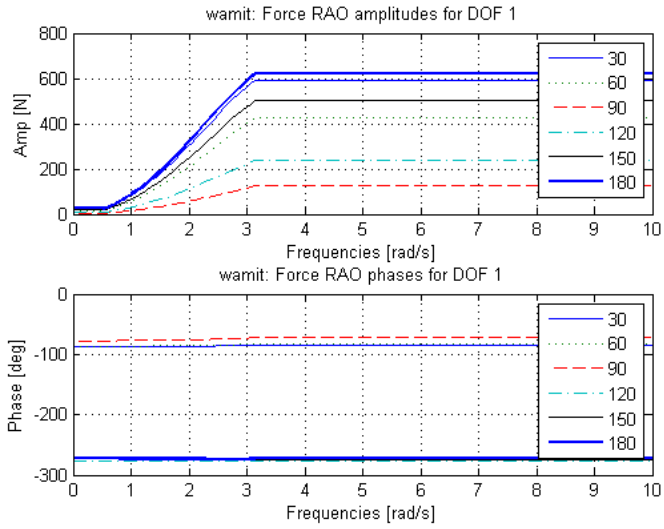

Figure B.8: Force RAO amplitude and phase for DOF 1

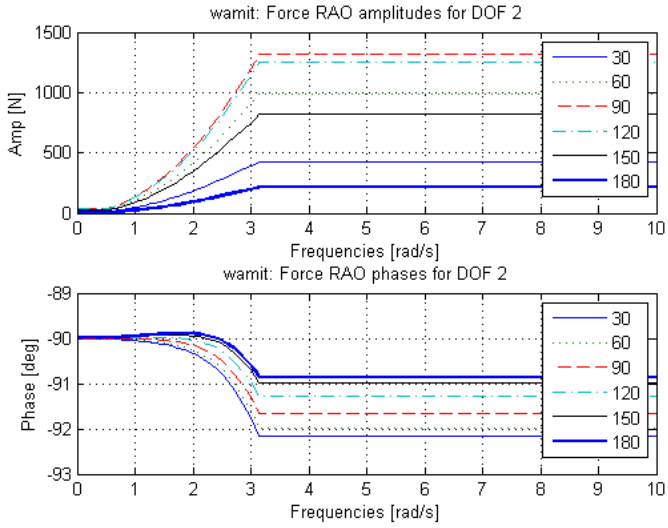

Figure B.9: Force RAO amplitude and phase for DOF 2

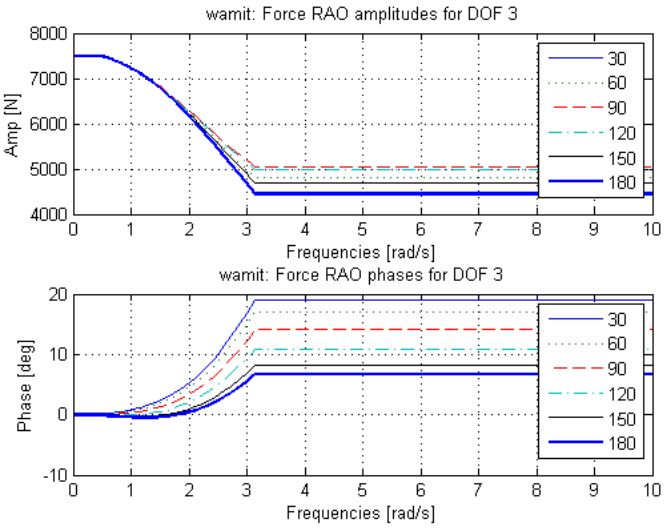

Figure B.10: Force RAO amplitude and phase for DOF 3

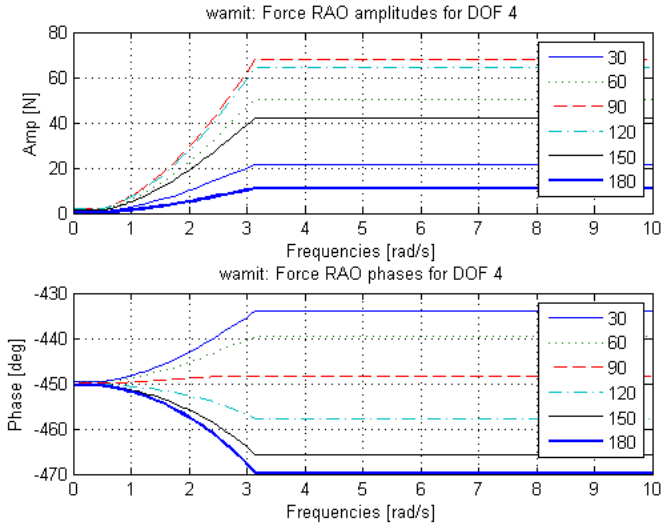

Figure B.11: Force RAO amplitude and phase for DOF 4

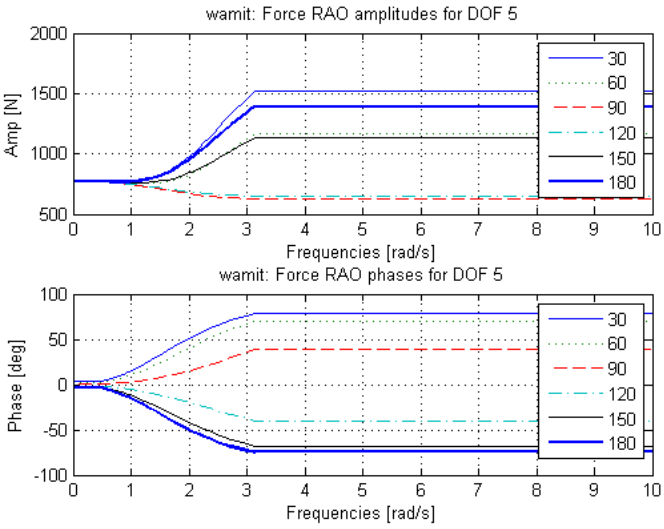

Figure B.12: Force RAO amplitude and phase for DOF 5

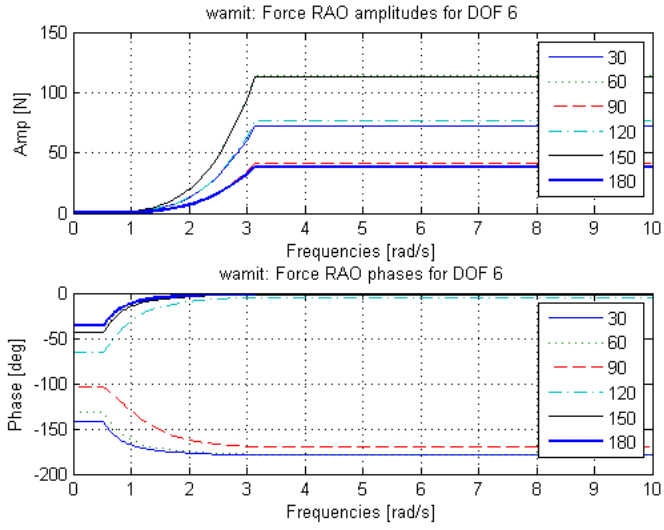

Figure B.13: Force RAO amplitude and phase for DOF 6

B.2 Wave Periods

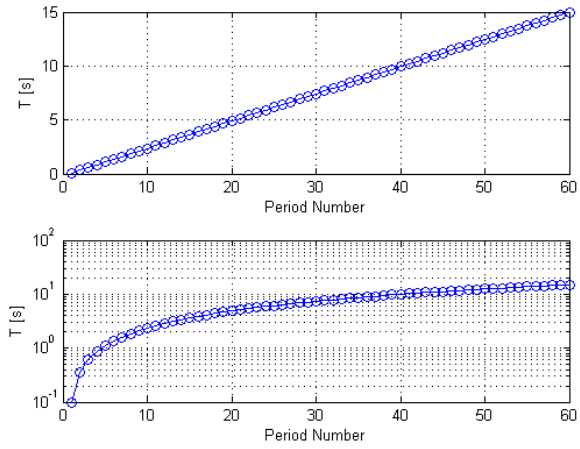

Figure B.14: Period Number

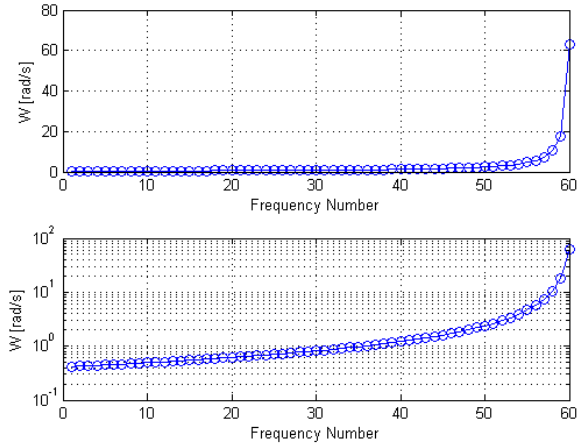

Figure B.15: Frequency Number

Appendix C

WAMIT Transcript

This Appendix contains the raw WAMIT transcript.

********** WAMIT RUN SETTINGS **********

WAMIT Version 6.414

Low-order panel method (ILOWHI=0)

Input from Geometric Data File: init.gdf
Rhino->WAMIT file export (mesh)

Input from Potential Control File: init.pot
Init pot file

POTEN run date and starting time: 27-Feb-2012 -- 15:28:16

Period	Time	RAD	DIFF (max iterations)
-1.0000	15:28:17	-1 (-1)	
1.9000	15:28:17	-1 (-1)	-1 (-1)
1.1000	15:28:18	-1 (-1)	-1 (-1)
0.9000	15:28:18	-1 (-1)	-1 (-1)

Gravity: 9.80665 Length scale: 1.00000
Water depth: infinite Water density: 1025.00000
Panel quadrature indices: IQUAD = 1 ILOG = 1 IDIAG = 1
Source formulation index: ISOR = 1
Diffraction/scattering formulation index: ISCATT = 0
Number of blocks used in linear system: ISOLVE = 1
Number of unknowns in linear system: NEQN = 293

BODY PARAMETERS:

Total panels: 586 Waterline panels: 36 Symmetry: Y=0
Irregular frequency index: IRR = 0

XBODY = 0.0000 YBODY = 0.0000 ZBODY = 0.0000 PHIBODY = 0.0
Volumes (VOLX,VOLY,VOLZ): 0.813706E-01 0.813936E-01 0.813839E-01
Center of Buoyancy (Xb,Yb,Zb): -0.030511 0.000000 -0.061371
Hydrostatic and gravitational restoring coefficients:
C(3,3),C(3,4),C(3,5): 0.75303 0.0000 0.77641E-01
C(4,4),C(4,5),C(4,6): 0.28167E-02 0.0000 0.17592E-02
C(5,5),C(5,6): 0.19932 0.0000
Center of Gravity (Xg,Yg,Zg): -0.010000 0.000000 0.040000

Output from WAMIT

FORCE run date and starting time: 27-Feb-2012 -- 15:28:18

I/O Filenames: init.frc init.p2f init.out
Init frc file

WAMIT geometry file: cybership3model.GDF.

---------- Vessel main parameters ----------
Lpp = 1.97 m
Boa = 0.44 m
Draught = 0.153 m
g = 9.8066
Center of gravity wrt midship and WL is: [xg yg zg] = [-0.01 -0.00 -0.04] (m)
Mass computed from displaced fluid from Wamit is: 0 (tonnes)
Mass input to Wamit : 0.0742 (tonnes)

---------- WAMIT periods and headings ----------
Number of headings = 19.
Number of period = 51, min period = 2.00 s, max period = 11.97 s.

------- Radii of gyration --------
R44 = 0.157 m corresponding to R44 = 0.36 Boa
R55 = 0.512 m corresponding to R55 = 0.26 Lpp
R66 = 0.512 m corresponding to R66 = 0.26 Lpp

------- heave Damping --------
B33 potential = 356
B33 viscous = 0
zeta heave pot = 0.1618
zeta heave visc = 0.0000
zeta heave total = 0.1618

------- Roll Damping --------
B44 potential = 0.0502
B44 viscous = 1.8
zeta roll pot = 0.0030
zeta roll visc = 0.1085
zeta roll total = 0.1115

------- Pitch Damping --------
B55 potential = 103
B55 viscous = 0
zeta pitch pot = 0.1840
zeta pitch visc = 0.0000
zeta pitch total = 0.1840

------- Stability Data --------
GM_T = 0.04 (m)
T roll specified = 1.85 (s)
T roll WAMIT = 1.85 (s)
GM_L = 2.75 (m)
T pitch specified = 1.05 (s)
T pitch WAMIT = 0.96 (s)
T heave specified = 0.94 (s)
T heave WAMIT = 0.93 (s)
---------- DP system ----------
The effect of a DP system is not accounted for.

---------- Mass, damping and spring matrices ----------
MRB =
74.20 0.00 0.00 0.00 3.16 0.00
0.00 74.20 0.00 -3.16 0.00 -1.08
0.00 0.00 74.20 0.00 1.08 0.00
0.00 -3.16 0.00 1.97 0.00 0.05
3.16 0.00 1.08 0.00 19.64 0.00
0.00 -1.08 0.00 0.05 0.00 19.50

D =
0.00 0.00 0.00 0.00 0.00 0.00
0.00 0.00 0.00 0.00 0.00 0.00
0.00 0.00 0.00 0.00 0.00 0.00
0.00 0.00 0.00 1.80 0.00 0.00
0.00 0.00 0.00 0.00 0.00 0.00
0.00 0.00 0.00 0.00 0.00 0.00

G =
0.00 0.00 0.00 0.00 0.00 0.00
0.00 0.00 0.00 0.00 0.00 0.00
0.00 0.00 0.00 0.00 0.00 0.00
0.00 0.00 0.00 0.00 0.00 0.00
0.00 0.00 0.00 0.00 0.00 0.00
0.00 0.00 0.00 0.00 0.00 0.00

Appendix D

Hull Configuration Plots

This Appendix contains the plots generated on the basis of the hydrodynamics from WAMIT and the completed hull configurations.

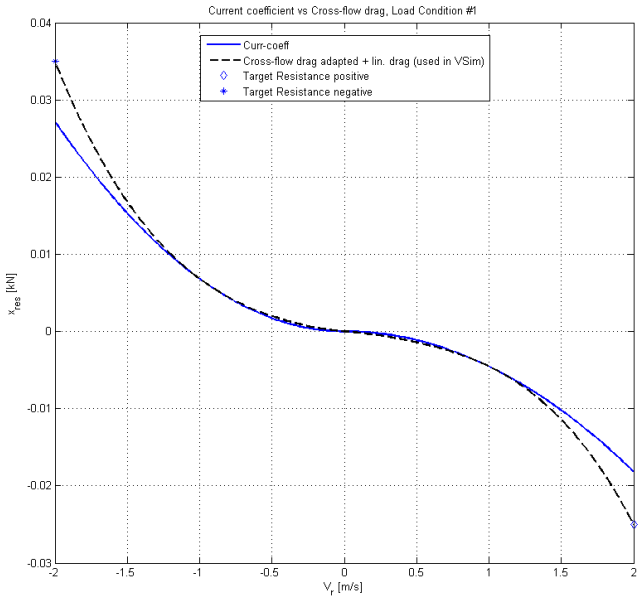

Figure D.1: Current coefficient vs Cross-flow drag

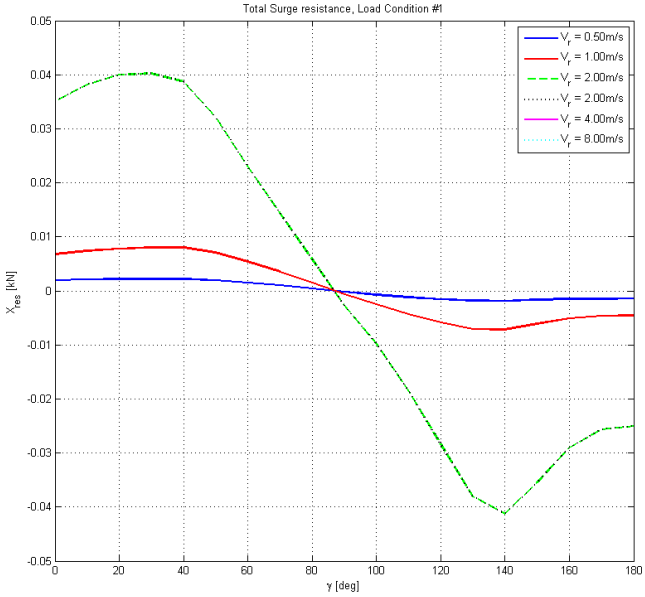

Figure D.2: Total Surge resistance

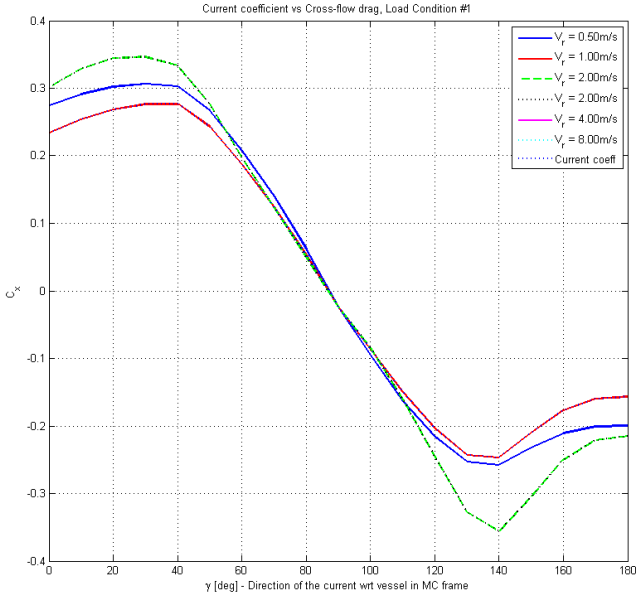

Figure D.3: Current coefficient vs Cross-flow drag, C_x

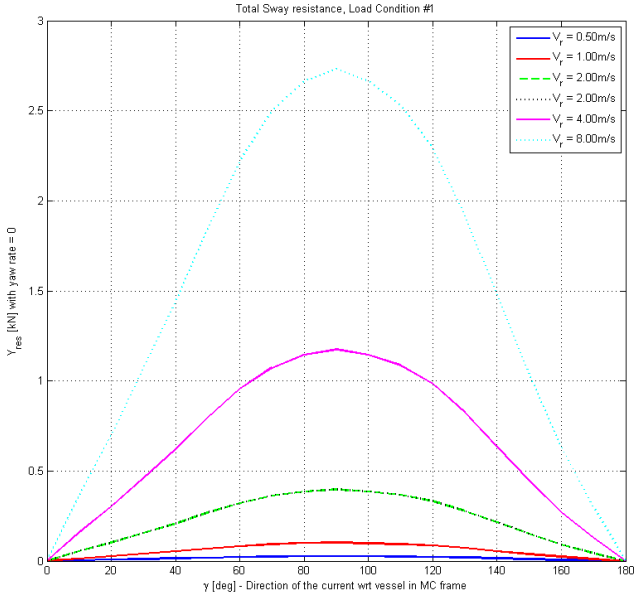

Figure D.4: Total sway force resistance

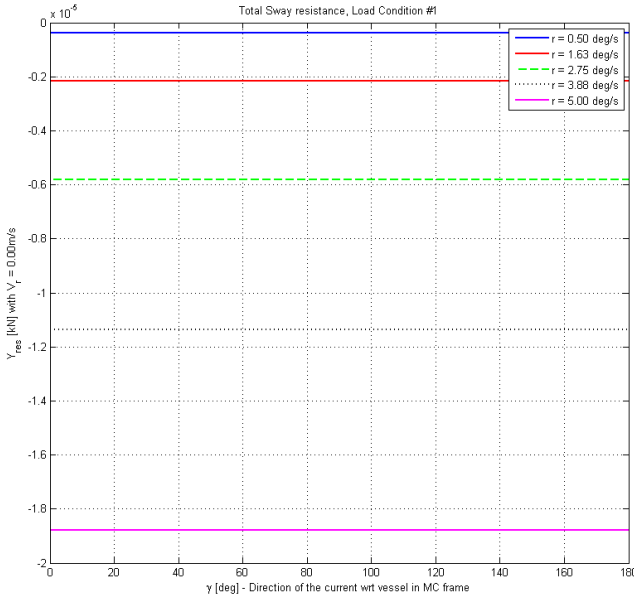

Figure D.5: Total sway resistance

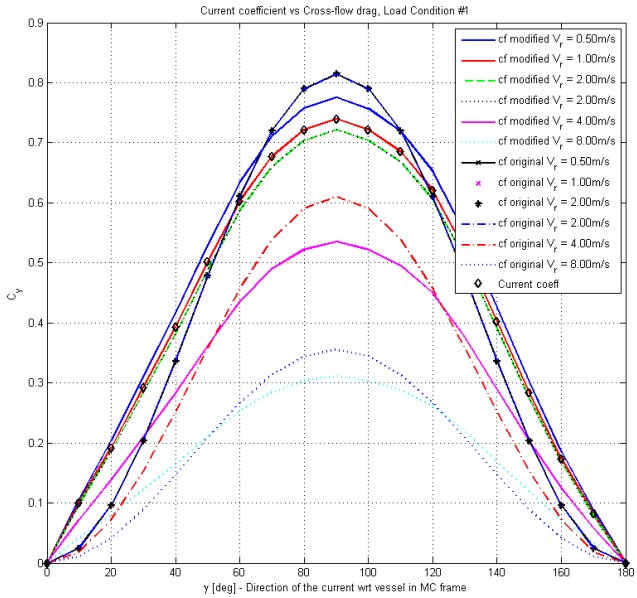

Figure D.6: Current coefficient vs Cross-flow drag, C_y

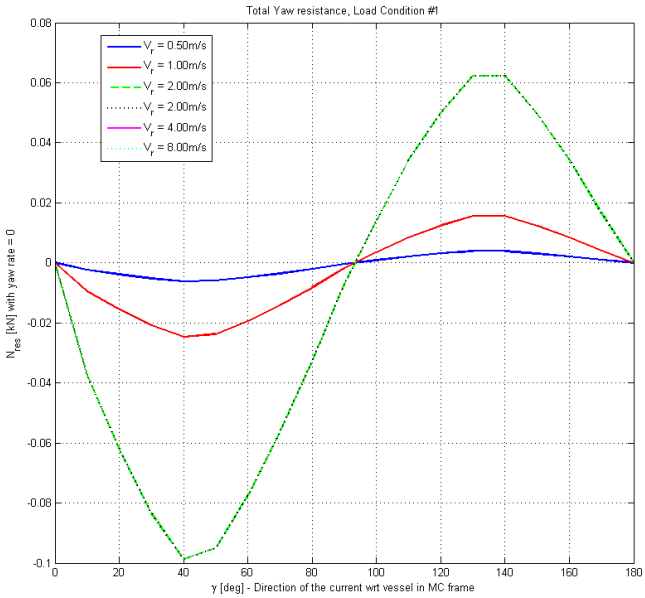

Figure D.7: Total yaw moment resistance

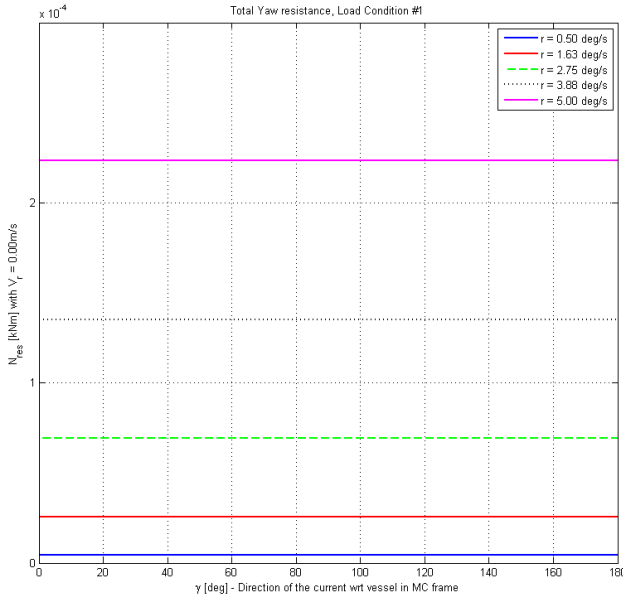

Figure D.8: Total yaw resistance

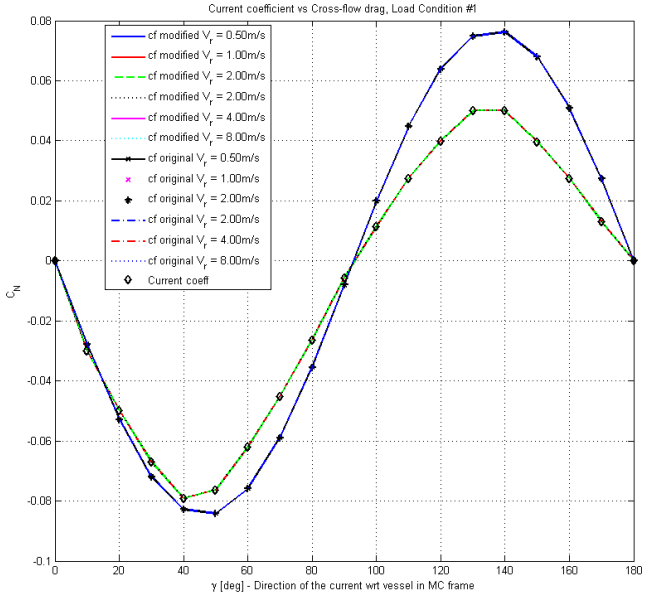

Figure D.9: Current coefficient vs Cross-flow drag, C_N

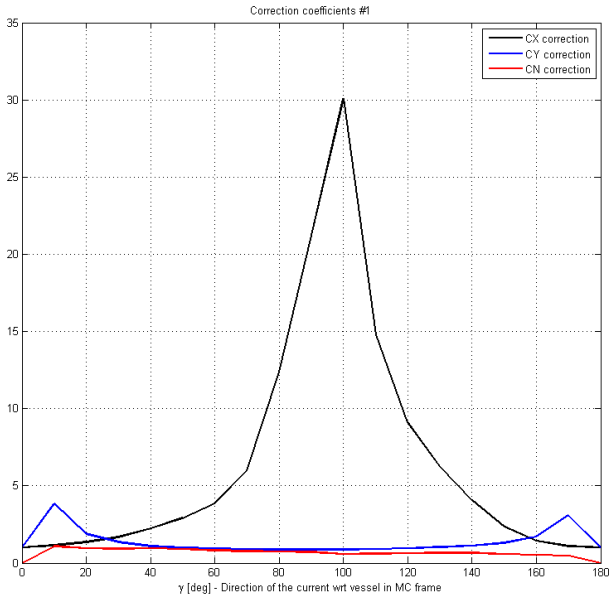

Figure D.10: Correction coefficients

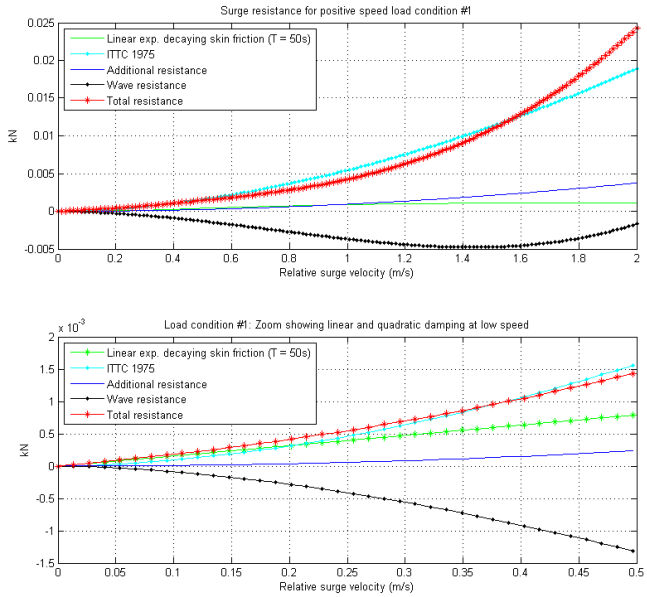

Figure D.11: Surge resistent for positive speed, and zoomed plot showing linear and quadric damping at low speed

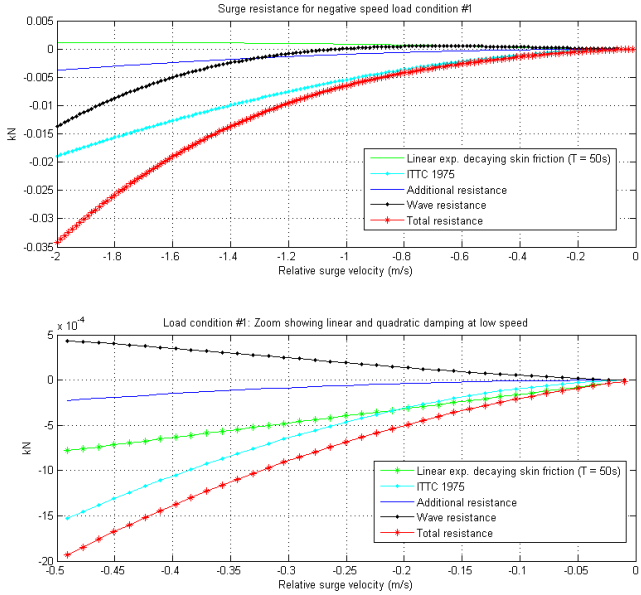

Figure D.12: Surge resistent for negative speed, and zoomed plot showing linear and quadric damping at low speed

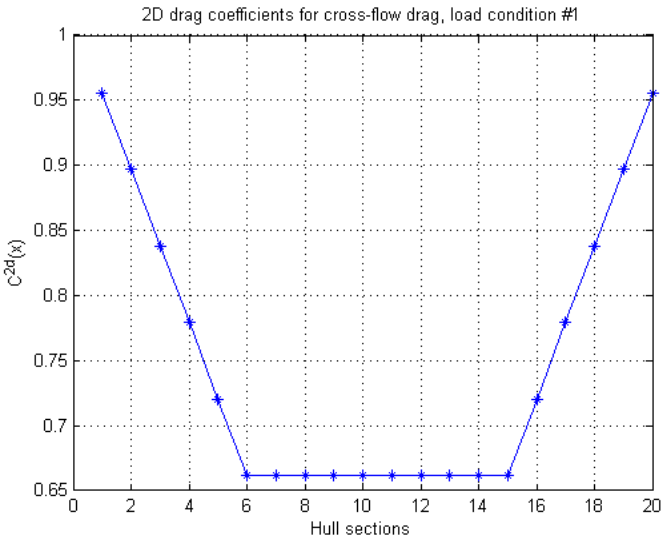

Figure D.13: 2D drag coefficients for cross-flow drag

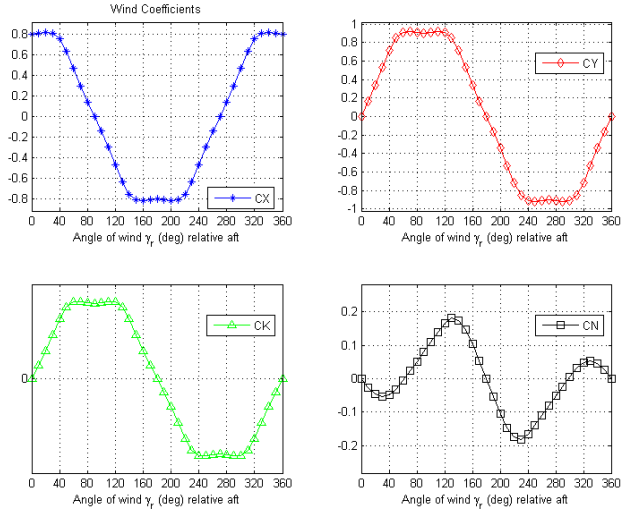

Figure D.14: Wind coefficients

Appendix E

Thruster Characteristics

```
Auto-generated combinator curves:
Par_Thruster.T_vec     = [ -22 -20 -18 -15 -13 -11  -9  -7  -4  -2  -1  -1   0   1   1   2   4   7   9  11  13  15  18  20  22];
Par_Thruster.RPM_p_vec = [ -2400 -2277 -2147 -2008 -1859 -1697 -1518 -1315 -1073 -759 -537 -379   0 379 537 759 1073 1315....
                           ....1518 1697 1859 2008 2147 2277 2400];
Par_Thruster.PD_vec    = [ 1.00 1.00 1.00 1.00 1.00 1.00 1.00 1.00 1.00 1.00 1.00 1.00 1.00 1.00 1.00 1.00 1.00 1.00 1.00....
                          ....1.00 1.00 1.00 1.00 1.00 1.00];
```

Table E.1: Thruster 1 combinator curves

```
Auto-generated combinator curves:
Par_Thruster.F2nPD_T_vec     = [ -22 -20 -18 -15 -13 -11  -9  -7  -4  -2  -1  -1   0   1   1   2   4   7   9  11  13  15  18  20  22];
Par_Thruster.F2nPD_RPM_p_vec = [ -2400 -2277 -2147 -2008 -1859 -1697 -1518 -1315 -1073 -759 -537 -379   0 379 537 759 1073 1315 1518....
                                 ....1697 1859 2008 2147 2277 2400];
Par_Thruster.F2nPD_PD_vec    = [ 1.00 1.00 1.00 1.00 1.00 1.00 1.00 1.00 1.00 1.00 1.00 1.00 1.00 1.00 1.00 1.00 1.00 1.00 1.00....
                                 1.00 1.00 1.00 1.00 1.00];
```

Table E.2: Thruster 2 combinator curves

```
Auto-generated combinator curves:
Par_Thruster.F2nPD_T_vec     = [ -22 -20 -18 -15 -13 -11  -9  -7  -4  -2  -1  -1   0   1   1   2   4   7   9  11  13  15  18  20  22];
Par_Thruster.F2nPD_RPM_p_vec = [ -2400 -2277 -2147 -2008 -1859 -1697 -1518 -1315 -1073 -759 -537 -379   0 379 537 759 1073 1315 1518....
                                 ....1697 1859 2008 2147 2277 2400];
Par_Thruster.F2nPD_PD_vec    = [ 1.00 1.00 1.00 1.00 1.00 1.00 1.00 1.00 1.00 1.00 1.00 1.00 1.00 1.00 1.00 1.00 1.00 1.00 1.00 1.00....
                                 1.00 1.00 1.00 1.00 1.00];
```

Table E.3: Thruster 3 combinator curves

Appendix F

Stability

This chapter will state some select definitions on stability and theorems, that are of relevance to the control system designed in Chapter 11

F.1 General Stability

Consider the nonlinear time-varying system

$$\dot{\boldsymbol{x}} = \boldsymbol{f}(t, \boldsymbol{x}), \quad \boldsymbol{x} \in \mathbb{R}^n \tag{F.1}$$

where $\boldsymbol{f} : \mathbb{R}^+ \times \mathbb{R}^n \to \mathbb{R}^+$ is assumed to be piecewise continious in t, and locally Lipschitz in$\boldsymbol{x}$.

According to Khalil (2002) we have that *uniformly stability* is given by:

Definition 3. *Uniform stability (Khalil (2002))*
The equilibrium point $x = 0$ of (F.1) is:

- *stable if, for each $\varepsilon > 0$, there is $\delta = \delta(\varepsilon, t_0)$ such that*

$$||x(t_0)|| < \delta \Rightarrow ||x(t)|| < \epsilon, \ \forall t \geq t_0 \geq 0 \tag{F.2}$$

- *uniformly stable if, for each $\varepsilon > 0$, there is $\delta = \delta(\varepsilon) > 0$, independent of t_0, such that (F.2) is satisfied.*

- *unstable if it is not stable*

- *asymptotically stable if it is stable and there is a positive constant* $c = c(t_0)$*, such that* $x(t) \to 0$ *as* $t \to \infty$*, for all* $||x(t_0)|| < c$

- *uniformly asymptotically stable if it is uniformly stable and there is a positive constant* c*, independent of* t_0*, such that for all* $||x(t_0)|| < c$*,* $x(t) \to 0$ *as* $t \to \infty$*, uniformly in* t_0*; that is, for each* $\eta > 0$*, there is* $T = T(\nu) > 0$*, such that*

$$||x(t)|| < \eta, \ \forall t \geq t_0 + T(\eta), \ \forall ||x(t_0)|| < c \tag{F.3}$$

- *globally uniformly asymptotically stable if it is uniformly stable,* $\delta(\varepsilon)$ *can be chosen to satisfy* $\lim_{\varepsilon \to \infty} \delta(\varepsilon) = \infty$*, and, for each pair of positive number* η *and* c*, there is* $T = T(\eta, c) > 0$ *such that*

$$||x(t)|| < \eta, \ \forall t \geq t_0 + T(\eta, c), \ \forall ||x(t_0)|| < c \tag{F.4}$$

Appendix G

Laboratory Log

This appendix contains the laboratory log, which was written during the CyberShip III capability experiment. By a manual line search the individual limits for all degrees where experimentally found, and results written in this log. In addition to the log, the data log from the experiment can be found in the digital appendix.

Wind and Wave scaling, by BIS method

Scale 1:1			Scale 1:30		
Wind	H_s	Periode	Wind	H_s	Periode
1,0	0,0214143	0,00	0,06	0,000713809	0,00
2,0	0,0856570	0,00	0,12	0,002855235	0,00
3,0	0,1927283	0,00	0,17	0,006424278	0,00
4,0	0,5353565	0,00	0,23	0,017845216	0,00
5,0	0,5353565	1,41	0,29	0,017845216	0,81
6,0	0,7709133	1,41	0,35	0,025697111	0,81
7,0	1,0492987	0,00	0,41	0,034976623	0,00
8,0	1,3705126	1,42	0,47	0,045683752	0,81
9,0	1,7345550	0,00	0,52	0,057818499	0,00
10,0	2,1414259	1,41	0,58	0,071380863	0,81
11,0	2,5911233	0,00	0,64	0,086370777	0,00
12,0	3,0836533	0,00	0,70	0,102788442	0,00
13,0	3,6190097	0,00	0,76	0,120633658	0,00
14,0	4,8182082	0,00	0,82	0,160606941	0,00
15,0	4,8820824	0,00	0,87	0,162736079	0,00
16,0	5,4805026	0,00	0,93	0,182683421	0,00
17,0	6,1887208	0,00	0,99	0,206290693	0,00
18,0	6,9382199	0,00	1,05	0,231273995	0,00
19,0	7,7305474	0,00	1,11	0,257684915	0,00
20,0	8,5657035	0,00	1,17	0,285523451	0,00

Constants	
Gravity	g 9,80655
Scale length	L 30,00

Scale	CS3
Linear Velocity	sqrt(L*g) 17,1522
Length	L 30
Time	sqrt(L/g) 1,7482

Wind/Wave Calculator	
U_(19,5)	H_s
9,5	1,93263686

Figure G.1: Laboratory Log - Wind and Wave scaling table and calculator

VARI-AC Lookup Table

Position	Voltage	Measured	
0	10	0	[m/s]
0	20	0	[m/s]
0	30	0	[m/s]
0	40	0	[m/s]
0	50	0	[m/s]
0	60	0	[m/s]
0	70	0	[m/s]
0	80	0	[m/s]
0	90	0	[m/s]
0	100	0	[m/s]
0	110	0	[m/s]
0	120	0,1	[m/s]
0	130	0,1	[m/s]
0	132,5	0,2	[m/s]
0	135	0,3	[m/s]
0	140	0,3	[m/s]
0	150	0,4	[m/s]
0	160	0,5	[m/s]
0	170	0,6	[m/s]
0	175	0,7	[m/s]
0	180	0,8	[m/s]
0	190	0,9	[m/s]

Figure G.2: Laboratory Log - Variable AC Lookup Table

Wind and wave scaling by BIS method

Status	Scale 1:1			Scale 1:30		
	Wind	H_s	Periode	Wind	H_s	Periode
OK	1,0	0,0214143	1,42	0,06	0,000713809	0,81
OK	2,0	0,0856570	1,42	0,12	0,002855235	0,81
OK	3,0	0,1927283	1,42	0,17	0,006424278	0,81
OK	4,0	0,5353565	1,42	0,23	0,017845216	0,81
OK	5,0	0,5353565	1,42	0,29	0,017845216	0,81
OK	6,0	0,7709133	1,42	0,35	0,025697111	0,81
OK	7,0	1,0492987	1,42	0,41	0,034976623	0,81
OK	8,0	1,3705126	1,42	0,47	0,045683752	0,81
Fail	*8,5*	*1,5471800*	1,42	*0,50*	*0,051572667*	*0,81*
Fail	9,0	1,7345550	1,42	0,52	0,057818499	0,81
Fail	10,0	2,1414259	1,42	0,58	0,071380863	0,81
Fail	11,0	2,5911233	1,42	0,64	0,086370777	0,81
Fail	12,0	3,0836533	1,42	0,70	0,102788442	0,81
Fail	13,0	3,6190097	1,42	0,76	0,120633658	0,81
Fail	14,0	4,8182082	1,42	0,82	0,160606941	0,81
Fail	15,0	4,8820824	1,42	0,87	0,162736079	0,81
N/A	16,0	5,4805026	0,00	0,93	0,182683421	0,00
N/A	17,0	6,1887208	0,00	0,99	0,206290693	0,00
N/A	18,0	6,9382199	0,00	1,05	0,231273995	0,00
N/A	19,0	7,7305474	0,00	1,11	0,257684915	0,00
N/A	20,0	8,5657035	0,00	1,17	0,285523451	0,00

* N/A = Not Applicable - due to limitations at the MCLab

Constants		
Gravity	g	9,80655
Scale leng	L	30,00

Scale	CS1
Linear Vel sqrt(L*g)	17,1522
Length L	30
Time sqrt(L/g)	1,7482

Wind/Wave Calculator	
U_(19,5)	H_s
8,50	1,54718
	0,051573

Line search

Run nr	Wind	Stabilize time	Duration	Result	Voltage	Experiment
1	6 m/s	10 min	15 min	OK	140 V	Completed
2	10 m/s	10 min	3 min	Fail	170 V	Aborted
3	8 m/s	10 min	15 min	OK	158 V	Completed
4	9 m/s	10 min	3 min	Fail	162 V	Aborted
5	8.5 m/s	10 min	9 min	Fail	160 V	Aborted
6						
7						
8						
9						
10						

Final result

8 m/s

Figure G.3: Laboratory Log - Heading 0 deg

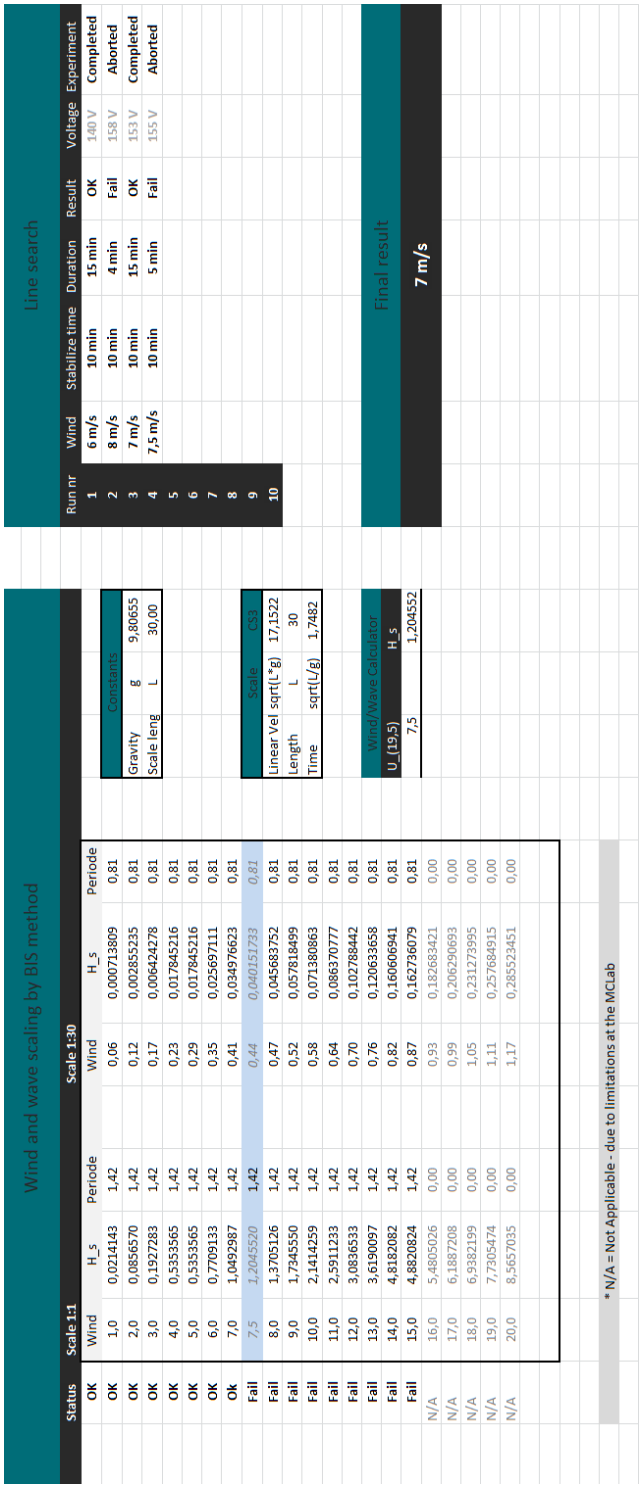

Figure G.4: Laboratory Log - Heading 10 deg

Wind and wave scaling by BIS method

Status	Scale 1:1			Scale 1:30			
	Wind	H_s	Periode	Wind	H_s	Periode	
OK	1,0	0,0214143	1,42	0,06	0,000713809	0,81	
OK	2,0	0,0856570	1,42	0,12	0,002855235	0,81	
OK	3,0	0,1927283	1,42	0,17	0,006424278	0,81	
OK	4,0	0,5353565	1,42	0,23	0,017845216	0,81	
OK	5,0	0,5353565	1,42	0,29	0,017845216	0,81	
OK	6,0	0,7709133	1,42	0,35	0,025697111	0,81	
OK	6,5	0,9047520	1,42	0,38	0,030158400	0,81	
Fail	7,0	1,0492987	1,42	0,41	0,034976623	0,81	
Fail	8,0	1,3705126	1,42	0,47	0,045683752	0,81	
Fail	9,0	1,7345550	1,42	0,52	0,057818499	0,81	
Fail	10,0	2,1414259	1,42	0,58	0,071380863	0,81	
Fail	11,0	2,5911233	1,42	0,64	0,086370777	0,81	
Fail	12,0	3,0836533	1,42	0,70	0,102788442	0,81	
Fail	13,0	3,6190097	1,42	0,76	0,120633658	0,81	
Fail	14,0	4,8182082	1,42	0,82	0,160606941	0,81	
Fail	15,0	4,8820824	1,42	0,87	0,162736079	0,81	
N/A	16,0	5,4805026	0,00	0,93	0,182683421	0,00	
N/A	17,0	6,1887208	0,00	0,99	0,206290693	0,00	
N/A	18,0	6,9382199	0,00	1,05	0,231273995	0,00	
N/A	19,0	7,7305474	0,00	1,11	0,257684915	0,00	
N/A	20,0	8,5657035	0,00	1,17	0,285523451	0,00	

Constants		
Gravity	g	9,80655
Scale leng	L	30,00

Scale	CS3
Linear Vel sqrt(L*g)	17,1522
Length L	30
Time sqrt(L/g)	1,7482

Wind/Wave Calculator	
U_(19,5)	H_s
6,5	0,904752

Line search

Run nr	Wind	Stabilize time	Duration	Result	Voltage	Experiment
1	6 m/s	10 min	15 min	OK	140 V	Completed
2	7 m/s	10 min	15 min	Fail	153 V	Completed
3	6,5 m/s	10 min	15 min	OK	145 V	Completed
4						
5						
6						
7						
8						
9						
10						

Final result

6,5 m/s

* N/A = Not Applicable - due to limitations at the MCLab

Figure G.5: Laboratory Log - Heading 20 deg

Wind and wave scaling by BIS method

Status	Scale 1:1			Scale 1:30		
	Wind	H_s	Periode	Wind	H_s	Periode
OK	1,0	0,0214143	0,00	0,06	0,000713809	0,00
OK	2,0	0,0856570	0,00	0,12	0,002855235	0,00
OK	3,0	0,1927283	0,00	0,17	0,006424278	0,00
OK	4,0	0,5353565	0,00	0,23	0,017845216	0,00
OK	5,0	0,5353565	1,42	0,29	0,017845216	0,81
OK	5,5	0,6477810	1,42	0,32	0,021592700	0,81
Fail	6,0	0,7709133	0,00	0,35	0,025697111	0,00
Fail	7,0	1,0492987	0,00	0,41	0,034976623	0,00
Fail	8,0	1,3705126	0,00	0,47	0,045683752	0,00
Fail	9,0	1,7345550	0,00	0,52	0,057818499	0,00
Fail	10,0	2,1414259	0,00	0,58	0,071380863	0,00
Fail	11,0	2,5911233	0,00	0,64	0,086370777	0,00
Fail	12,0	3,0836533	0,00	0,70	0,102788442	0,00
Fail	13,0	3,6190097	0,00	0,76	0,120633658	0,00
Fail	14,0	4,8182082	0,00	0,82	0,160606941	0,00
Fail	15,0	4,8820824	0,00	0,87	0,162736079	0,00
N/A	16,0	5,4805026	0,00	0,93	0,182683421	0,00
N/A	17,0	6,1887208	0,00	0,99	0,206290693	0,00
N/A	18,0	6,9382199	0,00	1,05	0,231273995	0,00
N/A	19,0	7,7305474	0,00	1,11	0,257684915	0,00
N/A	20,0	8,5657035	0,00	1,17	0,285523451	0,00

Constants		
Gravity	g	9,80655
Scale leng	L	30,00

Scale	CS3	
Linear Vel	sqrt(L*g)	17,1522
Length	L	30
Time	sqrt(L/g)	1,7482

Wind/Wave Calculator	
U (19,5)	H_s
5,5	0,647781

* N/A = Not Applicable - due to limitations at the MCLab

Line Search

Run nr	Wind	Stabilize time	Duration	Result	Voltage	Experiment
1	6 m/s	10 min	15 min	Fail	140 V	Completed
2	5,5 m/s	10 min	15 min	OK	135 V	Completed
3						
4						
5						
6						
7						
8						
9						
10						

Final result

5,5 m/s

Figure G.6: Laboratory Log - Heading 30 deg

Wind and wave scaling by BIS method

Status	Scale 1:1			Scale 1:30		
	Wind	H_s	Periode	Wind	H_s	Periode
OK	1,0	0,0214143	1,42	0,06	0,000713809	0,81
OK	2,0	0,0856570	1,42	0,12	0,002855235	0,81
OK	3,0	0,1927283	1,42	0,17	0,006424278	0,81
OK	4,0	0,5353565	1,42	0,23	0,017845216	0,81
OK	5,0	0,5353565	1,42	0,29	0,017845216	0,81
OK	5,5	0,6477810	1,42	0,32	0,021592700	0,81
Fail	6,0	0,7709133	1,42	0,35	0,025697111	0,81
Fail	7,0	1,0492987	1,42	0,41	0,034976623	0,81
Fail	8,0	1,3705126	1,42	0,47	0,045683752	0,81
Fail	9,0	1,7345550	1,42	0,52	0,057818499	0,81
Fail	10,0	2,1414259	1,42	0,58	0,071380863	0,81
Fail	11,0	2,5911233	1,42	0,64	0,086370777	0,81
Fail	12,0	3,0836533	1,42	0,70	0,102788442	0,81
Fail	13,0	3,6190097	1,42	0,76	0,120633658	0,81
Fail	14,0	4,8182082	1,42	0,82	0,160606941	0,81
Fail	15,0	4,8820824	1,42	0,87	0,162736079	0,81
N/A	16,0	5,4805026	0,00	0,93	0,182683421	0,00
N/A	17,0	6,1887208	0,00	0,99	0,206290693	0,00
N/A	18,0	6,9382199	0,00	1,05	0,231273995	0,00
N/A	19,0	7,7305474	0,00	1,11	0,257684915	0,00
N/A	20,0	8,5657035	0,00	1,17	0,285523451	0,00

* N/A = Not Applicable - due to limitations at the MCLab

Constants	
Gravity	g 9,80655
Scale leng	L 30,00

Scale	CS3
Linear Vel sqrt(L*g)	17,1522
Length	L 30
Time	sqrt(L/g) 1,7482

Wind/Wave Calculator	
U (19,5)	H_s
5,5	0,647781

Line Search

Run nr	Wind	Stabilize time	Duration	Result	Voltage	Experiment
1	5,5 m/s	10 min	15 min	OK	135 V	Completed
2	6 m/s	10 min	8 min	Fail	140 V	Aborted
3						
4						
5						
6						
7						
8						
9						
10						

Final result

5,5 m/s

Figure G.7: Laboratory Log - Heading 40 deg

Wind and wave scaling by BIS method

Status	Scale 1:1			Scale 1:30		
	Wind	H_s	Periode	Wind	H_s	Periode
OK	1,0	0,0214143	1,42	0,06	0,000713809	0,81
OK	2,0	0,0856570	1,42	0,12	0,002855235	0,81
OK	3,0	0,1927283	1,42	0,17	0,006424278	0,81
OK	4,0	0,3426280	1,42	0,23	0,011420933	0,81
OK	5,0	0,5353565	1,42	0,29	0,017845216	0,81
Fail	5,5	0,6477810	1,42	0,32	0,021592700	0,81
Fail	6,0	0,7709133	1,42	0,35	0,025697110	0,81
Fail	7,0	1,0492987	1,42	0,41	0,034976623	0,81
Fail	8,0	1,3705126	1,42	0,47	0,045683752	0,81
Fail	9,0	1,7345550	1,42	0,52	0,057818499	0,81
Fail	10,0	2,1414259	1,42	0,58	0,071380863	0,81
Fail	11,0	2,5911233	1,42	0,64	0,086370777	0,81
Fail	12,0	3,0836533	1,42	0,70	0,102788442	0,81
Fail	13,0	3,6190097	1,42	0,76	0,120633658	0,81
Fail	14,0	4,8182082	1,42	0,82	0,160606941	0,81
Fail	15,0	4,8820824	1,42	0,87	0,162736079	0,81
N/A	16,0	5,4805026	0,00	0,93	0,182683421	0,00
N/A	17,0	6,1887208	0,00	0,99	0,206290693	0,00
N/A	18,0	6,9382199	0,00	1,05	0,231273995	0,00
N/A	19,0	7,7305474	0,00	1,11	0,257684915	0,00
N/A	20,0	8,5657035	0,00	1,17	0,285523451	0,00

* N/A = Not Applicable - due to limitations at the MCLab

Constants		
Gravity	g	9,80655
Scale leng	L	30,00

Scale	CS3	
Linear Vel	sqrt(L*g)	17,1522
Length	L	30
Time	sqrt(L/g)	1,7482

Wind/Wave Calculator	
U (19,5)	H_s
5,5	0,647781

Line Search

Run nr	Wind	Stabilize time	Duration	Result	Voltage	Experiment
1	5,5 m/s	10 min	8 min	Fail	137V	Aborted
2	5 m/s	10 min	15 min	OK	135 V	Completed
3						
4						
5						
6						
7						
8						
9						
10						

Final result

5 m/s

Figure G.8: Laboratory Log - Heading 50 deg

Wind and wave scaling by BIS method

Status	Scale 1:1			Scale 1:30		
	Wind	H_s	Periode	Wind	H_s	Periode
OK	1,0	0,0214143	0,00	0,06	0,000713809	0,00
OK	2,0	0,0856570	0,00	0,12	0,002855235	0,00
OK	3,0	0,1927283	0,00	0,17	0,006424278	0,00
OK	4,0	0,3426280	0,00	0,23	0,011420933	0,00
Fail	4,5	0,4336390	1,42	0,26	0,014454633	0,81
Fail	5,0	0,5353565	1,42	0,29	0,017845217	0,81
Fail	6,0	0,7709133	1,42	0,35	0,025697110	0,81
Fail	7,0	1,0492987	0,00	0,41	0,034976623	0,00
Fail	8,0	1,3705126	0,00	0,47	0,045683752	0,00
Fail	9,0	1,7345550	0,00	0,52	0,057818499	0,00
Fail	10,0	2,1414259	0,00	0,58	0,071380863	0,00
Fail	11,0	2,5911233	0,00	0,64	0,086370777	0,00
Fail	12,0	3,0836533	0,00	0,70	0,102788442	0,00
Fail	13,0	3,6190097	0,00	0,76	0,120633658	0,00
Fail	14,0	4,8182082	0,00	0,82	0,160606941	0,00
Fail	15,0	4,8820824	0,00	0,87	0,162736079	0,00
N/A	16,0	5,4805026	0,00	0,93	0,182683421	0,00
N/A	17,0	6,1887208	0,00	0,99	0,206290693	0,00
N/A	18,0	6,9382199	0,00	1,05	0,231273995	0,00
N/A	19,0	7,7305474	0,00	1,11	0,257684915	0,00
N/A	20,0	8,5657035	0,00	1,17	0,285523451	0,00

* N/A = Not Applicable - due to limitations at the MCLab

Constants		
Gravity	g	9,80655
Scale leng	L	30,00

Scale	CS3
Linear Vel sqrt(L*g)	17,1522
Length	L 30
Time	sqrt(L/g) 1,7482

Wind/Wave Calculator	
U (19,5)	H_s
4,5	0,43639

Line Search

Run nr	Wind	Stabilize time	Duration	Result	Voltage	Experiment
1	5 m/s	10 min	15 min	Fail	140 V	Completed
2	4 m/s	10 min	15 min	OK	130 V	Completed
3	4,5 m/s	10 min	15 min	Fail	133,25 V	Completed
4						
5						
6						
7						
8						
9						
10						

Final result

4 m/s

Figure G.9: Laboratory Log - Heading 60 deg

Wind and wave scaling by BIS method

Status	Scale 1:1			Scale 1:30		
	Wind	H_s	Periode	Wind	H_s	Periode
OK	1,0	0,0214143	1,42	0,06	0,000713809	0,81
OK	2,0	0,0856570	1,42	0,12	0,002855235	0,81
OK	3,0	0,1927283	1,42	0,17	0,006424278	0,81
OK	4,0	0,5353565	1,42	0,23	0,017845216	0,81
OK	4,5	0,4336390	1,42	0,26	0,014454633	0,81
Fail	5,0	0,7709133	1,42	0,29	0,025697111	0,81
Fail	6,0	0,7709133	1,42	0,35	0,025697110	0,81
Fail	7,0	1,0492987	1,42	0,41	0,034976623	0,81
Fail	8,0	1,3705126	1,42	0,47	0,045683752	0,81
Fail	9,0	1,7345550	1,42	0,52	0,057818499	0,81
Fail	10,0	2,1414259	1,42	0,58	0,071380863	0,81
Fail	11,0	2,5911233	1,42	0,64	0,086370777	0,81
Fail	12,0	3,0836533	1,42	0,70	0,102788442	0,81
Fail	13,0	3,6190097	1,42	0,76	0,120633658	0,81
Fail	14,0	4,8182082	1,42	0,82	0,160606941	0,81
Fail	15,0	4,8820824	1,42	0,87	0,162736079	0,81
N/A	16,0	5,4805026	0,00	0,93	0,182683421	0,00
N/A	17,0	6,1887208	0,00	0,99	0,206290693	0,00
N/A	18,0	6,9382199	0,00	1,05	0,231273995	0,00
N/A	19,0	7,7305474	0,00	1,11	0,257684915	0,00
N/A	20,0	8,5657035	0,00	1,17	0,285523451	0,00

* N/A = Not Applicable - due to limitations at the MCLab

Constants		
Gravity	g	9,80655
Scale leng	L	30,00

Scale	CS3	
Linear Vel	sqrt(L*g)	17,1522
Length	L	30
Time	sqrt(L/g)	1,7482

Wind/Wave Calculator	
U (19,5)	H_s
4,5	0,433639

Line Search

Run nr	Wind	Stabilize time	Duration	Result	Voltage	Experiment
1	4 m/s	10 min	15 min	OK	130 V	Completed
2	4,5 m/s	10 min	15 min	OK	133,25 V	Completed
3	5 m/s	10 min	15 min	Fail	140 V	Completed
4						
5						
6						
7						
8						
9						
10						

Final result

4,5 m/s

Figure G.10: Laboratory Log - Heading 70 deg

Wind and wave scaling by BIS method

Status	Scale 1:1			Scale 1:30		
	Wind	H_s	Periode	Wind	H_s	Periode
OK	1,0	0,0214143	1,42	0,06	0,000713809	0,81
OK	2,0	0,0856570	1,42	0,12	0,002855235	0,81
OK	3,0	0,1927283	1,42	0,17	0,006424278	0,81
OK	4,0	0,3426280	1,42	0,23	0,011420933	0,81
Fail	4,5	0,4336390	1,42	0,26	0,014456633	0,81
Fail	5,0	0,5353565	1,42	0,29	0,017845217	0,81
Fail	6,0	0,7709133	1,42	0,35	0,025697110	0,81
Fail	7,0	1,0492987	1,42	0,41	0,034976623	0,81
Fail	8,0	1,3705126	1,42	0,47	0,045683752	0,81
Fail	9,0	1,7345550	1,42	0,52	0,057818499	0,81
Fail	10,0	2,1414259	1,42	0,58	0,071380863	0,81
Fail	11,0	2,5911233	1,42	0,64	0,086370777	0,81
Fail	12,0	3,0836533	1,42	0,70	0,102788442	0,81
Fail	13,0	3,6190097	1,42	0,76	0,120633658	0,81
Fail	14,0	4,8182082	1,42	0,82	0,160606941	0,81
Fail	15,0	4,8820824	1,42	0,87	0,162736079	0,81
N/A	16,0	5,4805026	0,00	0,93	0,182683421	0,00
N/A	17,0	6,1887208	0,00	0,99	0,206290693	0,00
N/A	18,0	6,9382199	0,00	1,05	0,231273995	0,00
N/A	19,0	7,7305474	0,00	1,11	0,257684915	0,00
N/A	20,0	8,5657035	0,00	1,17	0,285532451	0,00

Constants		
Gravity	g	9,80655
Scale leng	L	30,00

Scale	CS3
Linear Vel sqrt(L*g)	17,1522
Length L	30
Time sqrt(L/g)	1,7482

Wind/Wave Calculator	
U_(19,5)	H_s
4,5	0,433639

* N/A = Not Applicable - due to limitations at the MCLab

Line Search

Run nr	Wind	Stabilize time	Duration	Result	Voltage	Experiment
1	4 m/s	10 min	15 min	OK	130 V	Completed
2	4,5 m/s	10 min	2,39 min	Fail	133,25 V	Aborted
3						
4						
5						
6						
7						
8						
9						
10						

Final result

4 m/s

Figure G.11: Laboratory Log - Heading 80 deg

Wind and wave scaling by BIS method

Status	Scale 1:1			Scale 1:30		
	Wind	H_s	Periode	Wind	H_s	Periode
OK	1,0	0,0214143	1,42	0,06	0,000713809	0,81
OK	2,0	0,0856570	1,42	0,12	0,002855235	0,81
OK	3,0	0,1927283	1,42	0,17	0,006424278	0,81
OK	4,0	0,3426280	1,42	0,23	0,011420933	0,81
Fail	4,5	0,4336390	1,42	0,26	0,014454633	0,81
Fail	5,0	0,5353565	1,42	0,29	0,017845217	0,81
Fail	6,0	0,7709133	1,42	0,35	0,025697110	0,81
Fail	7,0	1,0492987	1,42	0,41	0,034976623	0,81
Fail	8,0	1,3705126	1,42	0,47	0,045683752	0,81
Fail	9,0	1,7345550	1,42	0,52	0,057818499	0,81
Fail	10,0	2,1414259	1,42	0,58	0,071380863	0,81
Fail	11,0	2,5911233	1,42	0,64	0,086370777	0,81
Fail	12,0	3,0836533	1,42	0,70	0,102788442	0,81
Fail	13,0	3,6190097	1,42	0,76	0,120633658	0,81
Fail	14,0	4,8182082	1,42	0,82	0,160606941	0,81
Fail	15,0	4,8820824	1,42	0,87	0,162736079	0,81
N/A	16,0	5,4805026	0,00	0,93	0,182683421	0,00
N/A	17,0	6,1887208	0,00	0,99	0,206290693	0,00
N/A	18,0	6,9382199	0,00	1,05	0,231273995	0,00
N/A	19,0	7,7305474	0,00	1,11	0,257684915	0,00
N/A	20,0	8,5657035	0,00	1,17	0,285523451	0,00

* N/A = Not Applicable - due to limitations at the MCLab

Constants		
Gravity	g	9,80655
Scale leng	L	30,00

Scale	CS3	
Linear Vel	sqrt(L*g)	17,1522
Length	L	30
Time	sqrt(L/g)	1,7482

Wind/Wave Calculator	
U (19,5)	H_s
4,5	0,433639

Line Search

Run nr	Wind	Stabilize time	Duration	Result	Voltage	Experiment
1	4 m/s	10 min	15 min	OK	130 V	Completed
2	4,5 m/s	10 min	4,29 min	Fail	133,5 V	Aborted
3						
4						
5						
6						
7						
8						
9						
10						

Final result

4 m/s

Figure G.12: Laboratory Log - Heading 90 deg

Wind and wave scaling by BIS method

Status	Scale 1:1			Scale 1:30		
	Wind	H_s	Periode	Wind	H_s	Periode
OK	1,0	0,0214143	1,42	0,06	0,000713809	0,81
OK	2,0	0,0856570	1,42	0,12	0,002855235	0,81
OK	3,0	0,1927283	1,42	0,17	0,006424278	0,81
OK	4,0	0,3426280	1,42	0,23	0,011420933	0,81
Fail	4,5	0,4336390	1,42	0,26	0,014454633	0,81
Fail	5,0	0,5353565	1,42	0,29	0,017845217	0,81
Fail	6,0	0,7709133	1,42	0,35	0,025697110	0,81
Fail	7,0	1,0492987	1,42	0,41	0,034976623	0,81
Fail	8,0	1,3705126	1,42	0,47	0,045683752	0,81
Fail	9,0	1,7345550	1,42	0,52	0,057818499	0,81
Fail	10,0	2,1414259	1,42	0,58	0,071380863	0,81
Fail	11,0	2,5911233	1,42	0,64	0,086370777	0,81
Fail	12,0	3,0836533	1,42	0,70	0,102788442	0,81
Fail	13,0	3,6190097	1,42	0,76	0,120633658	0,81
Fail	14,0	4,8182082	1,42	0,82	0,160606941	0,81
Fail	15,0	4,8820824	1,42	0,87	0,162736079	0,81
N/A	16,0	5,4805026	0,00	0,93	0,182683421	0,00
N/A	17,0	6,1887208	0,00	0,99	0,206290693	0,00
N/A	18,0	6,9382199	0,00	1,05	0,231273995	0,00
N/A	19,0	7,7305474	0,00	1,11	0,257684915	0,00
N/A	20,0	8,5657035	0,00	1,17	0,285523451	0,00

Constants		
Gravity	g	9,80655
Scale leng	L	30,00

Scale	CS3
Linear Vel sqrt(L*g)	17,1522
Length L	30
Time sqrt(L/g)	1,7482

Wind/Wave Calculator	
U_(19,5)	H_s
4,5	0,43639

Line Search

Run nr	Wind	Stabilize time	Duration	Result	Voltage	Experiment
1	4 m/s	10 min	15 min	OK	130 V	Completed
2	4,5 m/s	10 min	15 min	Fail	133,25 V	Completed
3						
4						
5						
6						
7						
8						
9						
10						

Final result

4 m/s

* N/A = Not Applicable - due to limitations at the MClab

Figure G.13: Laboratory Log - Heading 100 deg

Wind and wave scaling by BIS method

Status	Scale 1:1			Scale 1:30		
	Wind	H_s	Periode	Wind	H_s	Periode
OK	1,0	0,0214143	1,42	0,06	0,000713809	0,81
OK	2,0	0,0856570	1,42	0,12	0,002855235	0,81
OK	3,0	0,1927283	1,42	0,17	0,006424278	0,81
OK	4,0	0,3426280	1,42	0,23	0,011420933	0,81
OK	4,5	0,4336390	1,42	0,26	0,014454633	0,81
Fail	5,0	0,5353565	1,42	0,29	0,017845216	0,81
Fail	6,0	0,7709133	1,42	0,35	0,025697110	0,81
Fail	7,0	1,0492987	1,42	0,41	0,034976623	0,81
Fail	8,0	1,3705126	1,42	0,47	0,045683752	0,81
Fail	9,0	1,7345550	1,42	0,52	0,057818499	0,81
Fail	10,0	2,1414259	1,42	0,58	0,071380863	0,81
Fail	11,0	2,5911233	1,42	0,64	0,086370777	0,81
Fail	12,0	3,0836533	1,42	0,70	0,102788442	0,81
Fail	13,0	3,6190097	1,42	0,76	0,120633658	0,81
Fail	14,0	4,8182082	1,42	0,82	0,160606941	0,81
Fail	15,0	4,8820824	1,42	0,87	0,162736079	0,81
N/A	16,0	5,4805026	0,00	0,93	0,182683421	0,00
N/A	17,0	6,1887208	0,00	0,99	0,206290693	0,00
N/A	18,0	6,9382199	0,00	1,05	0,231273995	0,00
N/A	19,0	7,7305474	0,00	1,11	0,257684915	0,00
N/A	20,0	8,5657035	0,00	1,17	0,285523451	0,00

* N/A = Not Applicable - due to limitations at the MCLab

Constants		
Gravity	g	9,80655
Scale leng	L	30,00

Scale	CS3	
Linear Vel	sqrt(L*g)	17,1522
Length	L	30
Time	sqrt(L/g)	1,7482

Wind/Wave Calculator	
U_(19,5)	H_s
4,5	0,433639

Line Search

Run nr	Wind	Stabilize time	Duration	Result	Voltage	Experiment
1	4 m/s	10 min	15 min	OK	130 V	Completed
2	5 m/s	10 min	15 min	Fail	140 V	Completed
3	4,5 m/s	10 min	15 min	OK	133,25 V	Completed
4						
5						
6						
7						
8						
9						
10						

Final result

4,5 m/s

Figure G.14: Laboratory Log - Heading 110 deg

Wind and wave scaling by BIS method

Status	Scale 1:1			Scale 1:30			
	Wind	H_s	Periode	Wind	H_s	Periode	
OK	1,0	0,0214143	1,42	0,06	0,000713809	0,81	
OK	2,0	0,0856570	1,42	0,12	0,002855235	0,81	
OK	3,0	0,1927283	1,42	0,17	0,006424278	0,81	
OK	4,0	0,3426280	1,42	0,23	0,011420933	0,81	
OK	4,5	0,4336390	1,42	0,26	0,014454633	0,81	
Fail	5,0	0,5335565	1,42	0,29	0,017785217	0,81	
Fail	6,0	0,7709133	1,42	0,35	0,025697110	0,81	
Fail	7,0	1,0492987	1,42	0,41	0,034976623	0,81	
Fail	8,0	1,3705126	1,42	0,47	0,045683752	0,81	
Fail	9,0	1,7345550	1,42	0,52	0,057818499	0,81	
Fail	10,0	2,1414259	1,42	0,58	0,071380863	0,81	
Fail	11,0	2,5911233	1,42	0,64	0,086370777	0,81	
Fail	12,0	3,0836533	1,42	0,70	0,102788442	0,81	
Fail	13,0	3,6190097	1,42	0,76	0,120633658	0,81	
Fail	14,0	4,8182082	1,42	0,82	0,160606941	0,81	
Fail	15,0	4,8820824	1,42	0,87	0,162736079	0,81	
N/A	16,0	5,4805026	0,00	0,93	0,182683421	0,00	
N/A	17,0	6,1887208	0,00	0,99	0,206290693	0,00	
N/A	18,0	6,9382199	0,00	1,05	0,231273995	0,00	
N/A	19,0	7,7305474	0,00	1,11	0,257684915	0,00	
N/A	20,0	8,5657035	0,00	1,17	0,285523451	0,00	

Constants		
Gravity	g	9,80655
Scale leng	L	30,00

Scale	CS3
Linear Vel	sqrt(L*g) 17,1522
Length	L 30
Time	sqrt(L/g) 1,7482

Wind/Wave Calculator	
U_(19,5)	H_s
4,5	0,43639

* N/A = Not Applicable - due to limitations at the MCLab

Line Search

Run nr	Wind	Stabilize time	Duration	Result	Voltage	Experiment
1	4,5 m/s	10 min	15 min	OK	133,25 V	Completed
2	5 m/s	10 min	14,5 min	Fail	135 V	Aborted
3						
4						
5						
6						
7						
8						
9						
10						

Final result

4,5 m/s

Figure G.15: Laboratory Log - Heading 120 deg

Wind and wave scaling by BIS method

Status	Scale 1:1			Scale 1:30		
	Wind	H_s	Periode	Wind	H_s	Periode
OK	1,0	0,0214143	1,42	0,06	0,000713809	0,81
OK	2,0	0,0856570	1,42	0,12	0,002855235	0,81
OK	3,0	0,1927283	1,42	0,17	0,006424278	0,81
OK	4,0	0,3426280	1,42	0,23	0,011420933	0,81
OK	4,5	0,4336390	1,42	0,26	0,014454633	0,81
Fail	5,0	0,5353565	1,42	0,29	0,017845216	0,81
Fail	6,0	0,7709133	1,42	0,35	0,025697110	0,81
Fail	7,0	1,0492987	1,42	0,41	0,034976623	0,81
Fail	8,0	1,3705126	1,42	0,47	0,045683752	0,81
Fail	9,0	1,7345550	1,42	0,52	0,057818499	0,81
Fail	10,0	2,1414259	1,42	0,58	0,071380863	0,81
Fail	11,0	2,5911233	1,42	0,64	0,086370777	0,81
Fail	12,0	3,0836533	1,42	0,70	0,102788442	0,81
Fail	13,0	3,6190097	1,42	0,76	0,120633658	0,81
Fail	14,0	4,8182082	1,42	0,82	0,160606941	0,81
Fail	15,0	4,8820824	1,42	0,87	0,162736079	0,81
N/A	16,0	5,4805026	0,00	0,93	0,182683421	0,00
N/A	17,0	6,1887208	0,00	0,99	0,206290693	0,00
N/A	18,0	6,9382199	0,00	1,05	0,231273995	0,00
N/A	19,0	7,7305474	0,00	1,11	0,257684915	0,00
N/A	20,0	8,5657035	0,00	1,17	0,285523451	0,00

* N/A = Not Applicable - due to limitations at the MCLab

Constants		
Gravity	g	9,80655
Scale leng	L	30,00

Scale	CS3	
Linear Vel	sqrt(L*g)	17,1522
Length	L	30
Time	sqrt(L/g)	1,7482

Wind/Wave Calculator	
U_(19.5)	H_s
4,5	0,433639

Line Search

Run nr	Wind	Stabilize time	Duration	Result	Voltage	Experiment
1	5 m/s	10 min	4 min	Fail	135 V	Aborted
2	4,5 m/s	10 min	15 min	OK	133,25 V	Completed
3						
4						
5						
6						
7						
8						
9						
10						

Final result

4,5 m/s

Figure G.16: Laboratory Log - Heading 130 deg

Wind and wave scaling by BIS method

Status	Scale 1:1			Scale 1:30		
	Wind	H_s	Periode	Wind	H_s	Periode
OK	1,0	0,0214143	1,42	0,06	0,000713809	0,81
OK	2,0	0,0856570	1,42	0,12	0,002855235	0,81
OK	3,0	0,1927283	1,42	0,17	0,00642478	0,81
OK	4,0	0,3426280	1,42	0,23	0,011420933	0,81
OK	4,5	0,4336390	1,42	0,26	0,01445463	0,81
Fail	5,0	0,5353565	1,42	0,29	0,01784521	0,81
Fail	6,0	0,7709133	1,42	0,35	0,02569711	0,81
Fail	7,0	1,0492987	1,42	0,41	0,03497662	0,81
Fail	8,0	1,3705126	1,42	0,47	0,04568375	0,81
Fail	9,0	1,7345550	1,42	0,52	0,05781849	0,81
Fail	10,0	2,1414259	1,42	0,58	0,07138086	0,81
Fail	11,0	2,5911233	1,42	0,64	0,08637077	0,81
Fail	12,0	3,0836533	1,42	0,70	0,10278442	0,81
Fail	13,0	3,6190097	1,42	0,76	0,12063658	0,81
Fail	14,0	4,8182082	1,42	0,82	0,16060941	0,81
Fail	15,0	4,8820824	1,42	0,87	0,16273607	0,81
N/A	16,0	5,4805026	0,00	0,93	0,18268342	0,00
N/A	17,0	6,1887208	0,00	0,99	0,20629069	0,00
N/A	18,0	6,9382199	0,00	1,05	0,23127395	0,00
N/A	19,0	7,7305474	0,00	1,11	0,25768491	0,00
N/A	20,0	8,5657035	0,00	1,17	0,28552345	0,00

Constants		
Gravity	g	9,80655
Scale leng	L	30,00

Scale	CS3
Linear Vel sqrt(L*g)	17,1522
Length L	30
Time sqrt(L/g)	1,7482

Wind/Wave Calculator	
U_(19,5)	H_s
4,5	0,43639

* N/A = Not Applicable - due to limitations at the MCLab

Line Search

Run nr	Wind	Stabilize time	Duration	Result	Voltage	Experiment
1	5 m/s	10 min	15 min	Fail	135 V	Completed
2	4,5 m/s	10 min	15 min	OK	133,25 V	Completed
3						
4						
5						
6						
7						
8						
9						
10						

Final result

4,5 m/s

Figure G.17: Laboratory Log - Heading 140 deg

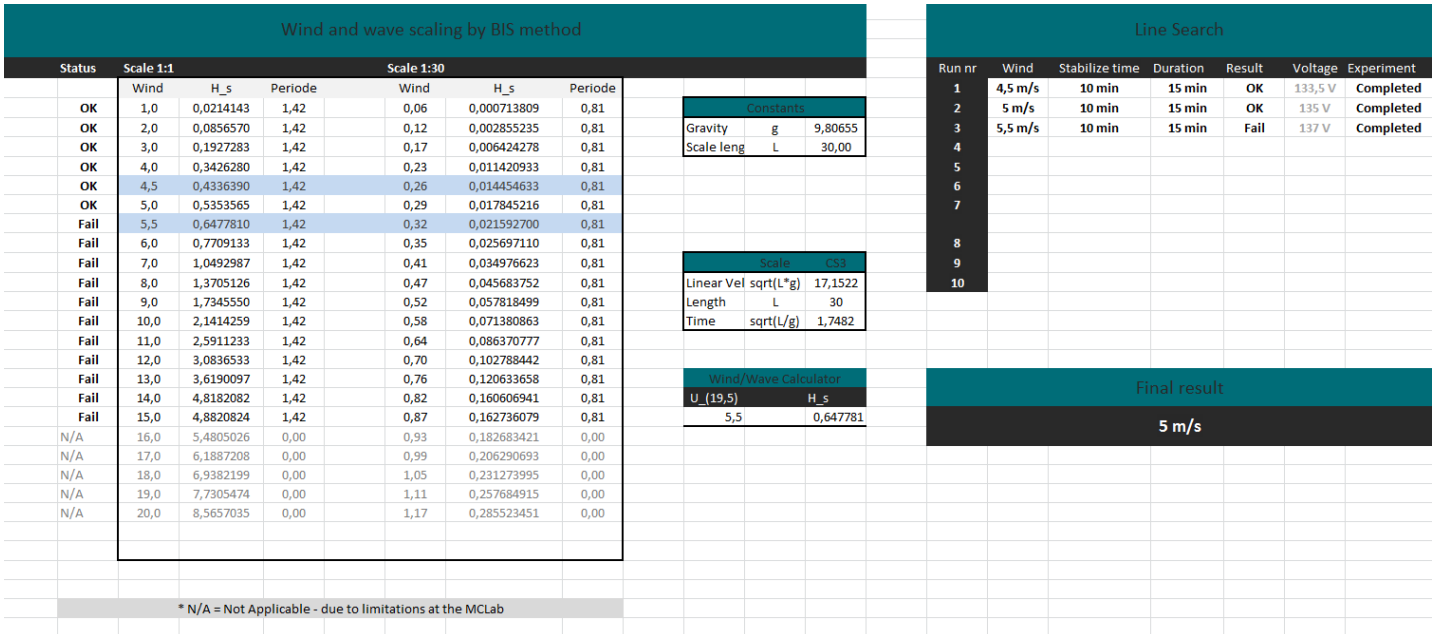

Wind and wave scaling by BIS method

Status	Scale 1:1			Scale 1:30		
	Wind	H_s	Periode	Wind	H_s	Periode
OK	1,0	0,0214143	1,42	0,06	0,000713809	0,81
OK	2,0	0,0856570	1,42	0,12	0,002855235	0,81
OK	3,0	0,1927283	1,42	0,17	0,006424278	0,81
OK	4,0	0,3426280	1,42	0,23	0,011420933	0,81
OK	4,5	0,4336390	1,42	0,26	0,014454633	0,81
OK	5,0	0,5353565	1,42	0,29	0,017845216	0,81
Fail	5,5	0,6477810	1,42	0,32	0,021592700	0,81
Fail	6,0	0,7709133	1,42	0,35	0,025697110	0,81
Fail	7,0	1,0492987	1,42	0,41	0,034976623	0,81
Fail	8,0	1,3705126	1,42	0,47	0,045683752	0,81
Fail	9,0	1,7345550	1,42	0,52	0,057818499	0,81
Fail	10,0	2,1414259	1,42	0,58	0,071380863	0,81
Fail	11,0	2,5911233	1,42	0,64	0,086370777	0,81
Fail	12,0	3,0836533	1,42	0,70	0,102788442	0,81
Fail	13,0	3,6190097	1,42	0,76	0,120633658	0,81
Fail	14,0	4,8182082	1,42	0,82	0,160606941	0,81
Fail	15,0	4,8820824	1,42	0,87	0,162736079	0,81
N/A	16,0	5,4805026	0,00	0,93	0,182683421	0,00
N/A	17,0	6,1887208	0,00	0,99	0,206290693	0,00
N/A	18,0	6,9382199	0,00	1,05	0,231273995	0,00
N/A	19,0	7,7305474	0,00	1,11	0,257684915	0,00
N/A	20,0	8,5657035	0,00	1,17	0,285523451	0,00

* N/A = Not Applicable - due to limitations at the MCLab

Constants		
Gravity	g	9,80655
Scale leng	L	30,00

	Scale	CS3
Linear Vel	sqrt(L*g)	17,1522
Length	L	30
Time	sqrt(L/g)	1,7482

Wind/Wave Calculator	
U_(19,5)	H_s
5,5	0,647781

Line Search

Run nr	Wind	Stabilize time	Duration	Result	Voltage	Experiment
1	4,5 m/s	10 min	15 min	OK	133,5 V	Completed
2	5 m/s	10 min	15 min	OK	135 V	Completed
3	5,5 m/s	10 min	15 min	Fail	137 V	Completed
4						
5						
6						
7						
8						
9						
10						

Final result

5 m/s

Figure G.18: Laboratory Log - Heading 150 deg

Wind and wave scaling by BIS method

Status	Scale 1:1			Scale 1:30		
	Wind	H_s	Periode	Wind	H_s	Periode
OK	1,0	0,0214143	1,42	0,06	0,000713809	0,81
OK	2,0	0,0856570	1,42	0,12	0,002855235	0,81
OK	3,0	0,1927283	1,42	0,17	0,006424278	0,81
OK	4,0	0,3426280	1,42	0,23	0,011420933	0,81
OK	5,0	0,5353565	1,42	0,29	0,017845216	0,81
Fail	5,5	0,6477810	1,42	0,32	0,021592700	0,81
Fail	6,0	0,7709133	1,42	0,35	0,025697110	0,81
Fail	7,0	1,0492987	1,42	0,41	0,034976623	0,81
Fail	8,0	1,3705126	1,42	0,47	0,045683752	0,81
Fail	9,0	1,7345550	1,42	0,52	0,057818499	0,81
Fail	10,0	2,1414259	1,42	0,58	0,071380863	0,81
Fail	11,0	2,5911233	1,42	0,64	0,086370777	0,81
Fail	12,0	3,0836533	1,42	0,70	0,102788442	0,81
Fail	13,0	3,6190097	1,42	0,76	0,120633658	0,81
Fail	14,0	4,8182082	1,42	0,82	0,160606941	0,81
Fail	15,0	4,8820824	1,42	0,87	0,162736079	0,81
N/A	16,0	5,4805026	0,00	0,93	0,182683421	0,00
N/A	17,0	6,1887208	0,00	0,99	0,206290693	0,00
N/A	18,0	6,9382199	0,00	1,05	0,231273995	0,00
N/A	19,0	7,7305474	0,00	1,11	0,257684915	0,00
N/A	20,0	8,5657035	0,00	1,17	0,285523451	0,00

Constants		
Gravity	g	9,80655
Scale leng	L	30,00

Scale	CS3
Linear Vel	sqrt(L*g) 17,1522
Length	L 30
Time	sqrt(L/g) 1,7482

Wind/Wave Calculator	
U_(19,5)	H_s
5,5	0,647781

* N/A = Not Applicable - due to limitations at the MCLab

Line Search

Run nr	Wind	Stabilize time	Duration	Result	Voltage	Experiment
1	5,5 m/s	10 min	15 min	Fail	137 V	Completed
2	5 m/s	10 min	15 min	OK	133,25 V	Completed
3						
4						
5						
6						
7						
8						
9						
10						

Final result

5 m/s

Figure G.19: Laboratory Log - Heading 160 deg

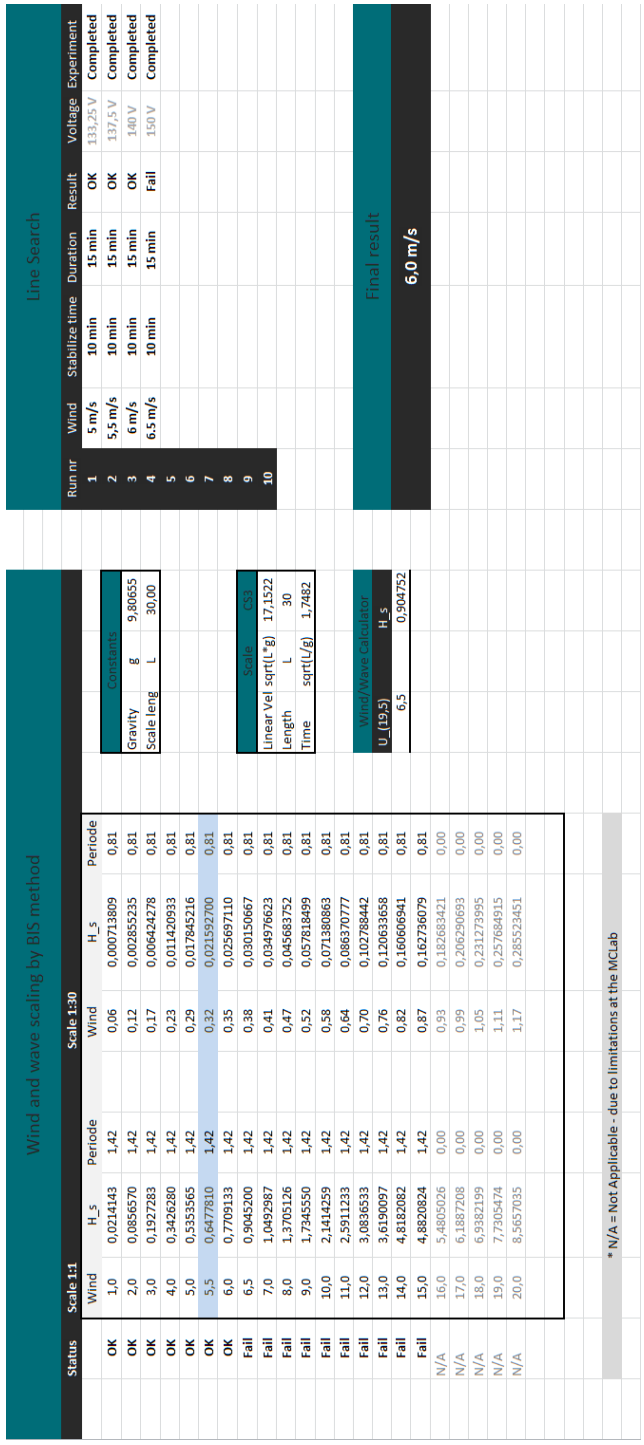

Figure G.20: Laboratory Log - Heading 170 deg

Wind and wave scaling by BIS method

Status	Scale 1:1			Scale 1:30		
	Wind	H_s	Periode	Wind	H_s	Periode
OK	1,0	0,0214143	1,42	0,06	0,00071809	0,81
OK	2,0	0,0856570	1,42	0,12	0,00285235	0,81
OK	3,0	0,1927283	1,42	0,17	0,00642478	0,81
OK	4,0	0,3426280	1,42	0,23	0,01142093	0,81
OK	5,0	0,5353565	1,42	0,29	0,01784521 6	0,81
OK	5,5	0,6477810	1,42	0,32	0,02159270 0	0,81
OK	6,0	0,7709133	1,42	0,35	0,02569711 0	0,81
Fail	7,0	1,0492987	1,42	0,41	0,03497662 3	0,81
Fail	8,0	1,3705126	1,42	0,47	0,04568375 2	0,81
Fail	9,0	1,7345550	1,42	0,52	0,05781849 9	0,81
Fail	10,0	2,1414259	1,42	0,58	0,07138086 3	0,81
Fail	11,0	2,5911233	1,42	0,64	0,08637077	0,81
Fail	12,0	3,0836533	1,42	0,70	0,10278842 2	0,81
Fail	13,0	3,6190097	1,42	0,76	0,12063658	0,81
Fail	14,0	4,8182082	1,42	0,82	0,16060694 1	0,81
Fail	15,0	4,8820824	1,42	0,87	0,16273607 9	0,81
N/A	16,0	5,4805026	0,00	0,93	0,18268342 1	0,00
N/A	17,0	6,1887208	0,00	0,99	0,20629069 3	0,00
N/A	18,0	6,9382199	0,00	1,05	0,23127399 5	0,00
N/A	19,0	7,7305474	0,00	1,11	0,25768491 5	0,00
N/A	20,0	8,5657035	0,00	1,17	0,28552345 1	0,00

Constants		
Gravity	g	9,80655
Scale leng	L	30,00

Scale	CS3
Linear Vel sqrt(L*g)	17,1522
Length L	30
Time sqrt(L/g)	1,7482

Wind/Wave Calculator	
U_(19,5)	H_s
7,5	1,204552

* N/A = Not Applicable - due to limitations at the MCLab

Line Search

Run nr	Wind	Stabilizetime	Duration	Result	Voltage	Experiment
1	6,5 m/s	10 min	15 min	OK	150 V	Completed
2	7 m/s	10 min	15 min	Fail	153 V	Completed
3						
4						
5						
6						
7						
8						
9						
10						

Final result

6,5 m/s

Figure G.21: Laboratory Log - Heading 180 deg

Appendix H

Wind Generator

This appendix contain the drawings and pictures of the wind generator rig. The rig was constructed by welding the two to mounting plates, to two extension rods. Both where made of steal. In this way the fan could be secured to the movable bridge over the pool at MCLab.

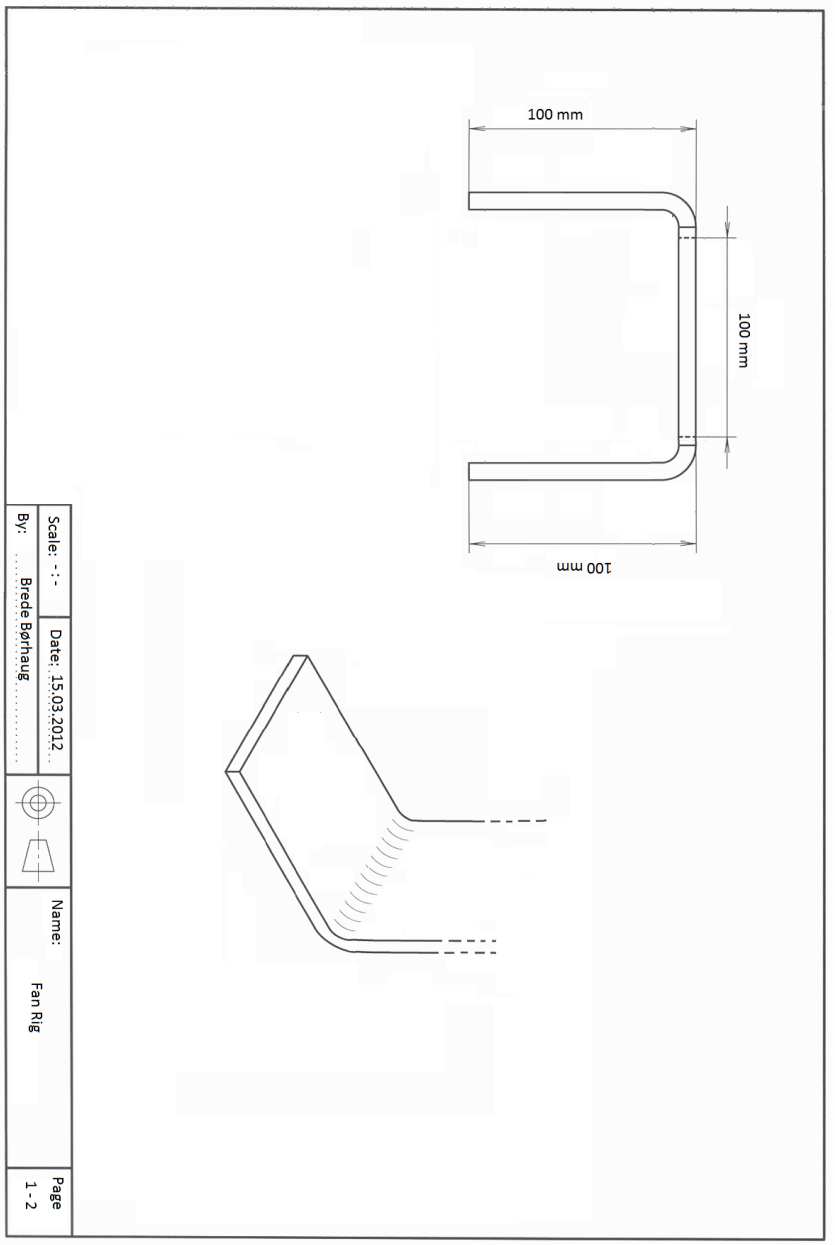

Figure H.1: Wind Rig Top Mounting Plate

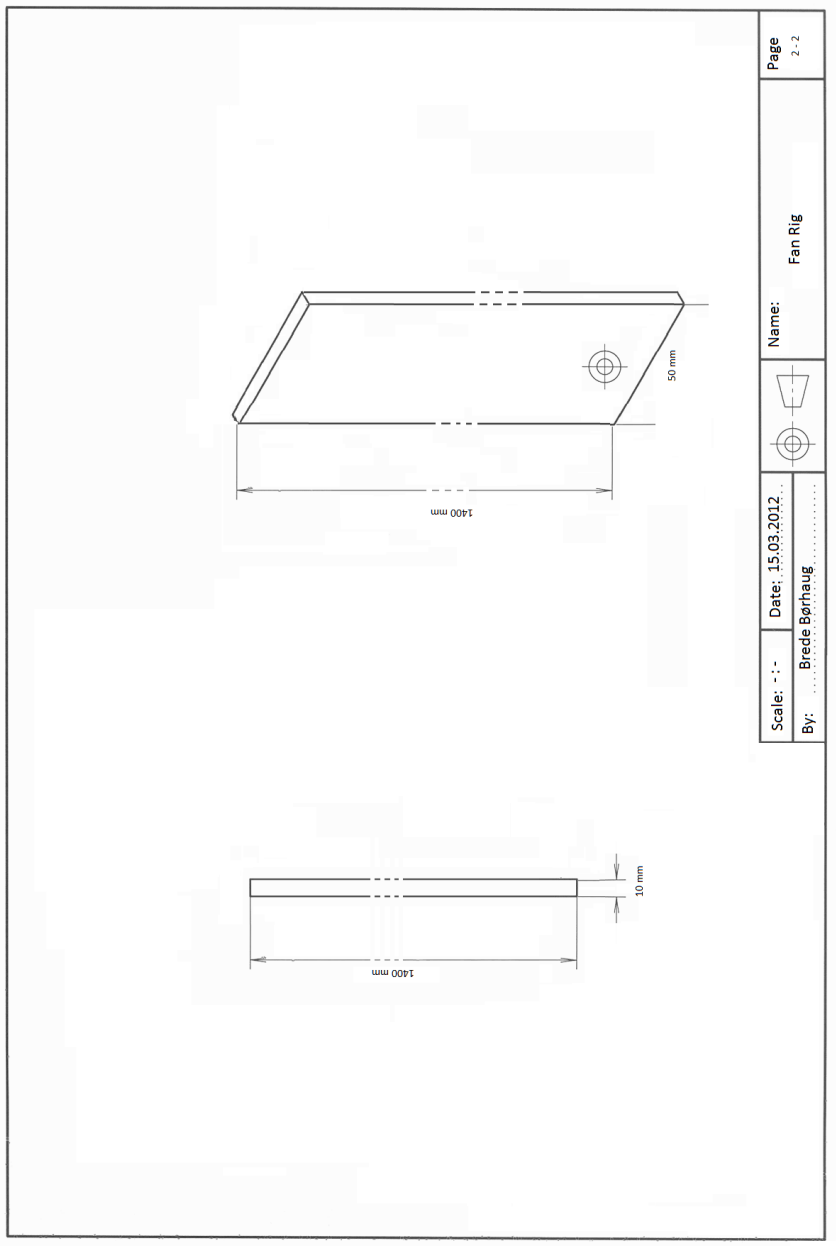

Figure H.2: Wind Rig Extension Rods

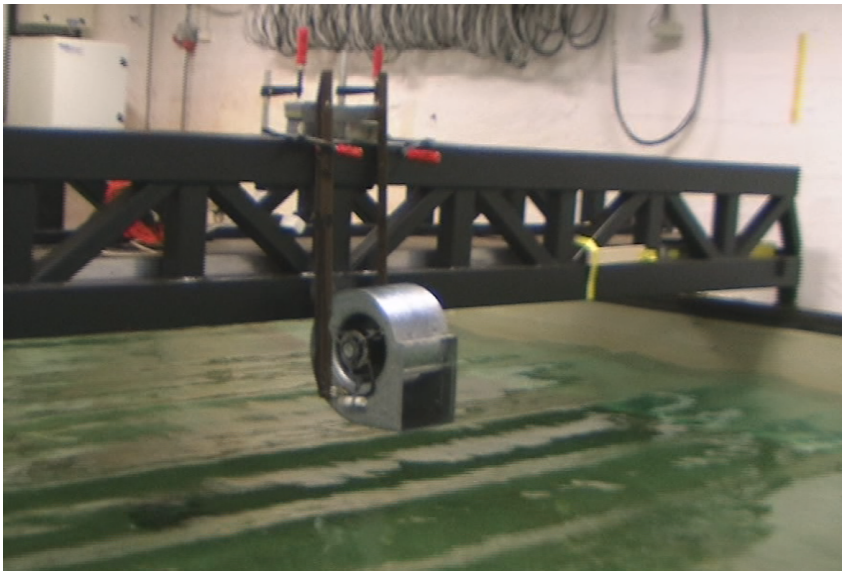

Figure H.3: Wind generator and rig